# Development of separation and condensation techniques using functional membrane for trace components in groundwater

Aosai, Daisuke

(Degree)
博士（工学）

(Date of Degree)
2016-03-25

(Date of Publication)
2017-03-01

(Resource Type)
doctoral thesis

(Report Number)
甲第6645号

(URL)
https://hdl.handle.net/20.500.14094/D1006645

Doctoral Dissertation

# Development of separation and condensation techniques using functional membrane for trace components in groundwater

（機能性膜を用いた地下水中微量成分の分離および濃縮技術の開発）

**January 2016**

**Graduate School of Engineering**
**Kobe University**

**Daisuke Aosai**

# Acknowledgment

Foremost, I would like to express my deep and sincere gratitude to my supervisor, Professor Dr. Hideto Matsuyama, for providing me this precious study opportunity as a PhD student in his laboratory. His continuous encouragement, support, and guidance have allowed me to complete my doctoral study. I will never forget this favor.

I am also deeply grateful to Dr. Daisuke Saeki for his advice and invaluable discussions. His attitude as researcher always impressed me. Without his kind help, I could not have completed this work.

I sincerely thank to Dr. Toru Ishigami for his kind support and helpful discussions. He always encouraged me.

I would like to thank Professor Dr. Hiroshi Suzuki and Professor Dr. Takashi Nishino for their kindness during the reviewing and examining of this thesis and giving constructive comments to improve upon it. I also owe my gratitude to the members in Professor Matsuyama's laboratory for their constructive comments for my study and their kindness.

I would like to express my appreciation to Yuichi Terasawa, Michiharu Inui, Katuji Kaneko, and Koji Onawa of Kobelco Research Institute, Inc. for their support and understanding throughout this work. I would like to offer my thanks to Teruki Iwatsuki and Takashi Mizuno of Japan Atomic Energy Agency, Yuhei Yamamoto of Tokushima University for their kind teaching and support.

Finally, I would like to express special thanks to my family, Yumiko, Mei and Kou for support and encouragement. I could not have succeeded without their love and understanding.

Daisuke Aosai

Graduate School of Engineering

Kobe University, 2016.

# Table of Contents

## Chapter I General Introduction



## Chapter II Size and composition analyses of colloids in deep granitic groundwater using microfiltration/ultrafiltration while maintaining in situ hydrochemical conditions

# Chapter I

## General Introduction

### I.1 Study of colloids on geological disposal of high level radioactive waste

#### I.1.1 Influence of colloids on radionuclides transport

Radioactivity of high level radioactive waste (HLW) originating from nuclear industry remains for very long periods of time, although that decays gradually. HLW could pose unacceptable risk to human health. Therefore, it is necessary to isolate HLW from human environment for long time. Various methods for isolation of HLW, such as geological disposal, space disposal, sea disposal, and ice sheets disposal, have been investigated by international organizations and countries. Geological disposal in stable underground environment is internationally recognized as a common concept for the most safe and suitable method (Table I.1). In japan, HLW vitrified in stainless steel containers is legislated to be disposed more than 300 m underground (Fig. I.1) according to the Designated Radioactive Waste Final Disposal Act [1]. The safety of geological disposal of HLW is ensured by retardation of released radionuclide migration in underground environment. Radionuclides such as uranium, plutonium, and americium in HLW hardly migrate in groundwater due to their low solubility to groundwater and strong sorption onto bed rocks [2]. For example, plutonium is stable as Pu(IV) under typical environmental water and easily precipitated by oxidation as $PuO_2$ [3], and solubility of trivalent americium is less than 1 μM/L [4].

Migration of radionuclides is mainly influenced by groundwater flow, precipitation, diffusion, and interaction with rocks (e.g., adsorption and filtration). Although, the

migration speed of radionuclides is generally slow, it is important to understand the migration behavior of radionuclides for long-term isolation. The migration speed of radionuclides is also influenced by the presence of colloids such as fragment of rock and humic substances (Fig. I 2). There are some evidences that the migration speed of radionuclides was accelerated by natural colloids. At the Nevada Test Site (NTS) in the United States, plutonium was detected as an associated state with colloids composed of clays, zeolites, and cristobalite in groundwater at 1.3 km away from the hypocenter of the nuclear weapons test site [5]. At the Los Alamos National Laboratory, plutonium and americium leaked from the Central Waste Treatment Plant were detected in groundwater 2 to 3 km away from a discharge site, and associated with mineral colloids [6]. At Mayak in Russia, plutonium and uranium were found with amorphous iron oxide colloids at 3 km away from a nuclear waste reprocessing plant site [7]. Therefore, understanding of colloid properties (e.g., concentration, size, shape, chemical composition, and interaction with radionuclides) in groundwater is indispensable for safety assessment of HLW.

**Table I.1 Disposal methods of HLW**

| Disposal methods | Summary |
|---|---|
| Geological disposal | Recognized as a common concept for the most safe and suitable method |
| Space disposal | Abandoned due to high cost and potential risks of launch failure. |
| Sea disposal | Not permitted by International agreements according to the Convention on the Prevention of Marine Pollution by Dumping of Wastes and Other Matter (1972). |
| Ice sheets disposal | Not permitted by International agreements according to the Antarctic Treaty (1959). |

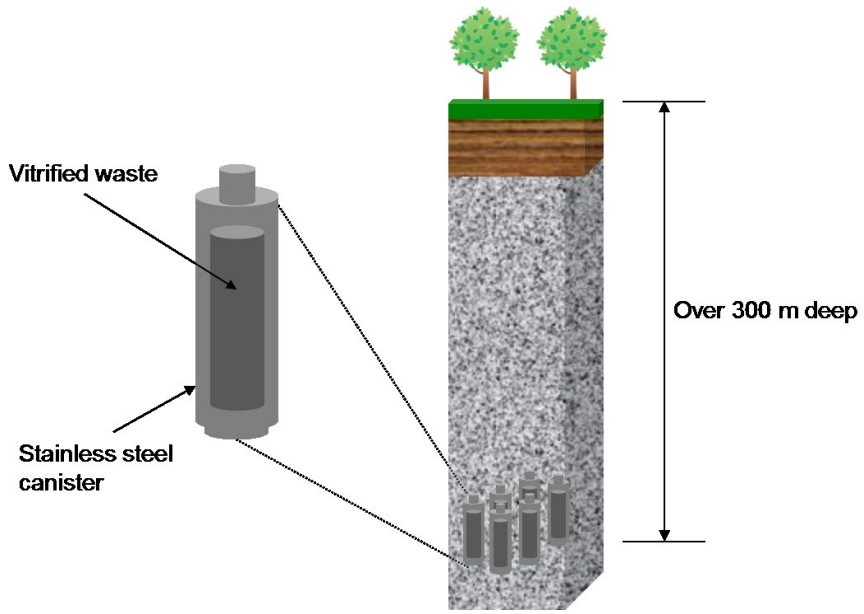


**Fig. I.1 Geological disposal of high level radioactive waste (in Japan).**

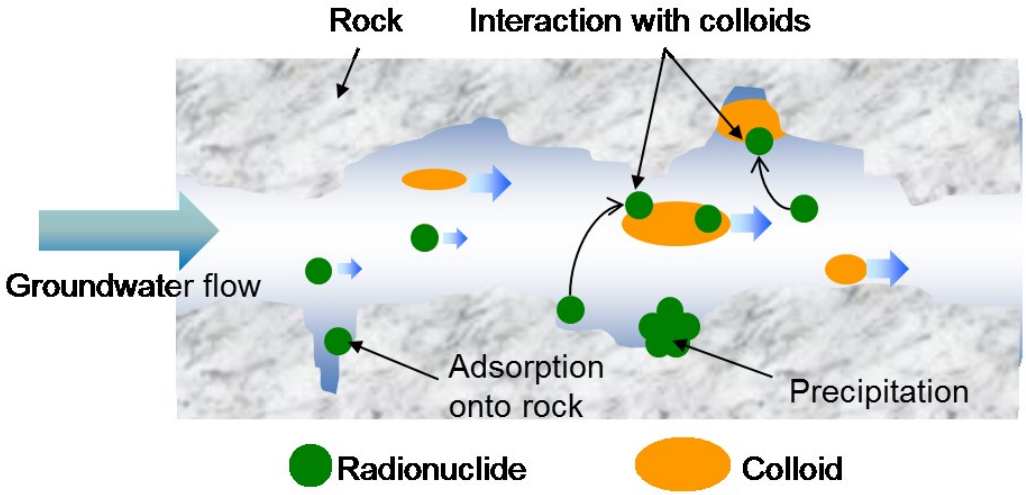


**Fig. I.2 Influence of colloids on radionuclides transport in groundwater.**

### I.1.2 Properties of Colloids in groundwater

#### I.1.2.1 Size and material

Colloids are particulates or macromolecules with diameters less than 1 μm [8] (Fig. I.3) and are ubiquitous in natural water [9]. Groundwater contain inorganic colloids and organic colloids. The former are produced by fragmentation, dissolution, and precipitation of rocks such as clays, silica, and metal (hydro) oxide, and the latter are humic substance, protein, bacteria and spores [10]. Most of organic colloids are considered as humic substance [11]. Colloids can adsorb various ions and be chemically bound by dissolved species, because colloids have large specific surface areas and charges. Thus, colloids play a significant role in groundwater as transferring carriers or blockers for radionuclides.

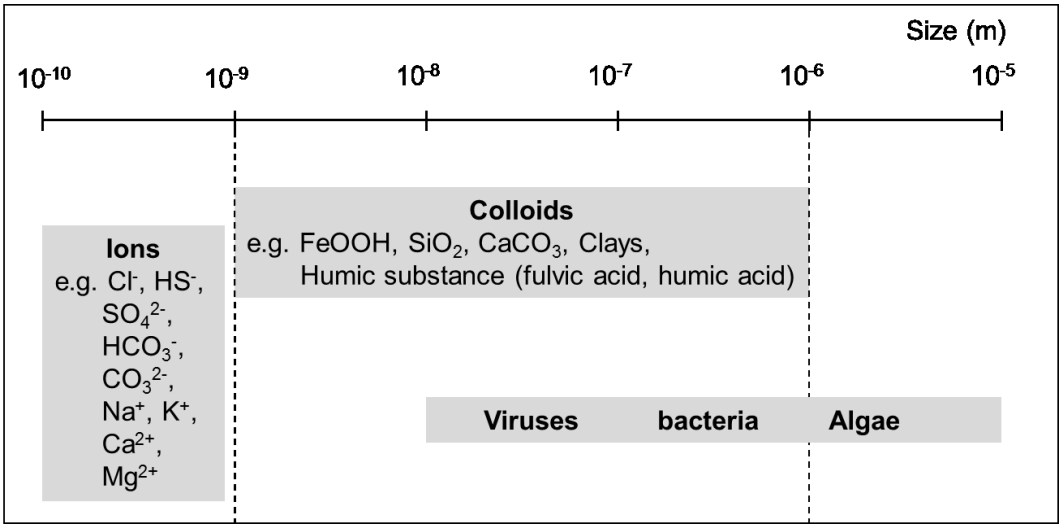


**Fig. I.3 Size distribution of groundwater material.**

### I.1.2.2 Stability

The stability of colloids is mainly determined by van der waals attractive force, which promotes aggregation, and by electrostatic repulsive force, which drives dispersion [8]. When colloids are dispersed stably in groundwater, colloids can be migrated by groundwater flow in underground environment. On the other hand, if colloids are precipitated due to aggregation, colloids cannot be migrated. Thus, migration of radionuclides adsorbed onto colloids is strongly influenced by the stability of colloids. Degueldre et al. discussed the stability of colloids in groundwater from various sites (crystalline, sedimentary, subsurface, and aquafers) [12]. They described the importance of pH, redox potential, concentration of salt ($Na^+$, $K^+$), water hardness ($Ca^{2+}$, $Mg^{2+}$), and organic material for the stability of colloids. Moreover, humic acids, which is a fraction of humic substances, is not soluble in aqueous solution under acidic condition (pH < 2) due to aggregation, but is soluble at high pH. Therefore, retaining the stability of colloids is important to analyze colloids accurately.

### I.1.3 Study of colloids in groundwater

To study geological disposal of radioactive waste, some countries operate Underground Research Laboratories (URLs), where researchers can obtain samples (groundwater, rock, and sediment) with less contamination or transformation (Table I.2). Vilks et al. investigated the size distribution, concentration, composition, and natural radionuclide content of colloids at the Cigra Lake U deposit located in northern Saskatchewan in the eastern part of the Athabasca Basin by size-fractionation and condensation using ultrafiltration (UF) membranes [13]. They reported that the composition of colloids was mostly clays, organic materials, and Fe oxides. Laaksoharji et al. reported that colloids in Swedish granitic groundwater were constituted by clay and quartz with size ranges from 10 to 450 nm [14]. Plaschke et al. characterized colloids obtained from the Gorleben site in the North German Plain by tapping-mode atomic force microscopy (AFM) with phase contrast imaging, and reported the presence of different types of colloids (e.g., spherical particles, fibrous structures, and structures which appear to be hollow), which may influence the migration of groundwater contaminants [15]. Artinger et al. investigated groundwaters from different aquifer systems in the Germany including Gorleben sediments for understanding their components and physicochemical properties and humic substances by isolation using reverse osmosis (RO) membranes and non-ionic macro porous resin (XAD resin) [16]. Humic substances were characterized of their elemental composition, ultra-violet/visible (UV/Vis) and fluorescence spectroscopic properties, and size distribution. They showed that the properties of aquatic humic substances from different aquifer systems were different each other. Kim et al. also investigated the humic substances in Gorleben groundwater and reported that rare earth elements (REEs), and components which are

susceptible to hydrolysis such as lanthanum and hafnium, were complex with humic acids [17]. In japan, Saito et al. studied nano colloids in granitic groundwater obtained from the Mizunami underground research laboratory (MIU) in terms of their size distribution by flow-field flow fractionation (FFF) with UV/Vis and fluorescence detectors, and inductively coupled plasma mass spectrometry (ICP-MS) [18]. Trace elements, lanthanides, actinides, and heavy metals showed the different size distribution due to association with mainly organic colloids. Kozai et al. analyzed colloids and ions in saline groundwater collected at the Horonobe URL in japan using a size exclusion chromatography (SEC) and ICP-MS [10]. They focused on the speciation of uranium and iodine and revealed that uranium present in the groundwater was associated with low molecular weight silica species with neutral charge.

As described above, property of colloids in groundwater is complicated and intricate. Thus, more accurate information of colloids are required.

**Table I.2 URLs in the world**

| Countries | Facilities |
|---|---|
| United States of America | Yucca mountain exploratory studies facility (ESF) |
| Switzerland | Grimsel test site (GTS) |
| Sweden | Äspö underground hard rock laboratory (HRL) |
| Germany | Gorleben site |
| Finland | Olkiluoto spent nuclear fuel repository (Onkalo) |

### I.1.4 Methodology of studying colloids in groundwater

#### I.1.4.1 Effect of changing in hydrochemical conditions on colloid properties

In general, colloids in groundwater exist under anaerobic and pressurized conditions. Exposure to an atmosphere and pressure release during sampling can lead alteration of colloid property due to changing of groundwater chemistry (Fig. I.4). Thus, a special sampling technique of colloids from groundwater is required avoiding alteration of colloids property and contamination. Hauser et al. developed a mobile Laser-Induced Breakdown Detection (LIBD) system which can conduct in-situ analysis of colloid migration [19]. The migration experiment was carried out in the Grimsel Test Site in Swiss. In order to investigate the role of colloids on the radionuclide migration, bentonite colloids dispersed in granite groundwater were injected into a rock fracture zone. After passing through the fracture, quantification of colloids was conducted. An average size of recovered colloids is slightly decreased from that of before injection. Ledin et al. applied photon correlation spectroscopy (PCS) to understand the concentration and size distribution of colloids in groundwater at the Äspö underground Hard Rock Laboratory, Oskarshamn, Sweden [20]. The on-line and in situ measurements showed that the stability and concentration of colloids in anaerobic groundwater with high Fe(II) concentration were sensitive to exposure to the atmosphere during the sampling. When air was allowed to diffuse into the sample, the size distribution of colloids was changed.

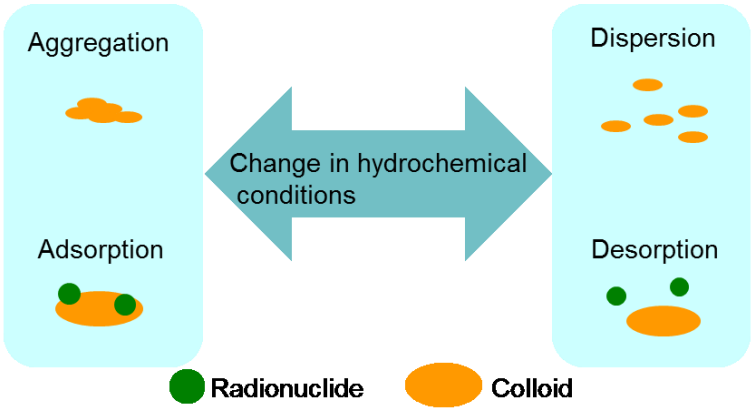


**Fig. I.4 Effect of changing in hydrochemical conditions on colloids property.**

### I.1.4.2 Analytical technique

Analyses of colloids in terms of their size, shape, composition, and concentration were important to understand the colloid property. Analytical techniques for colloids property are summarized in Table I.3. The chemical information is obtained by using inductively coupled plasma atomic emission spectrometry (ICP-AES) and inductively coupled plasma mass spectrometry (ICP-MS). The morphology is observed by using transmission electron microscopy (TEM), scanning electron microscopy (SEM), and Atomic force microscopy (AFM). The elemental information is obtained by using X-Ray spectroscope (EDS). Because SEM can mount EDS, element analysis and morphological analysis can be conducted simultaneously. The size distribution of elements and colloids are evaluated by using field flow fractionation (FFF), size exclusion chromatography (SEC), and membrane filtration. Single particle counter (SPC) [21], photon correlation spectroscopy (PCS), and laser induced breakdown detection (LIBD) were used to evaluate the size distribution of colloids at in-situ. The concentration of organic colloids is measured by ultra-violet and visible spectrophotometry (UV/Vis), and fluorescence spectrophotometry (FL). A functional

group of organic colloids is analyzed by fourier transform infrared spectroscopy (FT-IR) [22] and composition of them is analyzed by pyrolysis gas chromatography coupled with mass spectrometry (Py-GC/MS) [23].

Generally, analyses of organic colloids are less sensitive than that of inorganic colloids due to the difference in instrument performance. Therefore, an extraction technique or condensation technique of organic colloids are widely conducted (I.2.2). As extraction techniques of organic colloids, adsorption resins such as XAD resin [24] and weak anion exchanger resin (DEAE resin) [25] are applied. However, these techniques need acidification and alkalinization of samples to adsorb on the resin and to elute from the resin, and may cause chemical changes of organic colloids. On the other hands, condensation techniques for organic colloids are conducted by RO membranes to prevent chemical changes.

**Table I.3 Analytical techniques for colloid property**

| Analytical techniques | Features |
|---|---|
| Transmission electron microscopy (TEM) [21] | morphological observation<br>high resolution |
| Scanning electron microscopy (SEM) [13,21] | 3-dimensional observation<br>combining with EDS |
| Atomic force microscopy (AFM) [15,21] | 3-dimensional mapping<br>non-destructive |
| X-Ray spectroscope (EDS) [13,21] | element analysis<br>non-destructive |
| Single particle counter (SPC) [21] | in-situ<br>size distribution analysis |
| Photon correlation spectroscopy (PCS) [20,21] | in-situ<br>size distribution analysis |
| Laser induced breakdown detection (LIBD) [19,21] | in-situ<br>size distribution analysis |
| Field flow fractionation (FFF) [18] | size distribution analysis<br>combining with ICP-MS |
| Size exclusion chromatography (SEC) [10] | size distribution analysis<br>combining with ICP-MS |
| Inductively coupled plasma atomic emission spectrometry (ICP-AES) [18] | measuring inorganic concentration |
| Inductively coupled plasma mass spectrometry (ICP-MS) [10,18,19,31] | measuring inorganic substance concentration<br>high sensitive |
| Ultra-violet and visible spectrophotometry (UV/Vis) [10,18] | measuring organic colloid concentration |
| Fluorescence spectrophotometry (FL) [11,18] | measuring organic colloid concentration<br>high sensitive |
| Fourier transform infrared spectroscopy (FT-IR) [22] | functional group analysis of organic colloid<br>facile operating |
| Pyrolysis gas chromatography coupled with mass spectrometry (Py-GC/MS) [22,23] | composition analysis of polymer<br>high sensitive |

### I.1.4.3 Model organic colloids and analogue element

#### I.1.4.3.1 Humic substance

Most of organic colloids in groundwater are considered humic substances. Therefore, humic substances isolated from soil, sediment, peat, coal, and natural water are used as model organic colloids in laboratory experiment. Humic substances are metabolized through natural or biological degradation. They have a wide range of molecular weight and mainly involves aromatic carbon and carboxyl groups [11,26–28]. They have negative charges in their internal structures and adsorb radionuclides. Humic substances can be mainly divided into humic acids and fulvic acids. Humic acids are insoluble at low pH, while fulvic acids are soluble.

#### I.1.4.3.2 Rare earth elements (REEs)

REEs are a set of 15 lanthanides, Sc, and Y. Their chemical property is similar to each other. REEs are useful as tracers for various geochemical process and hydrothermal activity and especially important as analogues of radionuclides, because they have similarities in valence state, speciation, complexation, ionic radius for the radionuclides. Understanding the behavior of radionuclides in natural environment is very difficult, because numbers of sites contaminated radionuclides are very limited. Thus, study using REEs as analogues for artificial radionuclides such as $^{241}$ Am, $^{243}$Am, and $^{244}$Cm is conducted to predict the behavior of radionuclides [29]. Moreover, adsorption of REEs onto colloids in natural environment is studied. Sholkovitz et al. reported that there is large scale fractionation of REEs between colloidal and solution phases in river water and seawater by a filtration technique using UF and microfiltration (MF) membranes. Their results showed that light REEs (LREEs) have higher affinity

for colloids than heavy REEs (HREEs) [30]. Ingri et al. investigated the temporal and seasonal variations of REEs data from weekly sampling of the filtered and suspended particulate phase in the Kalix River, Northern Sweden [31]. They concluded that REEs were associated with both an organic-rich phase (with associated Al–Fe) and a Fe-rich (Fe–oxyhydroxide) inorganic phase, and LREEs had higher affinity for colloids than HREEs same as result of Sholkovitz et al. [30].

## I.2 Separation and condensation technique for colloids study using membrane

### I.2.1 Separation technique using membrane

Membrane filtration can be a very efficient way of separating colloids in a solution. A porous membrane has an ability to separate solutes or dispersions, depending on their physical properties. In general, membranes can be divided into four categories based on their pore sizes; MF membrane, UF membrane, nanofiltration (NF) membrane, and RO membrane (Fig. I.5). An MF membrane can reject micro particles larger than about 0.1 μm, while ions, dissolved organic matter, small colloids, and viruses pass through its pores. An MF membrane is usually used the process of removing microorganisms and pre-treatment for other separation processes. An UF membrane rejects the extremely small particles and macromolecules from fluids, while ions pass through its pores. The primary basis for separation is molecular size and can be defined by the molecular weight cut-off (MWCO). An UF membrane is typically used for pre-filtration of industrial RO plants and condensation of macromolecular. Especially in colloid study, an UF membrane has been widely used as a separation technique to understand the size distribution of colloids and to characterize the elements associated with colloids [9,13,14,25,27,28]. The size distribution of colloids and elements are understood by

comparing their concentrations of the filtered sample and that of the unfiltered sample. Using various UF membranes with different MWCO, the size distribution of colloids is determined in more detail.

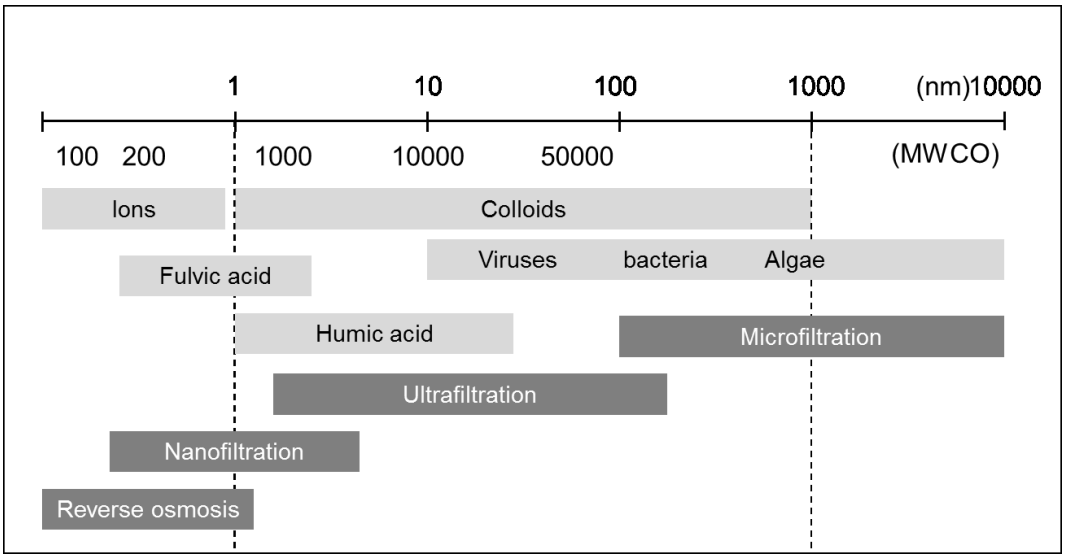


**Fig. I.5 Application range of membranes** [32]**.**

### I.2.2 Condensation technique using membrane

Condensation techniques using porous membranes with dead-end filtration and cross-flow filtration have been widely applied to obtain high concentration colloids (Fig. I.6). In dead-end filtration, all solution is passed through a membrane, resulting that some colloids will deposit on the membrane surface and subsequently block the pores (membrane fouling). On the other hands, in cross-flow filtration, a feed solution flow parallel to a membrane surface, and colloids rejected by the membrane are swept from the membrane surface by the feed flow. The feed flow prevents the accumulation of colloids on the membrane surface. Therefore, cross-flow filtration is more suitable for condensation of colloids than dead-end filtration.

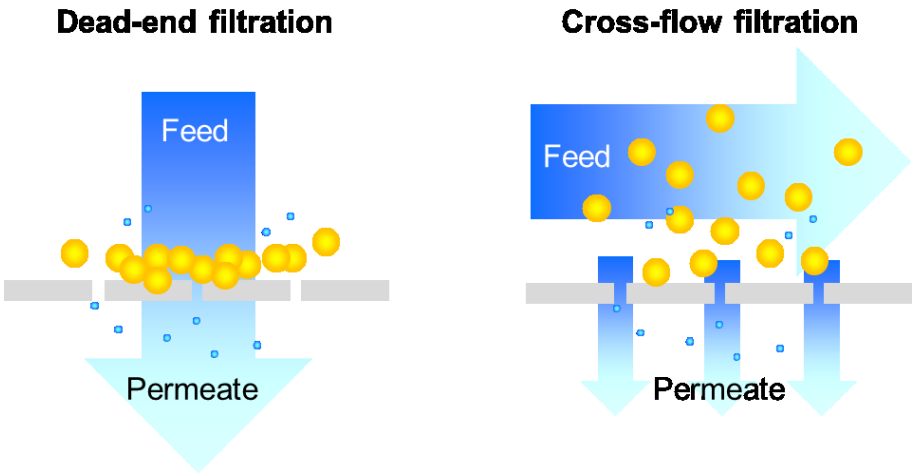


**Fig. I.6 Dead-end filtration and cross-flow filtration.**

As mentioned above, extraction techniques of organic colloids from natural water using adsorption resins are widely applied. However, extracted samples using adsorption resins are exposed to severe chemical disturbances, and there is concern over their chemical changes. On the other hands, condensation techniques of organic colloids using porous membranes do not expose samples to severe chemical disturbances. Some of humic substances with small size, mainly fulvic acid, pass through UF membranes, while not pass through NF and RO membranes. Therefore, NF and RO membranes are suitable for condensation of organic colloids. An RO membrane is a semi-permeable membrane to reject all ions. If two solutions with different concentrations are separated by an RO membrane, solvent will move across the membrane from low concentration solution side to high concentration solution side until the chemical potential of solutions reaches equilibrium. This phenomenon is called osmotic pressure. In RO process, when external pressure overcoming osmotic pressure is applied to high concentration solution side, solvent is forced to flow through the membrane from high to low concentration

solution side. RO membranes are normally rated by their rejection of sodium chloride, while UF are characterized according to MWCO. Condensation techniques of organic colloids using RO membranes were reported by Serkiz et al. and Sun et al. [33,34]. They achieved condensation of organic colloids from a large amount of river water efficiently and rapidly without strong chemical exposure. They recommended using a cation exchange resin as pre-treatment to remove cations that cause precipitation of less-soluble salts onto the membrane surface. RO process can also condense polyvalent cations such as Ca(II), Mg(II), Al(III), and Fe(III), and these condensed inorganic substances reach supersaturation, result in membrane fouling. Although membrane processes are useful, membrane fouling is still a great hindrance for applications based on membrane techniques including separation and condensation process.

NF membranes have separation properties between UF and RO membranes and distinguishing characteristics. NF membranes are low rejection of monovalent ions and high rejection of divalent ions. Thus, NF membrane may prevent the membrane fouling with inorganic substances.

### I.2.3 Membrane fouling

Membrane fouling can be categorized according to forms (Table I.4) and types of fouling material (foulant) (Table I.5). Fouling leads to several problems such as loss of samples, flux decline and long operation time. In particular, loss of sample, which results in interpretation of sample information, is a most severe problem for colloid studies. Therefore, effective control and mitigation of fouling in condensation techniques using membranes are very important to obtain the accurate information of colloids. To prevent membrane fouling, many studies about membrane preparation,

pre-treatment, optimization of operation condition, and surface modification have been conducted. Koo et al. reviewed the effect of factors (membrane morphology, feed water composition, hydrodynamic conditions) on membrane fouling from previous studies [35]. They concluded that a hydrophilic membrane is less susceptible to membrane fouling compared to a hydrophobic membrane. Elimelech et al. reported that a higher ionic strength solution contributes to higher fouling propensity [36]. Tang et al. reported that hydrodynamic conditions such as transmembrane pressure, cross-flow velocity, and permeate flux on the membrane filtration process strongly affect membrane fouling [37]. Moreover, Rana et al. reviewed the modification of membrane surfaces aimed at the reduction of membrane fouling [38].

**Table I.4 Fouling forms** [39]

| Fouling forms | Features |
|---|---|
| Adsorption | interaction between membrane and foulant occurred on the membrane surface or in pores |
| Pore blocking | blocking and clogging the membrane pores partially or fully by foulant |
| Cake layer formation | deposition of the foulant with layer formation on the membrane surface |
| Gel layer formation | formation of gel layer result from concentration polarization near the membrane surface |

**Table I.5 Fouling types** [39]

| Fouling types | Features |
|---|---|
| Inorganic fouling | accumulation of inorganic precipitates which are soluble salt exceed supersaturation |
| Organic fouling | adsorption and deposition of dissolved or colloidal organic matter |
| Colloidal fouling | accumulation of organic or inorganic colloids |
| Biofouling | adhesion and growth of microorganisms |

## I.3 PURPOSE OF THIS THESIS

Understanding the properties of colloids in groundwater is imperative for safety assessment of HLW, because colloids affect the migration process of radionuclides. Colloid studies have been conducted at various geological sites including URL operated by national authorities, and a great deal of useful information of organic and inorganic colloids have been obtained. Moreover, with the development of various analytical apparatuses and techniques, properties of colloids (concentration, size, shape, chemical composition, and interaction with trace elements such as heavy metals, actinides, and rare earth elements) have been understood. However, there are problems in the study of colloids in groundwater as follows.

(a) Properties of colloids in groundwater are sensitively influenced by exposure to the atmosphere and pressure release during sampling.

(b) Colloid concentration is generally very low in groundwater.

The purpose of this thesis is to develop a separation technique which can maintain anaerobic condition under high hydraulic pressure and a condensation technique to

analyze a low concentration of colloids accurately. I tried to develop the separation technique using MF and UF membranes without chemical changes of groundwater and the new condensation technique for organic colloids using NF membranes with cross flow filtration without chemical disturbance. Moreover, I tried to improve the condensation technique using NF membranes by optimization of operating conditions and surface-modification of NF membranes. In this thesis, actual groundwater, obtained from a depth of 300 m at the Mizunami Underground Research Laboratory (MIU) in Japan, was analyzed using above techniques and the properties of colloids in the groundwater were revealed.

**I.4 Scope of this thesis**

This thesis is composed of the five chapters. Each chapter is described briefly as follows:

**Chapter I** introduced the background of this study and summarized the findings reported in previous studies. Finally, the purpose of this thesis was described.

**In Chapter2**, separation technique using microfiltration/ultrafiltration which can maintain in situ physicochemical parameters (mainly hydraulic pressure and anaerobic condition) was developed. The size distribution and composition of colloids in granitic groundwater obtained from a depth of 300 m at the MIU were studied using the microfiltration/ultrafiltration technique without chemical change of groundwater. The shapes and composition of the fractionated colloids collected on the membrane surface were determined by scanning electron microscopy, energy dispersive X-ray spectroscopy, and attenuated total reflection infrared spectroscopy. Additionally, partitioning of REEs based on colloid size was studied using inductively coupled

plasma mass spectrometry (D. Aosai, et al., Colloids and Surfaces A: Physicochemical and Engineering Aspects, 461, 279–286, 2014).

**In Chapter3**, I focused on organic colloids, because results of chapter 2 and another study [40], which conducted speciation analysis of REEs complexes based on thermodynamic calculation, implicated that influence of organic colloids on radionuclides migration is stronger than that of inorganic colloids in the groundwater obtained from at the MIU.

A new condensation technique using NF membranes to condense organic colloids rapidly without chemical disturbance and to reject divalent ions, which may cause inorganic and/or organic fouling, was developed. The condensation performance of NF and RO membranes for aqueous solutions for humic acids was evaluated using a laboratory-scale membrane test unit. The time course of permeate flux and concentration of humic acids were measured. These membranes were applied to the condensation of the groundwater obtained at a depth of 300 m at the MIU. The permeate flux and concentration of major ions and organic colloids were measured. The organic colloids condensed by the NF membrane were successfully analyzed using pyrolysis gas chromatography coupled with mass spectrometry (Py-GC/MS) owing to their high concentrations and low concentrations of salts. (D. Aosai, et al., Colloids and Surfaces A: Physicochemical and Engineering Aspects, 485, 55–62, 2015)

**In Chapter4**, the condensation technique using NF membranes developed in chapter 3 was improved, because some part of components is lost by membrane fouling in chapter 3. Hydrodynamic conditions were optimized, and surfaces of NF membranes were modified using a cationic phosphorylcholine polymer, poly(2-methacryloyloxyethyl phosphorylcholine-co-2-aminoethyl methacrylate) (p(MPC-co-AEMA)), for preventing

membrane fouling and improving condensation efficiency. Aqueous solutions of humic acid and bovine serum albumin (BSA) were used as models of organic colloids, and they were condensed by a laboratory-scale cross-flow filtration apparatus equipped with a commercial NF membrane. The effects of hydrodynamic conditions, such as the applied transmembrane pressure (TMP), stirring rate, and membrane surface modification on condensation efficiency were evaluated.Groundwater, obtained from a depth of 300 m at the MIU, was condensed and the composition of organic colloids in the condensates was analyzed by Py-GC/MS. (D. Aosai, et al., Colloids and Surfaces A: Physicochemical and Engineering Aspects, 495, 68–78, 2016)

**In Chapter5**, findings in this thesis and conclusion were summarized.

**REFERENCES**

[1] Minister of Economy, Trade and Industry, Designated Radioactive Waste Final Disposal Act (Act No. 117 of 2000), 2000.

[2] H. Nitsche, R.C. Gatti, E.M. Standifer, Measured solubilities and speciations of neptunium, plutonium, and americium in a typical groundwater (J-13) from the Yucca Mountain region; Milestone report 3010-WBS 1.2. 3.4. 1.3. 1 (No. LA--12562-MS). Los Alamos National Lab., NM (United States); Lawrence Berkeley Lab., CA (United States), 1993.

[3] J.M. Haschke, and V.M. Oversby, Plutonium chemistry: a synthesis of experimental data and a quantitative model for plutonium oxide solubility. J. Nucl. Mater. 305 (2002) 187–201.

[4] C. Ekberg, G. Meinrath, B. Stromberg, A retraceable method to assess uncertainties in solubility estimations exemplified by a few americium solids. J. Chem. Thermodyn. 35 (2003) 55–66.

[5] A.B. Kersting, D.W. Efurd, D.L. Finnegan, D.J. Rokop, D.K. Smith, J.L. Thompson, Migration of plutonium in ground water at the Nevada Test Site, Nature 397 (1999) 56–59.

[6] W.R. Penrose, W.L. Polzer, E.H. Essington, D.M. Nelson, K.A. Orlandini, Mobility of plutonium and americium through a shallow aquifer in a Semiarid region, Environ. Sci. Technol. 24 (1990) 228–234.

[7] A.P. Novikov, S.N. Kalmykov, S. Utsunomiya, R.C. Ewing, F. Horreard, A. Merkulov, S.B. Clark, V.V. Tkachev, B.F. Myasoedov, Colloid transport of plutonium in the far-field of the Mayak Production Association, Russia, Science 314 (2006) 638–641.

[8] J.F. Mccarthy, J.M. Zachara, Subsurface transport of contaminants–mobile colloids in the subsurface environment may alter the transport of contaminants, Environ. Sci. Technol. 23 (1989) 496–502.

[9] M. Filella, Colloidal properties of submicron particles in natural waters, in: K.J. Wilkinson, J.R. Lead (Eds.), Environmental Colloids and Particles: Behaviour, Separation and Characterisation, Wiley, Chichester (2007) 17–94.

[10] N. Kozai, T. Ohnuki, T. Iwatsuki, Characterization of saline groundwater at Horonobe, Hokkaido, Japan by SEC-UV-ICP-MS: Speciation of uranium and iodine. Water res. 47 (2013) 1570–1584.

[11] R. Artinger, G. Buckau, S. Geyer, P. Fritz, M. Wolf, J.I. Kim, Characterization of groundwater humic substances: influence of sedimentary organic carbon, Appl. Geochem. 15 (2000) 97–116.

[12] C. Degueldre, I. Triay, J.I. Kim, P. Vilks, M. Laaksoharju, N. Miekeley, Groundwater colloid properties: a global approach, Appl. Geochem. 15 (2000) 1043–1051.

[13] P. Vilks, J. Cramer, D. Bachinski, D. Doern, and H. Miller, Studies of colloids and suspended particles, Cigar Lake Uranium Deposit, Saskatchewan, Canada, Appl. Geochem. 8 (1993) 605–616.

[14] M. Laaksoharji, Colloidal particles in deep Swedish granitic groundwater. SKB report AR-90-37, SKB, Stockholm, Sweden 1990.

[15] M. Plaschke, J. Romer, R. Klenze, J.I. Kim, In situ AFM study of sorbed humic acid colloids at different pH. Colloids Surf., A 160 (1999) 269–279.

[16] R. Artinger, B. Kienzler, W. Schüßler, J.I. Kim, Effects of humic substances on the 241Am migration in a sandy aquifer: batch and column experiments with Gorleben groundwater/sediment systems. J. Contam. Hydrol. 35 (1998) 261–275.

[17] J.I .Kim, P. Zeh, B. Delakowitz, Chemical interactions of actinide ions with groundwater colloids in Gorleben aquifer systems. Radiochim. Acta 58 (1992) 147–154.

[18] T. Saito, Y. Suzuki, T. Mizuno, Size and elemental analyses of nano colloids in deep granitic groundwater: Implications for transport of trace elements, Colloids Surf. A: Physiochem. Eng. Aspects 435 (2013) 48–55.

[19] W. Hauser, H. Geckeis, J.I. Kim, Th. Fierz, A mobile laser induced breakdown detection systems and its application for the in site monitering of colloid migrations. Colloids Surf., A 203 (2002) 37–45.

[20] A. Ledin, S. Karlsson, A. Düker, B. Allard, Measurements in situ of concentration and size distribution of colloidal matter in deep groundwaters by photon correlation spectroscopy. Water Res. 288 (1994) 1539–1545.

[21] C. Walther, Comparison of colloid investigations by single particle analytical techniques—a case study on thorium-oxyhydroxides. Colloids Surf., A 217 (2003) 81–92.

[22] X.Q. Lu, J.V. Hanna, W.D. Johnson, Source indicators of humic substances: an elemental composition, solid state 13 C CP/MAS NMR and Py-GC/MS study, Appl. Geochem. 15 (2000) 1019–1033.

[23] H. Iwai, M. Fukushima, M. Yamamoto, T. Komai, Y. Kawabe, Characterization of seawater extractable organic matter from bark compost by TMAH-py-GC/MS, J. Anal. Appl. Pyrolysis 99 (2013) 9–15.

[24] E.M Thurman, R.L Malcom, Preparative isolation of aquatic humic substances, Environ. Sci. Technol. 15 (1981) 463–466.

[25] C.J. Miles, J.R. Tuschall Jr, P.L. Brezonik, Isolation of aquatic humus with diethylaminoethylcellulose. Anal. Chem., 55 (1983) 410–411.

[26] S.W. Krasner, J. Croue, J. Buffle, E.M. Perdue, Three approaches forcharacterizing NOM, J. Am. Water Works Assoc. 88 (1996) 66–79.

[27] J.A. Leenheer, Systematic approaches to comprehensive analyses of naturalorganic matter, Ann. Environ. Sci. 3 (2009) 31–130.

[28] H.Z. Ma, H.E. Allen, Y.J. Yin, Characterization of isolated fractions of dissolvedorganic matter from natural waters and a wastewater effluent, Water Res. 35(2001) 985–996.

[29] N.A. Chapman, J.A. Smellie, Introduction and summary of the workshop. Chemical Geology 55 (1986) 167–173.

[30] E.R. Sholkovitz, Chemical evolution of rare earth elements: fractionation between colloidal and solution phases of filtered river water. Earth and Planetary Science Letters 114 (1992) 77–84.

[31] J. Ingri, A. Widerlund, M. Land, O. Gustafsson, P. Andersson, B. Ohlander, Temporal variations in the fractionation of the rare earth elements in a boreal river; the role of colloidal particles, Chem. Geol. 166 (2000) 23–45.

[32] M. Mulder, Basic principles of membrane technology. Springer Science & Business Media 1996.

[33] S.M. Serkiz, E.M. Perdue, Isolation of dissolved organic matter from the Suwannee River using reverse osmosis, Water Res. 24 (1990) 911–916.

[34] L. Sun, E.M. Perdue, J.F. McCarthy. Using reverse osmosis to obtain organic matter from surface and ground waters, Water Res. 29 (1995) 1471–1477.

[35] C.H. Koo, A.W. Mohammad, M.Z.M. Talib, Review of the effect of selected physicochemical factors on membrane fouling propensity based on fouling indices. Desalination 287 (2012) 167–177.

[36] M. Elimelech, J. Gregory, X. Jia, Particle Deposition and Aggregation: Measurement, Modelling and Simulation, Butterworth-Heinemann Oxford 1995.

[37] C.Y. Tang, Y.N. Kwon, J.O. Leckie, Fouling of reverse osmosis and nanofiltration membranes by humic acid—effects of solution composition and hydrodynamic conditions, J. Membr. Sci. 290 (2007) 86–94.

[38] A.W. Mohammad, Y.H. Teow, W.L. Ang, Y.T. Chung, D.L. Oatley-Radcliffe, N. Hilal, Nanofiltration membranes review: Recent advances and future prospects. Desalination 356 (2015) 226–254.

[39] D. Rana, T. Matsuura, Surface modifications for antifouling membranes, Chem. Rev. 110 (2010) 2448–2471.

[40] Y. Yamamoto, D. Aosai, T. Mizuno, Evaluation of behavior of rare earth elements based on determination of chemical state in groundwater in granite, Proceedings of the ASME 2010 13th International Conference on Environmental Remediation and Radioactive Waste Management, American Society of Mechanical Engineers 2010.

# Chapter II

## Size and composition analyses of colloids in deep granitic groundwater using microfiltration/ultrafiltration while maintaining in situ hydrochemical conditions

---

### II.1 Introduction

In this chapter, in order to understand properties of inorganic colloids, organic colloids, and analogue elements of radionuclides, groundwater was sampled and analyzed by separation technique using porous membrane without hydrochemical disturbance.

Understanding the behavior of elements in underground environments is important for geological disposal of high-level radioactive waste (HLW), carbon dioxide capture and storage, and groundwater pollution. In particular, the migration of radionuclides is of great concern in the geological disposal of HLW. The behavior of elements in underground environments is mainly controlled by groundwater flow, precipitation, diffusion, and interaction with rocks (e.g., adsorption and filtration). Additionally, it has been clearly shown that the migration velocity of elements either increases or decreases in the presence of colloids (particles and macromolecules in the size range from 1 to 1000 nm) [1–4]. Therefore, studying the physicochemical properties (e.g., concentration, size, shape, and chemical composition) of colloids is important for understanding the behavior of elements in underground environments.

Colloids in deep groundwater have been studied in several papers. Degueldre et al. [5] discussed the properties of colloids from various geological formations, ranging

from crystalline to sedimentary, from organic-rich to organic-poor systems, and from subsurface to very deep groundwater. The authors summarized the influence of geochemical conditions, such as pH, redox potential, and concentration of primary ions, on colloid properties. Geckeis et al. [6] reported the size distribution of smectitic colloids and the interaction between humic colloids in groundwater and trace metal ions, such as U, Th, and rare earth elements (REEs), using flow-field flow fractionation (Fl-FFF) combined with online inductively coupled plasma mass spectrometry (ICP–MS). However, there are difficulties in collecting and analyzing colloids in terms of their size, composition, and interaction with trace elements in groundwater because of the low concentrations of colloids in groundwater [7, 8]. To address this issue, enrichment and fractionation techniques based on colloid size have been developed. Saito et al. [9] reported a colloid enrichment technique, first using ultrafiltration, and then using the focusing technique with a large injection loop and the slot flow technique inherent to Fl-FFF. However, the most serious problem is that the physicochemical properties of colloids are likely to change owing to variations in the physicochemical parameters of groundwater, such as pH, redox potential, and hydraulic pressure, and exposure to the atmosphere during sampling [10]. For example, $CO_2$ degassing of groundwater resulting from a decrease in the hydraulic pressure may cause an increase in the pH. Precipitation of metal (hydr)oxides can occur upon oxidation of groundwater. These changes influence the properties of the colloids in groundwater. Thus, a method for collecting and analyzing colloids while maintaining in situ hydrochemical conditions (mainly hydraulic pressure and anaerobic condition) without chemical disturbance is required. Moreover, understanding the interaction between colloids and REEs in natural environments is important; REEs can be regarded as analogues of

trivalent actinides [11]. The hydrogeochemistry of REEs in groundwater has been studied in terms of their usefulness as tracers for various geochemical processes such as water–rock interactions and hydrothermal activity. REEs are known to have high affinities for colloids owing to their large ionic potential (ionic charge/ionic radius) [12–21]. However, the interaction between colloids and REEs is not well understood. Interactions evaluated on a laboratory scale do not necessarily correspond to that measured in in situ experiments possibly because of chemical disturbance. For example, preferential adsorption of heavy REEs (HREEs) onto iron (hydr)oxide colloids has been determined from laboratory experiments [22], whereas preferential adsorption of light REEs (LREEs) onto colloids has been reported in in situ experiments [23–25].

The objectives of this study are to develop a microfiltration/ultrafiltration technique while maintaining in situ hydraulic pressure and anaerobic condition and to understand the partitioning of REEs in the presence of colloids in complex natural environment without chemical disturbance. Using the technique developed herein, we sampled colloids and filtered groundwater in granite at a depth of 300 m that corresponds to the depth of geological disposal sites for HLW according to the Designated Radioactive Waste Final Disposal Act [26]. Moreover, to understand the influence of hydrochemical conditions (mainly hydraulic pressure and anaerobic condition) on colloid properties, the groundwater at a depth of 200 m was exposed to the atmosphere for different periods of time and fractionated by microfiltration/ultrafiltration. This study provides useful information on the size distribution and composition of colloids, and the interaction between colloids and REEs in complex natural environments.

## II.2 Development of the microfiltration/ultrafiltration apparatus

The microfiltration/ultrafiltration apparatus developed in this study consisted of two filter holders: an inlet pressure regulator and an outlet pressure regulator (Fig. II.1). The filter holders were made of stainless used steel (SUS) and designed to maintain anaerobic conditions under high hydraulic pressures (10 MPa). To prevent contamination from SUS, a part of the apparatus that had contact with groundwater was passivated. The concentration of Fe in ultrapure water flowing through the apparatus was less than 0.01 μg/L and that of REEs was less than 0.1 ng/L. The results confirmed that colloid characterization was not influenced by contamination from SUS. Microfiltration/ultrafiltration membranes with different pore sizes were packed into the filter holders. For example, when membranes with pore sizes of 0.45 and 0.01 μm were set into the pre- and post-filter holders, respectively, colloids in the size range of 0.01–0.45 μm were collected. The inlet and outlet pressure regulator valves connected to the filter holders were used to adjust the differential pressure to prevent excess resistance pressure (~0.4 MPa) of the microfiltration/ultrafiltration membrane filter in the filter holder. Thus, though the pressure of groundwater is higher than the resistance pressure of the membrane filter, microfiltration/ultrafiltration can be performed without failure of the membrane filter. The inlet pressure regulator, outlet pressure regulator, and two filter holders were connected using quick-connects (Swagelok, Solon, OH, USA) with double-end shut-off stems to prevent exposure to the atmosphere. Though the filter holders are separated from the inlet and outlet pressure regulators after microfiltration/ultrafiltration, hydraulic pressure and anaerobic condition in the filter holder can be maintained. Following discharge of residual groundwater in the filter holder using inert gas (e.g., Ar), the membrane filters were collected from the filter

holder in an anaerobic chamber purged with an inert gas. The relatively small package size (180 mm × 500 mm × 120 mm; 3.2 kg) of the microfiltration/ultrafiltration apparatus affords easy transport and assembly in underground facilities. Moreover, the present microfiltration/ultrafiltration technique can be conducted under artesian pressure as the driving force without pumping that may cause artificial alteration.

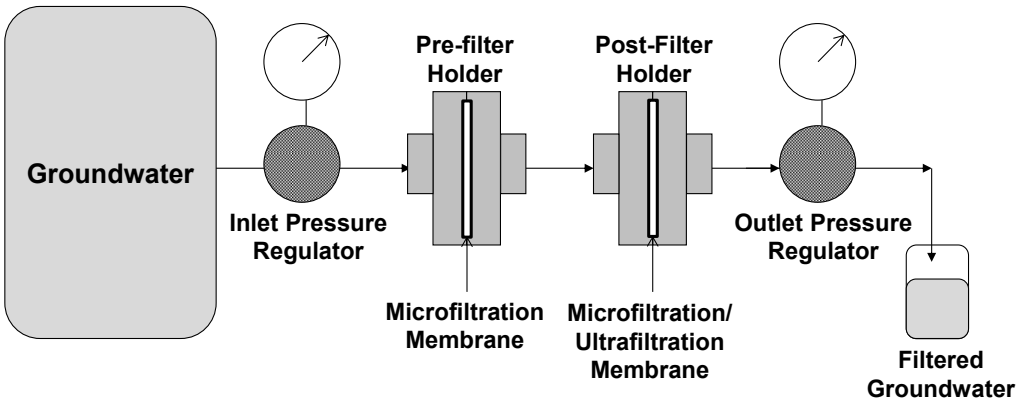


**Fig. II.1 Schematic illustration of the microfiltration/ultrafiltration apparatus operating under pressurized/anaerobic conditions.**

## II.3 Materials and methods

### II.3.1 Sampling point

Groundwater samples were collected from boreholes 07MI07 and 09MI20. 07MI07 and 09MI20 boreholes are both horizontal boreholes with the lengths of 55 and 102 m, respectively, located on the -200 and -300 m access/research galleries of MIU, respectively. The geological site at MIU consists of Cretaceous granitic rocks (Toki granite; ~60–70 Ma) and Miocene sedimentary rocks (Mizunami Group; ~15–20 Ma). The Mizunami Group unconformably overlies the Toki granite at a depth of ~160 m at the MIU site. The 07MI07 and 09MI20 boreholes are designed for investigations of any

hydrochemical changes related to facility construction. The 07MI07 and 09MI20 boreholes are divided into six sections by impermeable packers. The sections are numbered from 1 to 6 according to the distance from the base of the 07MI07 and 09MI20 boreholes. Groundwater samples were collected from each section through nylon tubing without exposure to the atmosphere. The outlet of the nylon tubing was directly connected to the microfiltration/ultrafiltration apparatus developed in this study using quick-connects with a double-end shut-off stem, i.e., a valve was used to simplify connection and disconnection of the microfiltration/ultrafiltration apparatus from the nylon tubing.

### II.3.2 Air exposure experiment

Microfiltration of groundwater samples collected from section 4 of borehole 07MI07 at a depth of 200 m was performed under different exposure times to the atmosphere (0, 180, and 43,200 min) following pressure release. The sample exposed to the atmosphere for 0 min was filtered using the apparatus mentioned above under artesian pressure (~1 MPa). A microfiltration membrane with a pore size of 0.2 μm (H020A047A, Advantec Toyo Kaisha, Ltd., Tokyo, Japan) was used. The samples exposed to the atmosphere for 180 and 43,200 min were filtered using a filter holder (SAKE-142, Advantec Toyo Kaisha, Ltd., Tokyo, Japan) in the laboratory under gas pressure (~0.3 MPa) after exposure to atmosphere and pressure release in a Teflon bottle. A microfiltration membrane with a pore size of 0.2 μm (H020A142C, Advantec Toyo Kaisha, Ltd., Tokyo, Japan) was used.

### II.3.3 Microfiltration/ultrafiltration under maintained in situ conditions

Microfiltration/ultrafiltration of groundwater samples collected from sections 1–6 of borehole 09MI20 at a depth of 300 m was performed using the apparatus mentioned above under artesian pressure. To remove large particles, membrane filters with a pore size of 0.45 μm (A045A047A, Advantec Toyo Kaisha, Ltd., Tokyo, Japan) were fitted into pre-filter holders. A microfiltration membrane with a pore size of 0.2 μm (H020A047A, Advantec Toyo Kaisha, Ltd., Tokyo, Japan) or an ultrafiltration membrane with a molecular weight cut-off (MWCO) of 10 kDa (13622, Merck, Darmstadt, Germany) was used for the post-filter. The filtered volume was 1 L for both types of filtration. The duration of the micro- and ultrafiltration was ~0.5 and 10 h, respectively. The in situ groundwater pressure as displayed on the inlet pressure gauge remained mostly constant and was comparable with the in situ pressure (~2 MPa) during filtration. The differential pressure between the inlet and outlet pressures was adjusted to ~0.3 MPa at the start of filtration, and remained mostly constant during filtration. The dissolved oxygen (DO) was measured by colorimetric method. The DO concentration in the unfiltered groundwater was less than 0.02 mg/L, however, rapidly increased upon exposure to the atmosphere. The DO concentration of groundwater filtered using the microfiltration/ultrafiltration apparatus was less than 0.02 mg/L even after sample collection and differed slightly from that of unfiltered groundwater. This indicates that the hydraulic pressure and anaerobic condition of groundwater are maintained during the filtration process.

### II.3.4 Characterization of colloids

#### II.3.4.1 ICP–MS measurements

The concentrations of Fe and REE in the filtered and unfiltered groundwater were determined by ICP–MS (ELAN DRC-II, PerkinElmer Inc., Waltham, MA, USA). The REE concentrations were determined after preconcentration using chelate resin (Chelate Disc Empore, Sumitomo 3M Ltd., Tokyo, Japan). The calibration curves were constructed from 0.01, 0.05, 0.1, 0.5, 1, 5, and 10 μg/L REE solutions prepared from 10 mg/L REE standard solution (SPEX CertiPrep Ltd. London, UK). Sample preparation and ICP–MS measurements were conducted in a clean room (Class 10,000). The detection limit values of Fe and REEs were 0.01 μg/L and 0.1 ng/L, respectively.

#### II.3.4.2 Scanning electron microscopy–energy-dispersive X-ray spectroscopy

After filtration, the 10 kDa MWCO membrane filters were dried in an anaerobic chamber under Ar atmosphere. The dry membrane filters were coated with Os. The filters were imaged using a field-emission scanning electron microscope (FE–SEM, Quanta 200, FEI Co., Hillsboro, OR, USA) equipped with an energy-dispersive X-ray analyzer (EDX, INCA Energy version 4.05, Oxford Instruments plc., Abingdon, UK) under high vacuum conditions. Sample preparation was performed in a clean room (Class 10,000). The accelerating voltage was 15 kV. The magnification was in the range of 100–40,000×. The equivalent circle diameters of the colloids were calculated by image processing of the obtained backscattered electron images.

### II.3.4.3 Fourier transform infrared spectroscopy

After filtration, the 10 kDa MWCO membrane filters were dried in an anaerobic chamber under Ar atmosphere. Each filter was examined by attenuated total reflection infrared spectroscopy (ATR-FTIR). The ATR-IR spectra (650-4000 $cm^{-1}$) were recorded on a Fourier transform infrared spectrophotometer (Spectrum Spotlight400, PerkinElmer Inc.).

## II.4 Results and discussion

### II.4.1 Air exposure experiment

To understand the influence of the hydrochemical conditions (mainly hydraulic pressure and anaerobic condition) on the colloid properties, filtrations were performed under different exposure times to the atmosphere (0,180, and 43,200 min) following pressure release.

Table II.1 shows the concentration of Fe in the filtered groundwater for different exposure times to the atmosphere. The Fe concentration in the filtered groundwater sample at 180 min was lower than that at 0 min. This indicates that Fe colloids larger than 0.2 μm formed by oxidation within 180 min after sample collection. The Fe concentrations at 180 and 43,200 min were not markedly different, suggesting that the formation of Fe colloids may be a rapid process reaching equilibrium quickly. The results of the Fe concentration indicate that exposure to the atmosphere during filtration impedes on the concentration determination of redox-sensitive elements in the filtered groundwater sample. For instance, Fe colloid formation as a result of oxidation may lead to an overestimation of the colloid size.

Fig. II.2 shows the relative REE concentrations in the filtered groundwater samples

for different exposure times to the atmosphere (180 and 43,200 min) after pressure release. Each concentration was normalized to filtered groundwater at 0 min. The data at 180 and 0 min were not markedly different, suggesting that REEs remained in the <0.2 μm fraction despite formation of Fe colloids. In contrast to the data at 180 min, the REE concentrations in the filtered groundwater sample at 43,200 min were less than those at 0 min, especially for LREEs (La, Ce, Pr, and Nd). This indicates that REE adsorption onto the Fe colloids occurred within 180–43,200 min; however, Fe colloids were formed within 180 min. This discrepancy may be due to the degassing of carbon dioxide from groundwater after pressure release. Carbonate ions can form stable complexes with REEs in groundwater, especially with heavier REEs [27] under both pressurized and anaerobic conditions. Most HREEs–carbonate complexes (<0.2 μm) were stable after 43,200 min. On the other hand, a part of LREE-carbonate complexes (<0.2 μm) might have dissociated within 180–43,200 min upon degassing of carbon dioxide owing to exposure to the atmosphere and pressure release because the stability of LREE-carbonate complexes are weaker than that of HREEs–carbonate complexes. Then, the free ion of LREEs may be adsorbed onto Fe colloids (>0.2 μm). However, this hypothesis was not verified because the concentration of inorganic carbon and pH were not measured. Based on these results, the oxidation of groundwater influenced the size distribution of the REEs though the REEs (except for Ce and Eu) were insensitive to the redox conditions.

**Table II.1 Average concentrations of total Fe in filtered groundwater.**

| | Exposure time | | | | | |
|---|---|---|---|---|---|---|
| | 0 (min) | | 180 (min) | | 43200 (min) | |
| | Avg. | S.D[a] | Avg. | S.D[a] | Avg. | S.D[a] |
| Fe (μg/L) | 5.5 | 0.52 | 3.2 | 0.42 | 2.7 | 0.28 |

[a]The standard deviation of three samples.

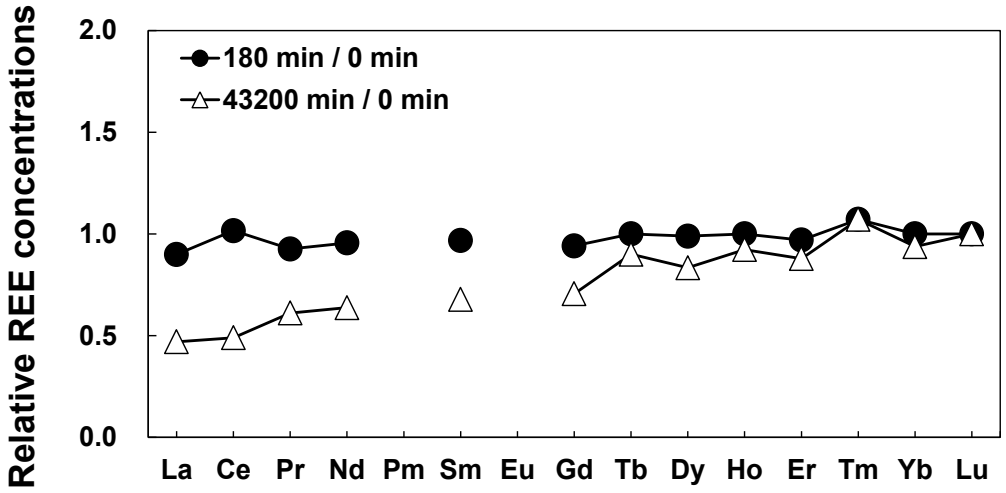


**Fig. II.2 Relative REE concentrations in the filtered groundwater samples at different exposure times to the atmosphere (180 and 43,200 min). Each concentration was normalized to filtered groundwater sample at 0 min.**

### II.4.2 Size distribution of colloids and REE partitioning

The REE concentrations in the unfiltered groundwater of the 09MI20 borehole are shown in Fig. II.3. The groundwater samples collected from all sections contained 0–25 ng/L REEs. The rock–water interaction is the main source of REEs because granitic rocks contain relatively large amounts of REE [28]. The difference in the REE concentrations between the sections suggests spatial variation of REEs. Mizuno et al.

[29] reported that the salinity of groundwater changes according to variations in the flow conditions of groundwater owing to the shaft construction at MIU. Therefore, the spatial variation of REEs may result from the shaft construction as well as the salinity. Moreover, a short sampling time is required to understand the size distribution of colloids and REEs in groundwater during construction of the facilities.

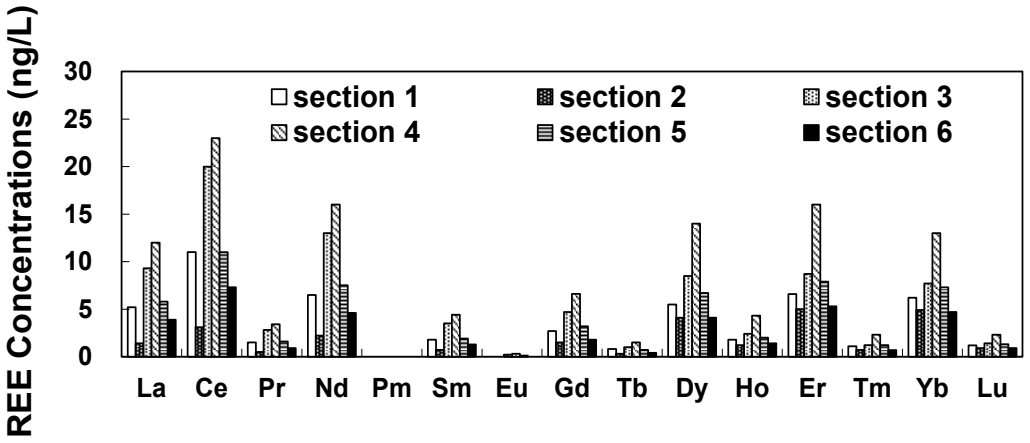


**Fig. II.3 Concentrations of REEs in the groundwater samples collected from all six sections of the 09MI20 borehole.**

Fig. II.4 shows the relative REE concentrations in the filtered groundwater samples collected from the six sections of 09MI20 borehole. The groundwater samples were filtered using membranes with different pore sizes (10 kDa MWCO and 0.2 μm). Each concentration was normalized to the unfiltered groundwater. All samples were collected on July 21, 2011 and July 26, 2011. For samples collected from section 2, the REE concentrations in the filtered groundwater samples were higher than those of the unfiltered groundwater. This was believed to be due to an analytical error during ICP–MS measurements because the REE concentrations of samples from section 2 were

the lowest among samples collected from all sections of 09MI20 borehole and comparable with the detection limit of the ICP–MS instrument. Thus, results relating to samples from section 2 are not discussed. The REE concentrations in the filtered groundwater decreased with decreasing membrane pore sizes (except for sample collected from section 2). The results indicate REE association with colloids present with size ranges of 10 kDa–0.2 μm and 0.2–0.45 μm. About 50% of the REEs present in all sections (except for section 2) associated with colloids with sizes larger than 10 kDa. Preferential association of LREEs with colloids with sizes ranging from 10 kDa to 0.2 μm and from 0.2 to 0.45 μm was observed in samples collected from sections 5 and 6, whereas that of LREEs with colloids with sizes ranging from 0.2 to 0.45 μm was observed in samples collected from section 1. Preferential association of LREEs with colloids, as observed in groundwater, has also been observed in river water [30].

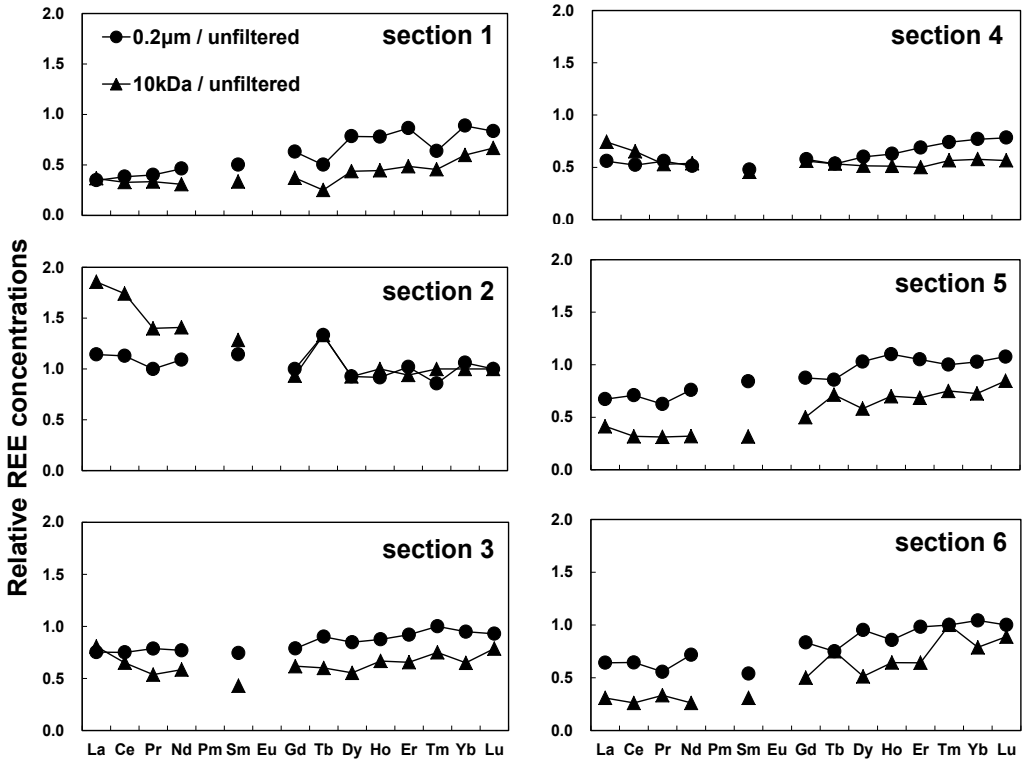


**Fig. II.4 Relative REE concentrations in the filtered groundwater samples collected from all six sections of the 09MI20 borehole. The groundwater samples were filtered using membranes with different pore sizes (10 kDa MWCO and 0.2 μm). Each concentration was normalized to the unfiltered groundwater sample.**

### II.4.3 Size distribution and composition of colloids on the ultrafiltration membrane

Fig. II.5 shows representative SEM images of the inorganic colloids in the groundwater samples collected from all six sections of 09MI20 borehole. The equivalent circle diameters of the inorganic colloids were estimated by image processing of backscattered electron images. For all sections, the equivalent circle diameters of most of the inorganic colloids were in the range of 0.05–0.45 μm. These results were consistent with the size distribution of the colloids estimated from the size distribution of REEs, as mentioned in section II.4.2. In this study, it was difficult to

measure the equivalent circle diameters of colloids smaller than 0.05 μm. High-resolution analysis techniques, such as transmission electron microscopy and atomic force microscopy, are required for such measurements.

Fig. II.6 (a) shows representative SEM images of the inorganic colloids in the groundwater samples collected from all six sections of the 09MI20 borehole and Fig. II.6 (b) shows EDX spectra of the inorganic colloids shown in Fig. II.6 (a). The spectra show the presence of C, O, and S that are from the polysulfone membrane filter. Inorganic particles containing Fe believed to be iron sulfide and iron (hydr)oxide were found in samples collected from sections 1 and 3. Inorganic particles containing Al, Si, alkaline earths, and alkaline earth metals were found in samples collected from sections 2, 5, and 6. Inorganic particles containing Al and Mg were found in samples collected from section 4. These particles are believed to be fragments of either granite or clay minerals. Because Fe (hydr)oxide and clay minerals have high affinities for REEs [14–18], inorganic colloids seem to form complexes with the REEs.

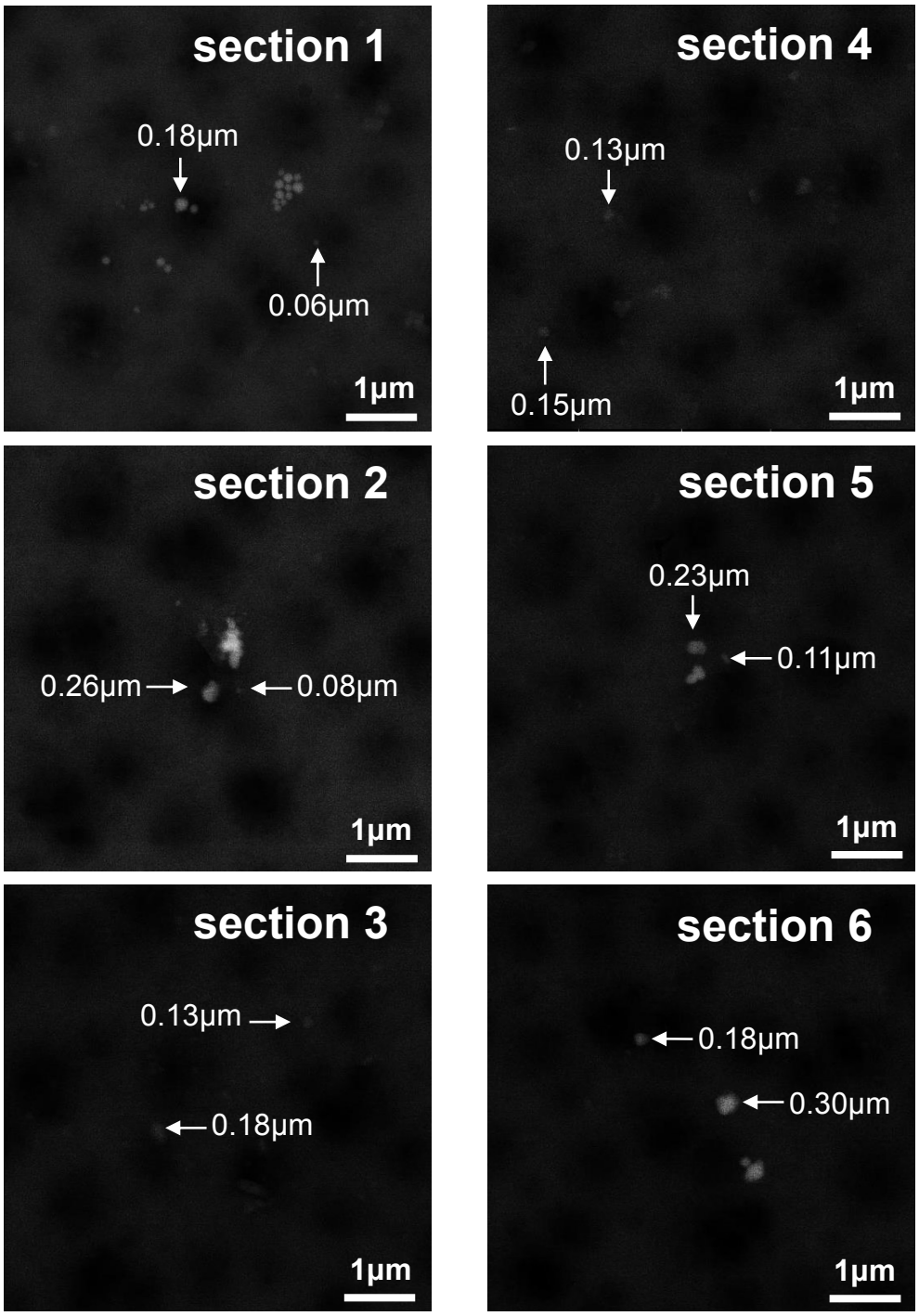


**Fig. II.5 Representative SEM images of inorganic colloids in the groundwater samples collected from all six sections of the 09MI20 borehole. The equivalent circle diameters of several colloids are shown.**

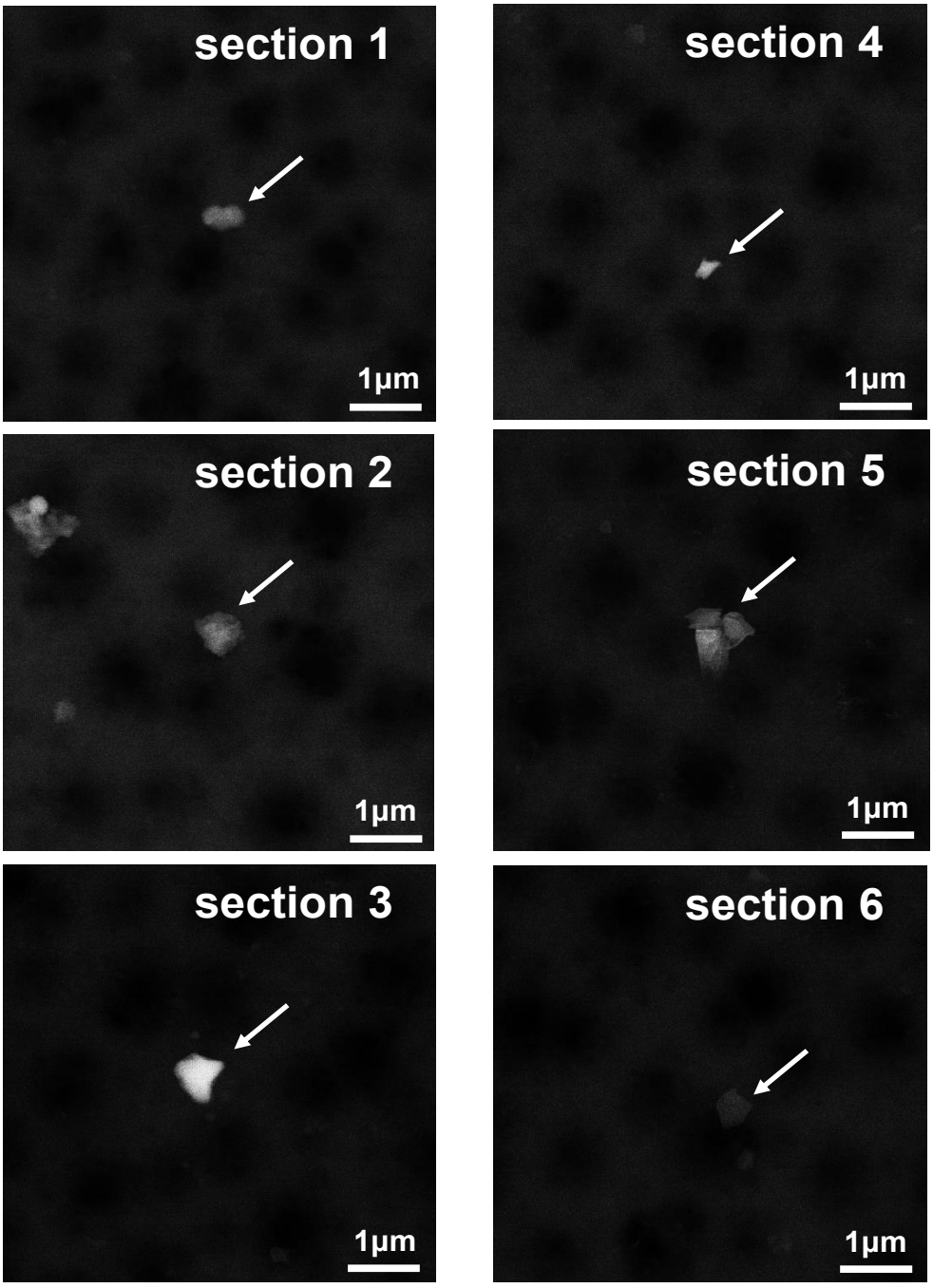


**Fig. II.6(a) Representative SEM images of inorganic colloids in the groundwater samples collected from all six sections of the 09MI20 borehole.**

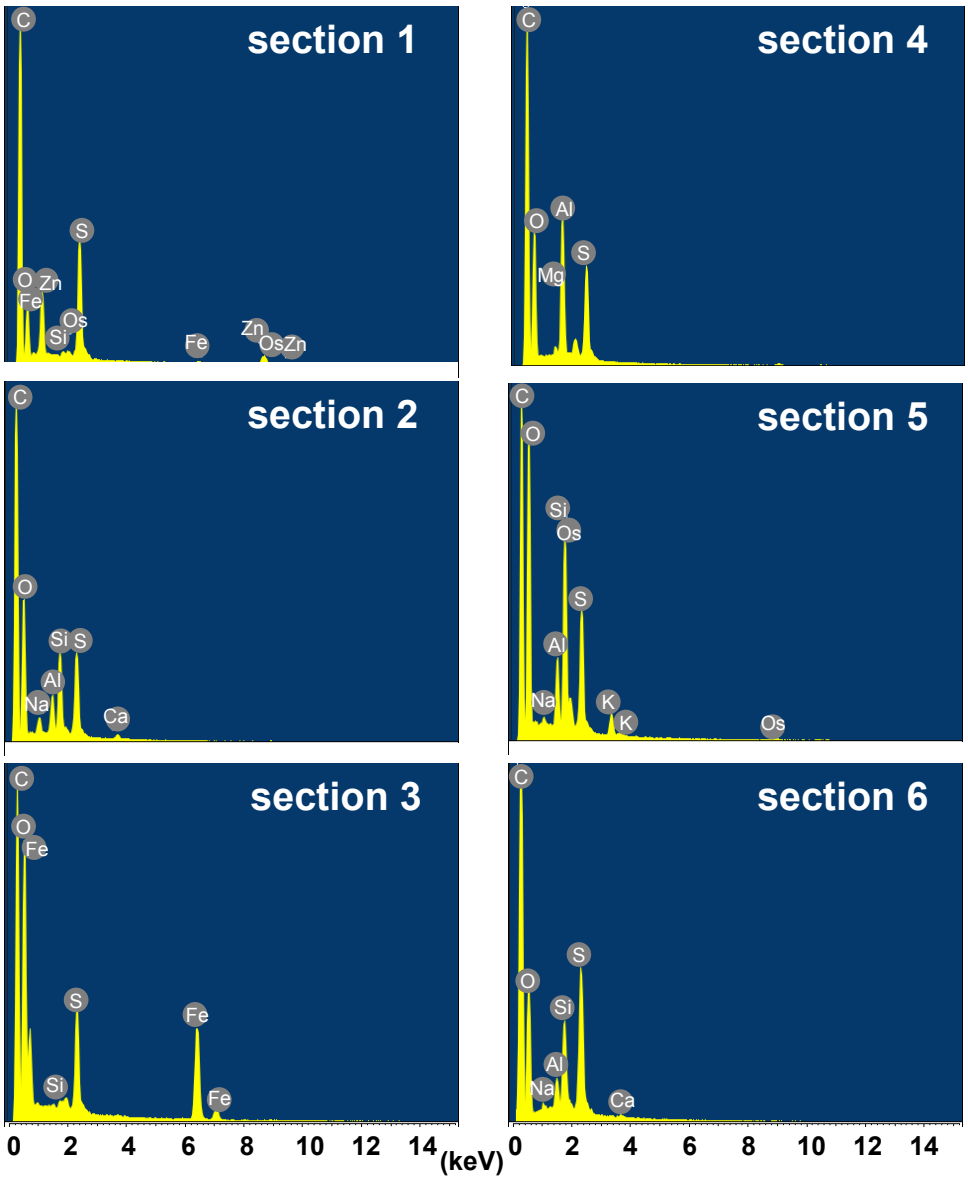


**Fig. II.6(b) Representative EDX spectra of the inorganic colloids shown in Fig. II.6 (a).**

Vilks et al. [31] reported that organic colloids with a range of sizes were present together with inorganic colloids. Thus, the effect of organic colloids on partitioning of REEs was considered. Identification of organic matter by SEM was difficult because the membrane filter was made of an organic substance. To confirm the presence of organic matter, IR analysis was performed. The FTIR spectra of all six sections and the Suwannee River humic acid standard (2S101H, International Humic Substances Society) are shown in Fig. 7. All FTIR spectra were characterized by a number of absorption bands, exhibiting varying relative intensities. The strong broad band at 2400–3700 $cm^{-1}$ is generally attributed to O–H stretching of hydroxyl groups involved in hydrogen links, carboxyl groups, and phenol groups. The band at 3292 $cm^{-1}$, which was weak in the humic acid spectrum, was attributed to the N–H stretch absorption band of amines and amides [32,33]. There were also a few absorption bands at 2923 and 2853 $cm^{-1}$. These bands were assigned to C–H stretching of methyl ($CH_3$) and methylene ($CH_2$) groups of aliphatic chains [34–36]. The bands at 1730 and 1701 $cm^{-1}$ are generally attributed to C=O stretching vibrations, mainly of carboxyl groups and, to a lesser extent, of ketones and aldehydes [34–36]. The band at 1644 $cm^{-1}$, which was absent from the humic acid spectrum, was ascribed to C=C stretching of aromatic rings [37] and C=O stretching vibration in amides (amide I band) [38]. The band at 1605 $cm^{-1}$, which was absent from the spectra in all groundwater samples, was ascribed to stretching of the C=C group conjugated with another C=C group (aromatic ring), C=O and/or $COO^-$ in unsaturated ketones, carboxylic acids, and amides [39]. The band at 1545 $cm^{-1}$, which was absent from the humic acid spectrum, was ascribed to NH bending in secondary amides (amide II band) [38]. All samples exhibit broad bands in the region 1000–1300 $cm^{-1}$, which are probably because of the C–O stretching vibration

in alcohols, ethers, phenols, carboxylic acids, and esters [38, 40]. For the groundwater samples collected from all sections of the borehole, it was difficult to detect absorption bands in the region of 650–1400 $cm^{-1}$ because of the strong absorption bands of the blank.

The FTIR spectra of organic matter present in samples collected from all sections showed similar shapes and intensities, suggesting that all sections of the 09MI20 borehole were similar structures. Some differences were observed between the FTIR spectra of organic matter and humic acid. Although the organic matter showed some absorption bands relating to nitrogen, such as absorption bands at 1545, 1644, and 3292 $cm^{-1}$, these absorption bands were weak or different from those of humic acid. These differences indicated that the nitrogen content of the organic matter in the groundwater samples collected from all sections of the borehole was greater than that of humic acid. Previous studies reported that most of the REEs in groundwater bound to humic substances by forming stable complexes [41]. Organic matter present in 09MI20 borehole may associate with REEs as well as inorganic colloids.

Vilks et al. [31] reported that inorganic colloids consisting of clay minerals, ferrioxide, and carbonate minerals were present in a wide size range with organic matter in groundwater. Saito et al. [9] reported that Al-, Mg-, and Fe-bearing colloids associated with organic matter at a depth of 300 m at the MIU site. Additionally, in this study, we reveal that organic matter in groundwater associated with inorganic colloids and clarified the structures of organic matter. Although the results obtained from this study are qualitatively similar to those of previous studies [9, 31], our results may give more useful information owing to the newly developed sampling technique that can be operated under in situ hydrochemical conditions.

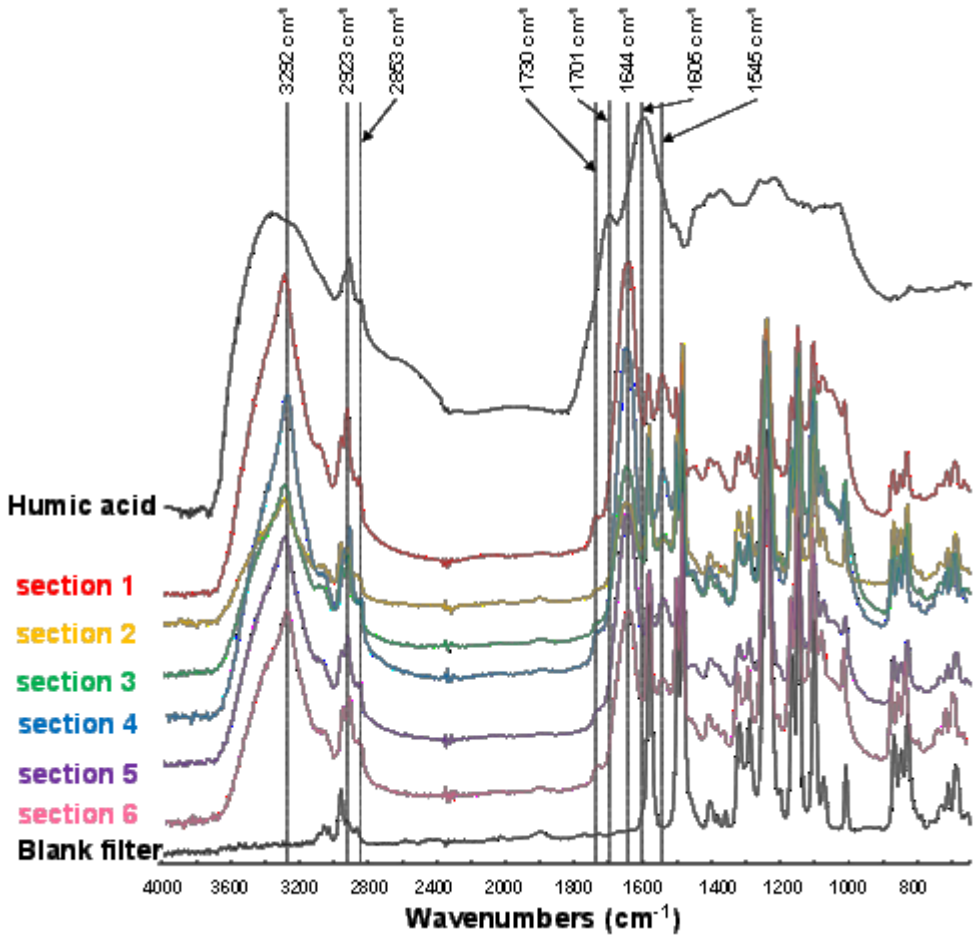


**Fig. II.7 FTIR spectra of the reference humic acid and organic colloids in the groundwater samples collected from all six sections of the 09MI20 borehole. FTIR spectra of the reference humic acid and organic colloids in the groundwater samples collected from all six sections of the 09MI20 borehole.**

## II.5 Conclusions

In this study, we developed a microfiltration/ultrafiltration technique that can maintain in situ physicochemical parameters and afford collection of colloids without chemical disturbance. The microfiltration/ultrafiltration technique can solve some of the uncertainties regarding colloid properties such as size distribution and interaction with REEs.

Using the microfiltration/ultrafiltration technique developed in this study, we obtained useful information on the presence of inorganic (e.g., Fe, Al, Mg, and Si) and organic colloids with a wide size range, and REEs characteristic partitioning in granite groundwater at a depth of 300 m. The latter depth corresponds to that of geological disposal sites for high-level radioactive waste. The inorganic colloids are primary minerals (i.e. fragments of granites) or secondary minerals such as clay minerals resulting from dissolution and precipitation of the host rock. Moreover, the findings indicated the co-existence of inorganic and organic colloids, and colloids bound metal ions. REEs characteristic partitioning, such as preferential association of LREEs with colloids with sizes ranging from 10 kDa to 0.2 μm and from 0.2 to 0.45 μm in a specific section of borehole, may be due to the influence of the wide variety of colloids. In future studies, we will investigate the effect of these colloids on radioactive behaviors using combined microfiltration/ultrafiltration technique and bulk analyses.

REFERENCES

[1] A.B. Kersting, D.W. Efurd, D.L. Finnegan, D.J. Rokop, D.K. Smith, J.L. Thompson, Migration of plutonium in ground water at the Nevada Test Site, Nature 397 (1999) 56–59.

[2] W.R. Penrose, W.L. Polzer, E.H. Essington, D.M. Nelson, K.A. Orlandini, Mobility of plutonium and americium through a shallow aquifer in a Semiarid region, Environ. Sci. Technol. 24 (1990) 228–234.

[3] G.J. Moridis, Q. Hu, Y.S. Wu, G.S. Bodvarsson, Preliminary 3-D site-scale studies of radioactive colloid transport in the unsaturated zone at Yucca Mountain, Nevada, J. Contam. Hydrol. 60 (2003) 251–286.

[4] A.P. Novikov, S.N. Kalmykov, S. Utsunomiya, R.C. Ewing, F. Horreard, A. Merkulov, S.B. Clark, V.V. Tkachev, B.F. Myasoedov, Colloid transport of plutonium in the far-field of the Mayak Production Association, Russia, Science 314 (2006) 638–641.

[5] C. Degueldre, I. Triay, J.I. Kim, P. Vilks, M. Laaksoharju, N. Miekeley, Groundwater colloid properties: a global approach, Appl. Geochem. 15 (2000) 1043–1051.

[6] H. Geckeis, T.N. Manh, M. Bouby, J.I. Kim, Aquatic colloids relevant to radionuclide migration: characterization by size fractionation and ICP-mass spectrometric detection, Colloids Surf. A: Physiochem. Eng. Aspects 217 (2003) 101–108.

[7] J. Gaillardet, J. Viers, B. Dupré, Trace Elements in River Waters, in: J.I. Drever (Ed.), Treatise on Geochemistry, Elsevier, Amsterdam (2003) 225–272.

[8] M. Plaschke, J. Romer, J.I. Kim, Characterization of Gorleben groundwater colloids

by atomic force microscopy, Environ. Sci. Technol. 36 (2002) 4483–4488.

[9] T. Saito, Y. Suzuki, T. Mizuno, Size and elemental analyses of nano colloids in deep granitic groundwater: Implications for transport of trace elements, Colloids Surf. A: Physiochem. Eng. Aspects 435 (2013) 48–55.

[10] C. Degueldre, M. Bolek, Modelling colloid association with plutonium: The effect of pH and redox potential, Appl. Geochem. 24 (2009) 310–318.

[11] N. Chapman, J Smellie, Introduction and summary of the workshop, Chem. Geol. 55(3-4) (1986) 167–173.

[12] J.W. Tang, K.H. Johannesson, Speciation of rare earth elements in natural terrestrial waters: assessing the role of dissolved organic matter from the modeling approach, Geochim. Cosmochim. Acta 67 (13) (2003) 2321–2339.

[13] Y. Yamamoto, Y. Takahashi, H. Shimizu, Systematic change in relative stabilities of REE-humic complexes at various metal loading levels, Geochem. J. 44 (2010) 39–63.

[14] F.J. Millero, Stability constants for the formation of rare earth-inorganic complexes as a function of ionic strength, Geochim. Cosmochim. Acta 56(8) (1992) 3123–3132.

[15] M. Bau, Scavenging of dissolved yttrium and rare earths by precipitating iron oxyhydroxide: experimental evidence for Ce oxidation, Y-Ho fractionation, and lanthanide tetrad effect, Geochim. Cosmochim. Acta 63 (1) (1999) 67–77.

[16] A. Ohta, I. Kawabe, REE(III) adsorption onto Mn dioxide (δ-MnO2) and Fe oxyhydroxide: Ce(III) oxidation by δ-MnO2, Geochim. Cosmochim. Acta 65(5) (2001) 695–703.

[17] F. Coppin, G. Berger, A. Bauer, S. Castet, M. Loubet, Sorption of lanthanides on

smectite and kaolinite, Chem. Geol. 182 (2002) 57–68.

[18] Y. Takahashi, A. Tada, H. Shimizu, Distribution pattern of rare earth ions between water and montmorillonite and its relation to the sorbed species of the ions, Anal. Sci. 20(9) (2004) 1301–1306.

[19] M. Leybourne, W. Goodfellow, D. Boyle, G. Hall, Rapid development of negative Ce anomalies in surface waters and contrasting REE patterns in groundwaters associated with Zn–Pb massive sulphide deposits, Appl. Geochem. 15(6) (2000) 695–723.

[20] B. Nelson, S. Wood, J. Osiensky, Partitioning of REE between solution and particulate matter in natural waters: a filtration study, J. Solid State Chem. 171(1-2) (2003) 51–56.

[21] P. Rönnback, M. Åström, J. Gustafsson, Comparison of the behaviour of rare earth elements in surface waters, overburden groundwaters and bedrock groundwaters in two granitoidic settings, Eastern Sweden, Appl. Geochem. 23(7) (2008) 1862–1880.

[22] L. Congqiang, W Jiahong, Y Wenhui, Controls of interactions between iron hydroxide colloid and water on REE fractionations in surface waters: Experimental study on pH-controlling mechanism, Science in China (Series D) 45 (2002) 449–458.

[23] H. De Baar, M. Bacon, P. Brewer, Rare-earth distributions with a positive Ce anomaly in the Western North Atlantic Ocean, Nature 301 (1983) 324–327.

[24] E. Sholkovitz, Chemical evolution of rare earth elements: fractionation between colloidal and solution phases of filtered river water, Earth Planet. Sci. Lett., 114 (1992) 77–84.

[25] H. Elderfield, R. Upstill-Goddard, E. Sholkovitz, The rare earth elements in rivers, estuaries, and coastal seas and their significance to the composition of ocean waters, Geochim. Cosmochim Acta, 54 (1990) 971–991

[26] Minister of Economy, Trade and Industry, Designated Radioactive Waste Final Disposal Act (Act No. 117 of 2000) (2000) [in Japanese].

[27] J. Tang, K. Johannesson, Controls on the geochemistry of rare earth elements along a groundwater flow path in the Carrizo Sand aquifer, Texas, USA, Chem. Geol., 225(1-2) (2006) 156–171.

[28] Y. Takahashi, H. Yoshida, N. Sato, K. Hama, Y. Yusa, H. Shimizu, W- and M-type tetrad effects in REE patterns for water-rock systems in the Tono uranium deposit, central Japan, Chem. Geol. 184 (2002) 311–335.

[29] T. Mizuno, D. Aosai, S Shingu, H. Hagiwara, Y. Yamamoto, A. Fukuda, Hydrochemical changes associated with construction of Mizunami Underground Research Laboratory, Transactions of the Atomic Energy Society of Japan 12 (2013) 89-102.

[30] J. Ingri, A. Widerlund, M. Land, O. Gustafsson, P. Andersson, B. Ohlander, Temporal variations in the fractionation of the rare earth elements in a boreal river; the role of colloidal particles, Chem. Geol. 166(1–2) (2000) 23–45.

[31] P. Vilks, J. Cramer, D. Bachinski, D. Doern, and H. Miller, Studies of colloids and suspended particles, Cigar Lake Uranium Deposit, Saskatchewan, Canada, Appl. Geochem. 8 (1993) 605–616.

[32] H.C. Kim, M.J. Yu, Characterization of natural organic matter in conventional water treatment processes for selection of treatment processes focused on DBPs control, Water Res. 39 (2005) 4779–4789.

[33] J.P. Simjouw, E.C. Minor, K. Mopper, Isolation and characterization of estuarine dissolved organic matter: comparison of ultrafiltration and C-18 solid-phase extraction techniques. Mar. Chem. 96 (2005) 219–235.

[34] R.M.B.O. Duarte, A.C. Duarte, Application of non-ionic solid sorbents (XAD resins) for the isolation and fractionation of water-soluble organic compounds from atmospheric aerosols, J. Atmos. Chem. 51 (2005) 79–93.

[35] V.I. Esteves, M. Otero, A.C. Duarte, Comparative characterization of humic substances from the open ocean, estuarine water and fresh water, Org. Geochem. 40 (2009) 942–950.

[36] P.S.M. Santos, M. Otero, R.M.B.O. Duarte, A.C. Duarte, Spectroscopic characterization of dissolved organic matter isolated from rainwater, Chemosphere 74 (2009) 1053–1061.

[37] S. Nagao, T. Iwatsuki, K. Hama, Characteristics of dissolved humic substances isolated from groundwater in Tono area, Gifu Prefecture, Japan, J. Nucl. Fuel Cycle Environ. 15 (2008) 2 (in Japanese).

[38] R.M. Silverstein, F.X. Webster, in: Spectrometric Identification of Organic Compounds, sixth ed., John Wiley & Sons, Inc., Canada. (1997).

[39] I. Simkovic, P. Dlapa, S.H. Doerr, J. Mataix-Solera, V. Sasinkova, Thermal destruction of soil water repellency and associated changes to soil organic matter as observed by FTIR spectroscopy, Catena 74 (2008) 205–211.

[40] J. Tarchitzky, O. Lerner, U. Shani, G. Arye, A. Lowengart-Aycicegi, A. Brener, Y. Chen, Water distribution pattern in treated wastewater irrigated soils: hydrophobicity effect, Eur. J. Soil Sci. 58 (2007) 573–588.

[41] J.P.L. Dearlove, G. Longworth, M. Ivanovich, J.I. Kim, B. Delakowitz, P. Zeh, A

study of groundwater-colloids and their geochemical interactions with natural radionuclides in Gorleben aquifer systems, Radiochim. Acta 52/53 (1991) 83–89.

# Chapter III

## Concentration and characterization of organic colloids in deep granitic groundwater using nanofiltration membranes for evaluating radionuclide transport

### III.1 Introduction

Result of chapter II implicated that influence of organic colloids on radionuclides is stronger than inorganic colloids in the deep granitic groundwater. Thus study in chapter III focused on organic colloids.

Colloids, such as particles and macromolecules ranging from 1 to 1000 nm in size, are widespread in various natural water sources [1]. Groundwater contains inorganic colloids, such as fragments of rock and clay minerals from dissolution and precipitation of the rock, and organic colloids such as humic substances [2-5]. Additionally, it has been clearly shown that the migration velocity of radionuclides can either increase or decrease in the presence of colloids [6-11]. Therefore, investigation of the physicochemical properties (e.g., concentration, size, shape, and chemical composition) of colloids is of great importance for geological disposal of high-level radioactive waste (HLW). In particular, the detailed structures of organic colloids, which have more complex structures than inorganic colloids, are not yet well understood.

Organic colloids, most of which are humic substances, are metabolized through natural or biological degradation, and involve mainly aromatic carbon and carboxyl groups [12-15]. Organic colloids have negative charges in their internal structures and

adsorb radionuclides in groundwater. Although field investigations have been conducted to understand the effect of organic colloids on radionuclide transport [16,17], precise analysis of organic colloids in groundwater is difficult owing to their low concentrations [18,19]. To solve this issue, groundwater concentration techniques using adsorption resins [20,21] and reverse osmosis (RO) membranes [22,23] have been attempted. Although the method using adsorption resins concentrates samples into disproportionately enriched organic colloids, the samples are exposed to severe chemical conditions, resulting in chemical or physicochemical changes of the organic colloids. The method using RO membranes can concentrate organic colloids highly efficiently and rapidly without strong chemical exposure. However, this method requires sample pretreatment using a cation exchange resin to remove cations that cause precipitation onto the membrane surface [22,23]. This pretreatment using a cation exchange resin affects the composition of rare earth elements (REEs) in the sample, which are regarded as analogues of trivalent actinides [24] and are important for HLW analysis.

In this study, we propose a novel concentration method using nanofiltration (NF) membranes, which can be operated rapidly without chemical disturbance, and does not require additional sample treatment such as cation exchange. NF membranes are generally looser than RO membranes [25]. Typically, monovalent ion rejection of NF membranes is not very high, while multivalent ions can be rejected at high levels. To compare the concentration performance of membranes with different properties, an aqueous solution of commercial humic acid was concentrated as a model of organic colloids using two types of NF membranes and an RO membrane. The recovery yield of humic acid was measured using a UV-vis spectrophotometer. Then, we sampled

groundwater in granite at a depth of 300 m and concentrated the groundwater using the membranes. To confirm the applicability of this method for groundwater, concentrations of cations and anions in both the concentrate and permeate water were measured by ion chromatography (IC). To characterize the chemical structures of the concentrated organic colloids, the concentrate water was analyzed by pyrolysis gas chromatography coupled with mass spectrometry (Py-GC/MS). Py-GC/MS is commonly used to obtain detailed structural information on the components of natural organic matter, although salt removal is required [26]. Moreover, REE concentrations in the concentrated groundwater enriched by the two types of NF membranes and the RO membrane were measured by inductively coupled plasma mass spectrometry (ICP-MS).

## III.2 Materials and methods

### III.2.1 Materials for performance evaluation of NF and RO membranes

Two types of commercial NF membranes (NTR7410 and NTR7450; Nitto Denko, Osaka, Japan) composed of sulfonated polyethersulfone and a commercial RO membrane (ES20; Nitto Denko, Osaka, Japan) composed of aromatic polyamide were used. The properties of the membranes are shown in table III.1. All solutions used in this study were prepared using ultrapure water and analytical-grade chemicals. Humic acid derived from peat (H16752; Sigma-Aldrich, St. Louis, MO, USA) was used after the following pretreatment process. The humic acid was dissolved in a NaOH solution (pH 10) and the pH was adjusted to 1 with a HCl solution to remove fulvic acid and heavy metals. The sample was centrifuged to remove ash, and then the residue was freeze-dried. The elemental composition of this humic acid has been previously

reported: 55.5% C, 38.9% O, 4.6% H, and 0.6% N [27]. This humic acid has been used extensively as a model organic colloid by many researchers [28-31] owing to its easy availability and well-characterized properties.

**Table III.1 Properties of membranes.**

| Membrane | Material | NaCl Rejection [%][a] |
|---|---|---|
| NTR7410 | Sulfonated polyethersulfone | 15 |
| NTR7450 | Sulfonated polyethersulfone | 51 |
| ES20 | Aromatic polyamide | 99.7 |

[a] Nominal value.

### III.2.2 Groundwater sampling

Groundwater was collected from the 09MI20 borehole in the −300 m access/research gallery of Mizunami Underground Research Laboratory (MIU) on December 25, 2014. The Miocene sedimentary rocks (Mizunami Group) unconformably overlie the Cretaceous granitic rocks (Toki granite) at a depth of ~160 m at the MIU site. The groundwater in the granite was weakly alkaline Na–(Ca)–Cl-type, and the salinity increased with depth as a result of mixing of deeply lying saline water with recharged meteoric water [32]. The 09MI20 borehole is a horizontal borehole with a length of 102 m and was designed for investigations of hydrochemical changes related to facility construction. The borehole is divided into six sections by impermeable packers and the sections are numbered from 1 to 6 according to the distance from the base of the borehole. Groundwater samples were collected from section 1. Hydrochemistry of the groundwater is summarized in Table III.2.

**Table III.2 Hydrochemistry of groundwater sampled from 09MI20 borehole section 1 at a depth of 300 m on December 25, 2014.**

| pH | EC | $Na^+$ | $K^+$ | $Ca^{2+}$ | $Cl^-$ | $F^-$ | $SO_4^{2-}$ | Mg | Al | Fe | Mn |
|---|---|---|---|---|---|---|---|---|---|---|---|
| | [mS/m] | [mg/L] | [mg/L] | [mg/L] | [mg/L] | [mg/L] | [mg/L] | [mg/L] | [mg/L] | [mg/L] | [mg/L] |
| 8.5 | 43 | 76 | 0.4 | 9.0 | 64 | 9.8 | 13 | 0.11 | <0.01 | <0.005 | <0.003 |

| Dissolved inorganic carbon | Dissolved organic carbon | M-Alkalinity |
|---|---|---|
| [mg/L] | [mg/L] | [meq/L] |
| 13 | <0.5 | 1.19 |

### III.2.3 Concentration apparatus

A laboratory-scale cross-flow concentration apparatus was used to concentrate aqueous solutions (Fig. III.1) [33]. A feed solution was fed into a membrane cell using a plunger pump (NPL-120; Nihon Seimitsu Kagaku Co., Tokyo, Japan) with a constant flow rate of 9.0 mL/min. The applied pressure was maintained at 1.5 MPa using a back pressure valve. The effective area of sample membranes was 8.0 $cm^2$. The permeate solution was collected in a permeate reservoir. The feed solution was recycled into the feed reservoir and was concentrated from 500 mL to a minimum of 25 mL. The feed solution side of the membrane cell was magnetically stirred at 150 rpm. The permeate flux was calculated from the weight gain.

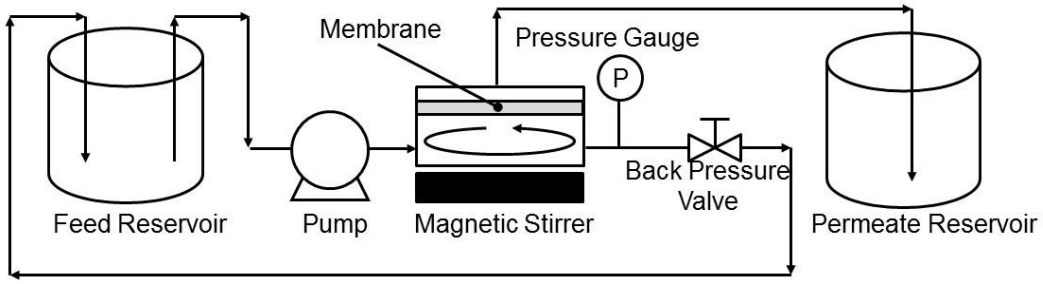


**Fig. III.1 Schematic diagram of the cross-flow concentration apparatus**

### III.2.4 Concentration test of humic acid

A feed solution of 1 mg/L of humic acid was used. The recovery yield was evaluated through the concentration ratio of humic acid in the feed solution before and after the concentration test. The concentration of the humic acid was measured using a UV-vis spectrometer at 254 nm (V-650; Jasco Corp., Tokyo, Japan).

### III.2.5 Concentration of groundwater

The groundwater was concentrated from 500 mL to 25 mL using the NF membranes (NTR7410, NTR7450) and from 500 mL to 80 mL using the RO membrane (ES20). Organic colloid concentration was calculated on the assumption that all organic colloids were humic acid. The recovery yield of organic colloids was evaluated by using the organic colloid concentrations in the concentrated solution and raw solution. Cationic species ($Na^+$, $K^+$, $Ca^{2+}$) and anionic species ($F^-$, $Cl^-$, $SO_4^{2-}$) in the concentrate and permeate water of the groundwater were analyzed by ion chromatography (ICS-3000; Dionex Corp., Sunnyvale, CA, USA). For cation separations, an IonPac CS16 (250 × 5 mm, Dionex Corp.) analytical column and IonPac CG16 (50 × 5 mm, Dionex Corp.) guard column were used, and the eluent was $CH_3SO_3H$. For anion separations, an IonPac AS18 (250 × 4 mm, Dionex Corp.) analytical column and IonPac AG18 (50 × 4 mm, Dionex Corp.) guard column were used, and the eluent was KOH. REE concentrations in the raw and concentrated groundwater were measured by ICP-MS (Agilent 7000x; Agilent Technologies Inc., Palo Alto, CA, USA). The REE isotopes monitored with ICP-MS were $^{139}La$, $^{140}Ce$, $^{141}Pr$, $^{146}Nd$, $^{149}Sm$, $^{151}Eu$, $^{157}Gd$, $^{159}Tb$, $^{163}Dy$, $^{165}Ho$, $^{166}Er$, $^{169}Tm$, $^{172}Yb$, and $^{175}Lu$. The calibration curves were constructed from 1, 5, 10, 50, 100, and 500 ng/L REE

solutions prepared from a 10 mg/L REE standard solution (SPEX CertiPrep Ltd., London, UK). The detection limit values of the REEs were 1 ng/L. After concentration of the groundwater, membranes were dried and analyzed by attenuated total reflectance Fourier transform infrared spectroscopy (ATR-FTIR). These measurements were carried out using a Nicolet iS5 FT-IR spectrometer with an iD5 diamond advanced attenuated total reflectance attachment (Thermo Fisher Scientific, Waltham, MA, USA).

### III.2.6 Characterization of concentrated organic colloids

The groundwater concentrated by NF7450 was further evaporated, dried under $N_2$, and analyzed by Py-GC/MS. The Py-GC/MS analysis was performed using a double-shot pyrolyzer (PY-2020id; Frontier Laboratories Ltd., Fukushima, Japan) attached to a GC/MS instrument (Agilent 6890N/Agilent 5973; Agilent Technologies Inc., Palo Alto, CA, USA) with a DB-5ms fused silica column (30 m × 0.25 mm i.d. × 0.25 μm film thickness, Agilent Technologies Inc.). The sample was heated at 600 °C for 1 min, and the evolved gases were then directly injected into the GC/MS instrument for analysis. Helium was used as a carrier gas at a constant flow of 1 mL/min. The column temperature was programmed from 40 to 300 °C at 10 °C/min and held at 300 °C for 15 min. The mass spectrometer was operated in electron impact ionization mode with an ionizing energy of 70 eV. Compound identification was based on comparisons of the mass spectra and relative retention times with those in the NIST and Wiley library databases.

## III.3 Results and discussion

### III.3.1 Concentration of model humic acid

Fig. III.2 shows the time courses of the permeate flux and humic acid concentration in the concentrated solutions in the concentration tests using the three types of membranes (NTR7410, NTR7450, and ES20). In this figure, the calculated concentrations in the concentrated solutions with 100% recovery yield are plotted as red dotted lines. Fig. III.3 shows the relationship between the humic acid concentration in the concentrated solution and the concentration magnification. The concentration magnification is defined as the volume of the raw solution divided by that of the concentrated solution. The dotted lines in these figures show the calculated relationships in the case of 100% recovery yield. The concentration test using NTR7410 showed the highest initial permeate flux followed by an immediate decrease (Fig. III.2a and 3a). The humic acid concentrations in concentrated solutions were below the dotted line, indicating low recovery yields. The recovery yield at 20-fold concentration was only 26%. The decrease in the permeate flux and the low recovery yield were probably due to the membrane fouling caused by humic acid. Large amounts of the humic acids were adsorbed on the membrane surface and reduced the water permeation. On the other hand, the water flux hardly decreased throughout the concentration test using NTR7450, and the recovery yield of humic acid at 20-fold concentration was as high as 81% (Fig. III.2b and 3b). Although the two membranes are basically composed of the same material, sulfonated polyethersulfone, the tendencies of the flux changes were clearly different, suggesting that the high initial flux causes severe flux decline and low recovery yield of humic acid. This result is consistent with those of previous studies [29-31,33], which reported that humic acid

fouls membranes via a hydrodynamic drag force caused by the water flux toward a membrane surface. The concentration using ES20 hardly showed a permeate flux decrease and achieved the highest recovery yield of 90% at 20-fold concentration (Fig. III.2c and 3c). Although the initial fluxes of NTR7450 and ES20 were similar, the difference in the membrane materials, sulfonated polyethersulfone of NTR7450 and aromatic polyamide of ES20, probably affected the membrane fouling by humic acid.

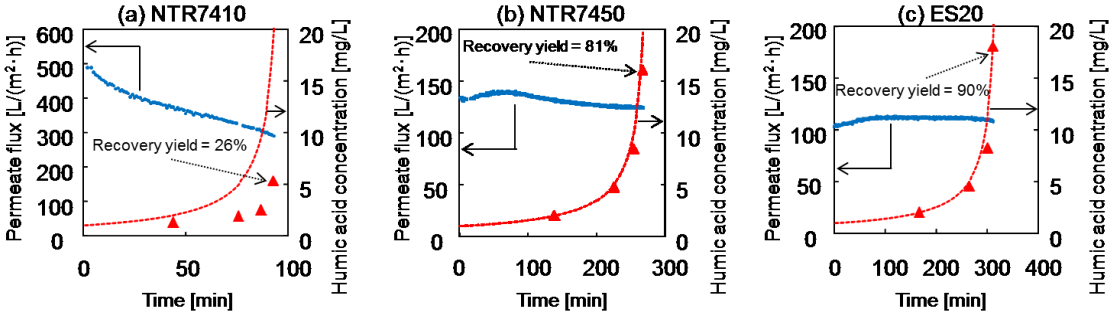


**Fig. III.2 Time courses of the permeate fluxes and humic acid concentrations in the concentrated solutions in the concentration tests of humic acid with (a) NTR7410, (b) NTR7450, and (c) ES20. Blue circles and red triangles indicate permeate flux and humic acid concentration, respectively. Red dotted lines indicate calculated concentrations if recovery yield = 100%.**

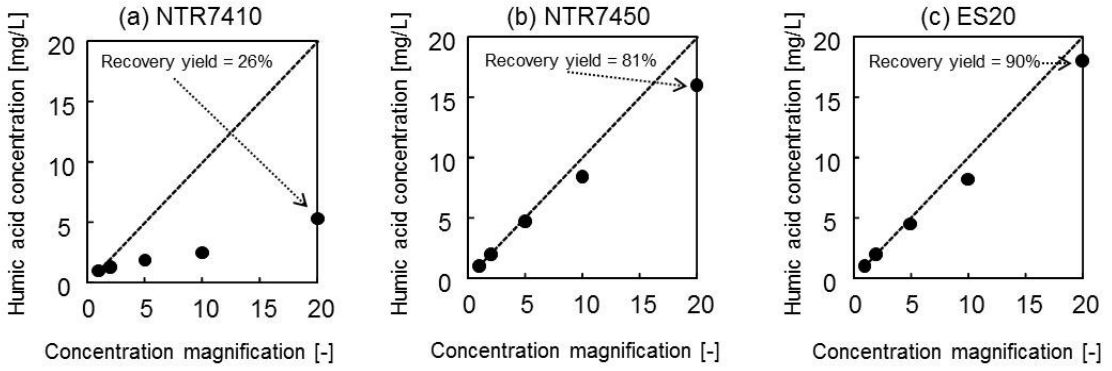


**Fig. III.3 Relationship between the humic acid concentration in the concentrated solution and the concentration magnification of (a) NTR7410, (b) NTR7450, and (c) ES20. Dotted lines indicate the calculated concentration if recovery yield = 100%.**

### III.3.2 Concentration of groundwater

#### III.3.2.1 Concentration of organic colloids in groundwater

Fig. III.4 shows the time courses of the permeate flux and organic colloid concentration in the concentrated solutions in the groundwater test. Fig. III.5 shows the relationship between the organic colloid concentration in the concentrated solution and the concentration magnification. The permeate flux of NTR7410 decreased slightly throughout the concentration test, and the recovery yield of the organic colloids at 20-fold concentration was only 8.8% (Fig. III.4a and 5a). The permeate flux decline and low recovery yield were considered to be due to organic colloid fouling, similar to the case of the humic acid experiment. In the case of using NTR7450, the recovery yield at 20-fold concentration was 57%, and the initial permeate flux was maintained throughout the concentration test (Fig. III.4b and 5b). In the case of using ES20, the permeate flux was constant for approximately 300 min, and then declined suddenly over the twofold concentration (Fig. III.4c and 5c). Therefore, it was difficult to concentrate the solution to more than 6-fold concentration. This drastic decline in the permeate flux did not occur in the concentration test of model humic acid. Therefore, it is suggested that inorganic substances in the groundwater precipitate on the membrane surface and bring about the permeate flux decline. This will be discussed in section 3.2.2.

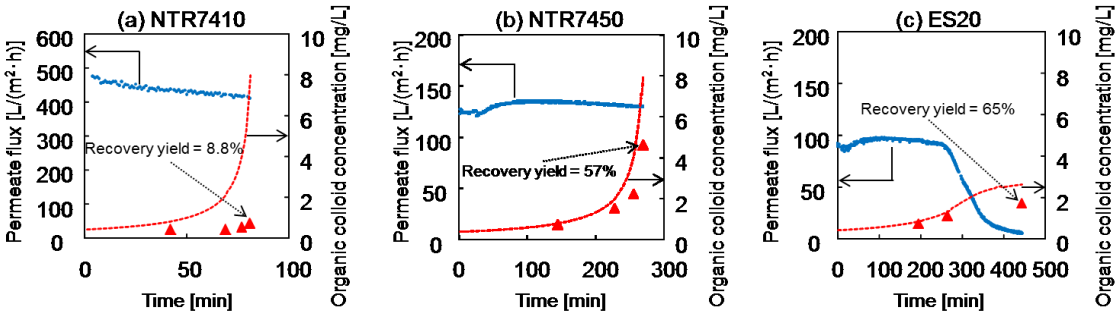


**Fig. III.4 Time courses of the permeate fluxes and organic colloid concentrations in the concentrated solutions in the concentration tests of the groundwater using (a) NTR7410, (b) NTR7450, and (c) ES20. Blue circles and red triangles indicate permeate flux and humic acid concentration, respectively. Red dotted lines indicate the calculated value if recovery yield = 100%.**

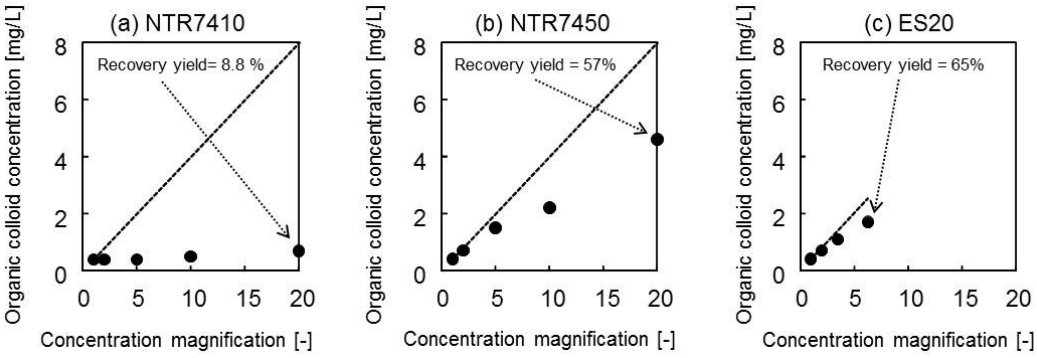


**Fig. III.5 Relationship between the organic colloid concentration in the concentrated solution and the concentration magnification of (a) NTR7410, (b) NTR7450, and (c) ES20. Dotted lines indicate the calculated value if recovery yield = 100%.**

### III.3.2.2 Effect of inorganic substances on concentration of organic colloids

To understand the effect of the inorganic substances on the recovery yield of the organic colloids and the decline of the permeate flux, the concentrations of major ions $Na^+$, $K^+$, $Ca^{2+}$, $Cl^-$, $F^-$, and $SO_4^{2-}$ in both the concentrated and permeate solutions from the groundwater were measured. As shown in Table III.1, since the major components of the groundwater were $Na^+$, $K^+$, $Ca^{2+}$, $Cl^-$, $F^-$, and $SO_4^{2-}$, we measured these ion concentrations. Fig. III.6 shows the relationship between the cation concentrations in

both the concentrated and the permeate solutions and the concentration magnification in the concentration tests using the three types of membranes. Fig. III.7 shows the results of the anions. The dotted lines in both figures represent the calculated concentrations in the case of 100% recovery yield. In the case of using NTR7410, the concentrations of all ions in the permeate solution and concentrated solution were approximately equal, suggesting that these ions were not rejected by this membrane (Fig. III.6a and 7a). In the NTR7450 test, although the concentrations of monovalent ions in the permeate solution were slightly lower than those in the concentrated solution, the concentrations of $Ca^{2+}$ and $SO_4^{2-}$ increased more than those of monovalent ions (Fig. III.6b and 7b). On the other hand, for ES20, most ions were not detected in the permeate solution and recovery yields were almost 100% except for $Ca^{2+}$ and $F^-$ in the regions of high concentration magnification (Fig. III.6c and 7c). This result indicates that $Ca^{2+}$ and $F^-$ may form less-soluble salts such as $CaCO_3$ and $CaF_2$, and precipitated on the membranes when the concentrations exceeded the supersaturation values.

The FTIR spectra of the membrane surfaces after the concentration test are shown in Fig. III.8. A strong broad band at 1400 $cm^{-1}$ was observed in the FTIR spectrum of ES20, but not in the spectra of NTR7410 and NTR 7450. The strong broad band was generally attributed to $CO_3$ [34]. This result indicates that $CaCO_3$ precipitated on ES20. However, it was difficult to confirm the precipitation of $CaF_2$, because $CaF_2$ shows no band. A previous study reported that less-soluble salts were supersaturated by membrane concentration, precipitated on the membrane surface, and blocked the membrane pore [22,23]. Moreover, the high calcium concentration induces severe membrane fouling in the presence of humic acid. Increasing calcium concentrations

significantly reduces negative net charges of humic acids [27,29-31,35], resulting in a more compact, energetically stable conformation [35,36]. In addition, $Ca^{2+}$ ions bridge humic acid molecules [37]. Thus, the bridged humic acid molecules caused by the increased $Ca^{2+}$ concentration accelerated the membrane fouling. Therefore, in the concentration test using ES20 with high rejection properties, it is suspected that $Ca^{2+}$ was concentrated over the supersaturation value by concentration polarization and precipitated on the membrane surfaces, resulting in the sudden flux decrease shown in Fig. III.4c.

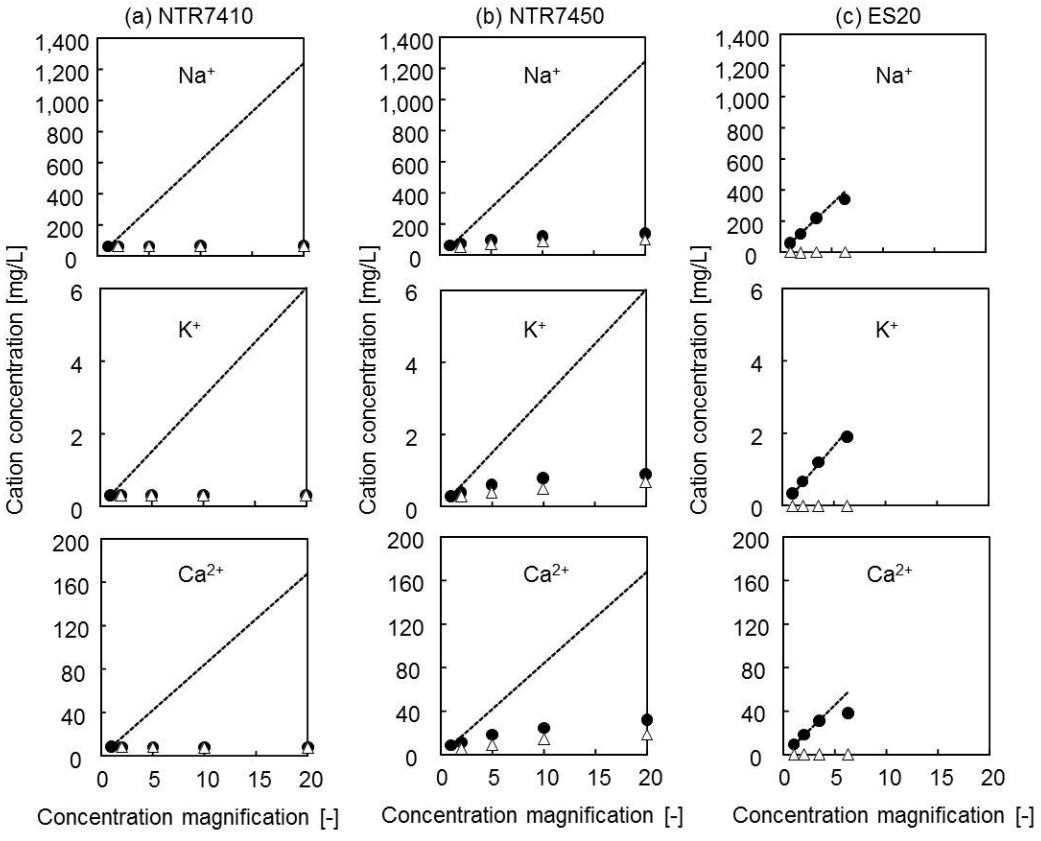


**Fig. III.6 Relationship between the cation concentrations in both the concentrated and permeate solutions from groundwater and the concentration magnification in the concentration tests using (a) NTR7410, (b) NTR7450, and (c) ES20. Black circles and white triangles indicate the concentration in the concentrate and permeate, respectively. Dotted lines indicate the calculated value if recovery yield = 100%.**

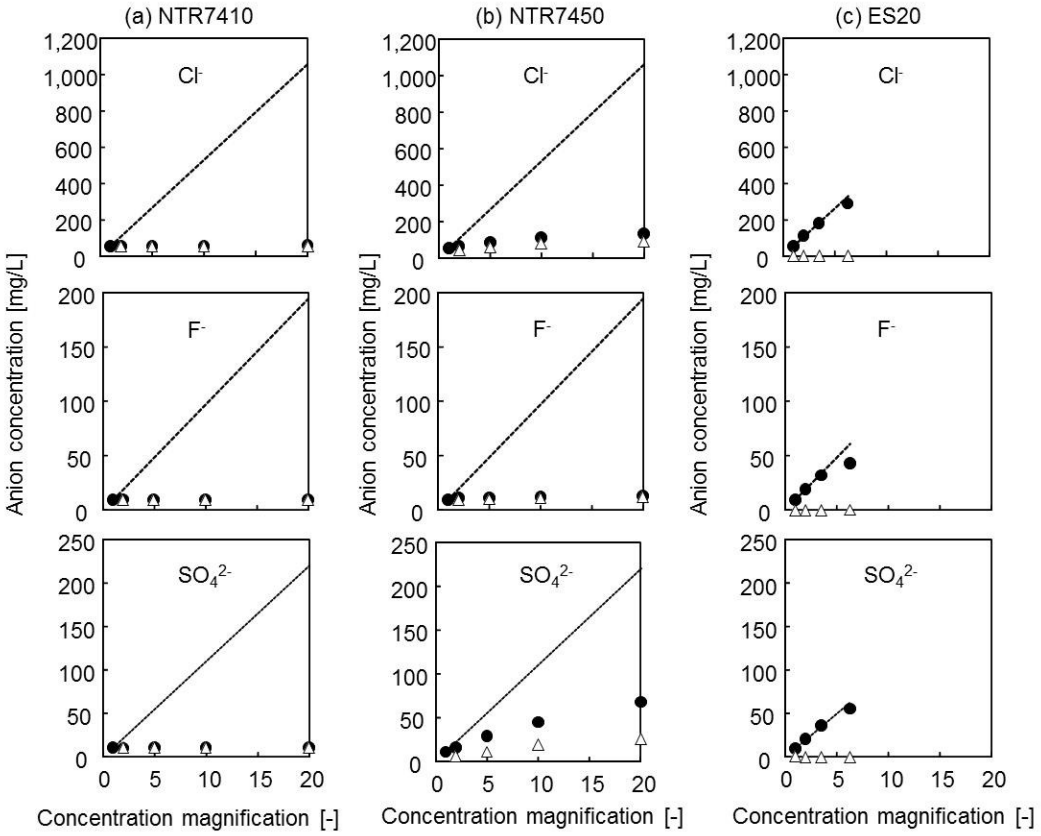


**Fig. III.7 Relationship between the anion concentrations in both the concentrated and permeate solutions from groundwater and the concentration magnification in the concentration tests using (a) NTR7410, (b) NTR7450, and (c) ES20. Black circles and white triangles indicate the concentration of the concentrate and permeate, respectively. Dotted lines indicate the calculated value if recovery yield = 100%.**

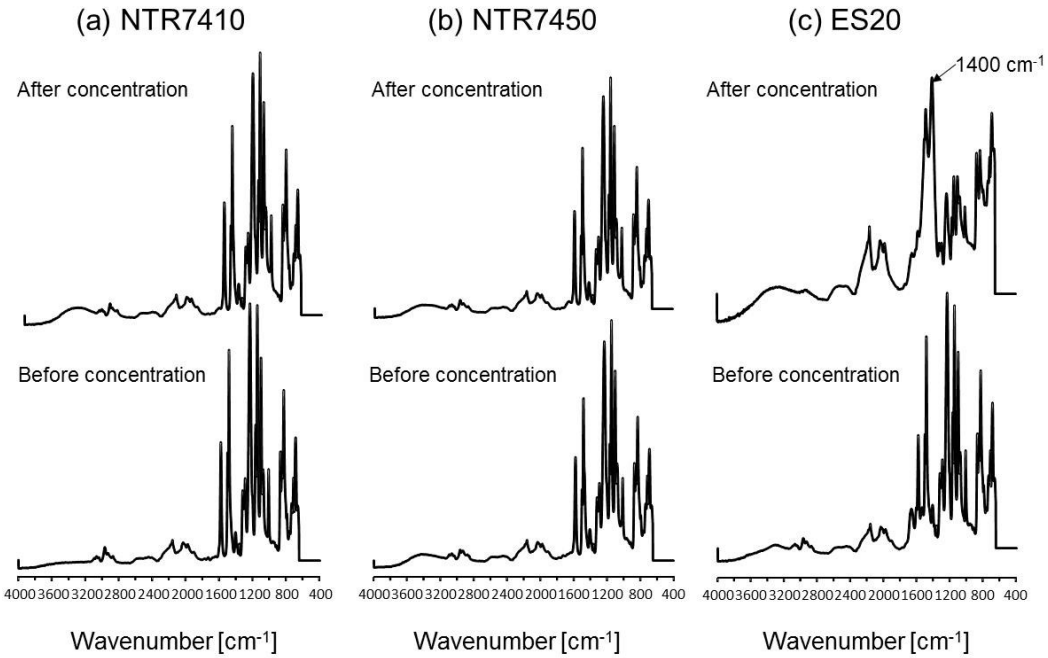


**Fig. III.8 FTIR spectra of the membrane surfaces after the concentration tests of groundwater using (a) NTR 7410, (b) NTR7450, and (c) ES20.**

### III.3.2.3 Applicability of NF and RO membranes for concentration of organic colloids

As shown in Fig. III.5, organic colloids were concentrated from 0.4 mg/L to 1.7 mg/L using ES20. However, it was difficult to concentrate further owing to the precipitation of the concentrated inorganic substances on the membrane surfaces and the fouling of the organic colloids caused by concentrated $Ca^{2+}$. In the case of using NTR7410, organic colloids were only concentrated from 0.4 mg/L to 0.7 mg/L owing to organic fouling caused by the high initial permeate flux. In the case of using NTR7450, the organic colloids were concentrated from 0.4 mg/L to 4.6 mg/L with high recovery yield due to prevention of concentration polarization by removing ions. The NTR7450 membrane has high applicability for concentration of organic colloids in groundwater because of the moderate initial permeate flux and ion rejection.

### III.3.2.4 Structure of organic colloids

The organic colloids in the concentrated groundwater samples were analyzed by Py-GC/MS. The samples concentrated by NTR7410 or ES20 were not applied to Py-GC/MS due to their low concentrations of organic colloids and/or high concentrations of salts. The Py-GC/MS pyrogram of the organic colloid in the groundwater concentrated by NTR7450 is presented in Fig. III.9. More than 30 compounds were detected, which are listed in Table III.3. Most of the compounds are the same as those detected in previous pyrolysis studies of humic substances from soil, peat, lignites, and aquatic sources [38-41]. The main pyrolysis compounds can be identified by source polymer such as carbohydrates, proteins, lignin, and lipids [42]. As shown in Fig. III.9, pyrolysis compounds arising from carbohydrates such as furan and its derivatives were not detected, while trace amounts of N-containing compounds (n = 1, 10) arising from proteins were detected. Phenol (n = 10) and alkyl phenols (n = 14) arising from lignin-derived subunits in wood material [43,44] were weakly detected. The series of aliphatic compounds (n = 3, 7, 11, 16, 19, 21, 24, 26) arising from polymethylene structures such as lipids with long aliphatic chains and paraffinic material was detected, but relatively weakly. Thus, the major pyrolysis products of organic colloids were aromatic products. Lu et al. [42] reported that a high abundance of aromatic products indicates high humification, and carbohydrates are lost during humification. Therefore, it is suspected that most parts of the organic colloid structures in deep groundwater were similar to humic substances with high humification. The concentration method using NTR7450 enabled the analysis of organic colloids in groundwater without adsorption resins or cation exchange, which affect the REE composition.

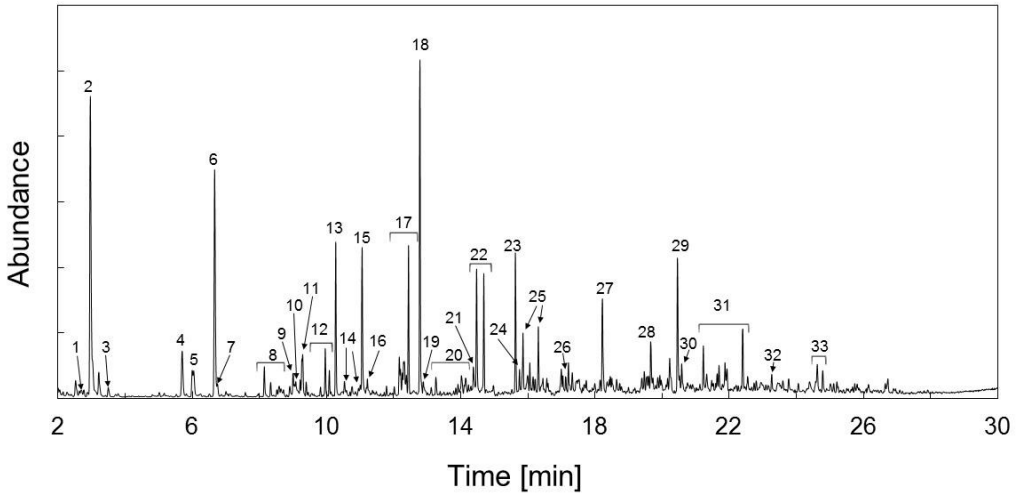


**Fig. III.9 Py-GC/MS pyrogram of organic colloids in groundwater concentrated by NTR7450. Peak numbers are shown in Table III.3.**

### III.3.2.5 Concentration of REEs

For concentrated groundwater, the composition of REEs was measured. Table III.4 shows the REE concentrations in the raw and concentrated groundwater in the concentration tests using the three types of membranes. Some REE concentrations in the groundwater concentrated by NTR7450 and ES20 could be detected by ICP-MS, while those in the raw groundwater were lower than the detection limit. Although the obtained REE concentrations were not very high, NTR7450 could concentrate the samples to much higher concentrations for a longer time for a more accurate analysis. Thus, this concentration method would be promising for concentrating organic colloids and REEs in groundwater efficiently and for understanding the interaction between organic colloids and REEs.

**Table III.3 Typical pyrolysis compounds of organic colloids in groundwater concentrated by NTR7450**

| Peak No. | Compound | Group |
|---|---|---|
| 1 | Pyrrole | N-containing |
| 2 | Toluene | aromatic |
| 3 | Octene | aliphatic carbon |
| 4 | Ethylbenzene | aromatic |
| 5 | Xylene | aromatic |
| 6 | Styrene | aromatic |
| 7 | Nonene | aliphatic carbon |
| 8 | $C_3$-Alkylbenzene | aromatic |
| 9 | Methylstyrene | aromatic |
| 10 | Phenol and Benzonitrile | hydroxy benzene and N-containing |
| 11 | Decene and $C_3$-Alkylbenzene | aliphatic carbon and aromatic |
| 12 | $C_3$-Alkylbenzene | aromatic |
| 13 | Indene | aromatic |
| 14 | Cresol | hydroxy benzene |
| 15 | Methylbenzaldehyde | aromatic |
| 16 | Undecene | aliphatic carbon |
| 17 | $C_4$-Alkylbenzene | aromatic |
| 18 | Naphthalene | aromatic |
| 19 | Dodecene | aliphatic carbon |
| 20 | $C_5$-Alkylbenzene | aromatic |
| 21 | Tridecene | aliphatic carbon |
| 22 | Methylnaphthalene | aromatic |
| 23 | Biphenyl | aromatic |
| 24 | Tetradecene | aliphatic carbon |
| 25 | Methylbiphenyl or Dimethylnaphthalene | aromatic |
| 26 | Pentadecene | aliphatic carbon |
| 27 | Fluorene | aromatic |
| 28 | Dihydrophenanthrene or Dihydroanthracene | aromatic |
| 29 | Phenanthrene | aromatic |
| 30 | Anthracene | aromatic |
| 31 | Methylphenanthrene and Methylanthracene | aromatic |
| 32 | Pyrene | aromatic |
| 33 | Methylpyrene | aromatic |

**Table III.4 REE concentrations of raw and concentrated groundwater**

| | La [ng/L] | Ce [ng/L] | Pr [ng/L] | Nd [ng/L] | Sm [ng/L] | Eu [ng/L] | Gd [ng/L] |
|---|---|---|---|---|---|---|---|
| Raw groundwater | <1 | <1 | <1 | 1 | <1 | <1 | <1 |
| 20-fold concentrate (NTR7410) | 1 | 2 | <1 | <1 | <1 | <1 | <1 |
| 20-fold concentrate (NTR7450) | <1 | 3 | <1 | 2 | <1 | <1 | <1 |
| 6.25-fold concentrate (ES20) | <1 | 2 | <1 | 3 | <1 | <1 | 1 |

| | Tb [ng/L] | Dy [ng/L] | Ho [ng/L] | Er [ng/L] | Tm [ng/L] | Yb [ng/L] | Lu [ng/L] |
|---|---|---|---|---|---|---|---|
| Raw groundwater | <1 | 1 | <1 | 2 | <1 | 2 | <1 |
| 20-fold concentrate (NTR7410) | <1 | <1 | <1 | <1 | <1 | <1 | <1 |
| 20-fold concentrate (NTR7450) | <1 | 1 | <1 | 3 | <1 | 5 | 2 |
| 6.25-fold concentrate (ES20) | <1 | 4 | 2 | 7 | 2 | 6 | 2 |

## III.4 Conclusions

In this study, we applied NF and RO membranes to the concentration of organic colloids. Although the recovery yield using the RO membrane was high in the model humic acid concentration test, concentration of groundwater was difficult owing to the precipitation of inorganic substances on membranes and membrane fouling caused by organic colloids with $Ca^{2+}$. On the other hand, an NF membrane with moderate initial flux and ion rejection achieved 20-fold concentration of groundwater with 57% recovery yield of organic colloids. Based on the Py-GC/MS measurement of the concentrated groundwater, it is suspected that organic colloid structures in granite groundwater at a depth of 300 m are similar to those of humic substances with high humification. Thus, the groundwater concentration technique using NF membrane presented in this work could be a useful method to investigate the physicochemical properties of colloids in the groundwater.

REFERENCES

[1] M. Filella, Colloidal properties of submicron particles in natural waters, in: K.J. Wilkinson, J.R. Lead (Eds.), Environmental Colloids and Particles: Behaviour, Separation and Characterization, Wiley, Chichester (2007) 17–94.

[2] D. Backhus, Sampling colloids and colloid-associated contaminants in groundwater, Ground Water 31 (1993) 466–479.

[3] P. Vilks, D.B. Bachinski, Characterization of organics in Whiteshell Research area groundwater and the implications for radionuclide transport, Appl. Geochem. 11 (1996) 387–402.

[4] T. Saito, Y. Suzuki, T. Mizuno, Size and elemental analyses of nano colloids in deep granitic groundwater: implications for transport of trace elements, Colloids Surf. A: Physicochem. Eng. Asp. 435 (2013) 48–55.

[5] D. Aosai, Y. Yamamoto, T. Mizuno, T. Ishigami, H. Matsuyama, Size and composition analyses of colloids in deep granitic groundwater using microfiltration/ultrafiltration while maintaining in situ hydrochemical conditions, Colloids and Surf. A: Physicochem. Eng. Asp. 461 (2014) 279–286.

[6] A.B. Kersting, D.W. Efurd, D.L. Finnegan, D.J. Rokop, D.K. Smith, J.L. Thompson, Migration of plutonium in ground water at the Nevada Test Site, Nature 397 (1999) 56–59.

[7] W.R. Penrose, W.L. Polzer, E.H. Essington, D.M. Nelson, K.A. Orlandini, Mobility of plutonium and americium through a shallow aquifer in a semiarid region, Environ. Sci. Technol. 24 (1990) 228–234.

[8] G.J. Moridis, Q. Hu, Y.S. Wu, G.S. Bodvarsson, Preliminary 3-D site-scale studies of radioactive colloid transport in the unsaturated zone at Yucca Mountain,

Nevada, J. Contam. Hydrol. 60 (2003) 251–286.

[9] A.P. Novikov, S.N. Kalmykov, S. Utsunomiya, R.C. Ewing, F. Horreard, A. Merkulov, S.B. Clark, V.V. Tkachev, B.F. Myasoedov, Colloid transport of plutonium in the far-field of the Mayak Production Association, Russia, Science 314 (2006) 638–641.

[10] J.N. Ryan, M. Elimelech, Colloid mobilization and transport in groundwater, Colloids and Surf. A 107 (1996) 1–56.

[11] J.F. McCarthy, J.M. Zachara, Subsurface transport of contaminants, Environ. Sci. Technol. 23 (1989) 496–502.

[12] R. Artinger, G. Buckau, S. Geyer, P. Fritz, M. Wolf, J.I. Kim, Characterization of groundwater humic substances: influence of sedimentary organic carbon, Appl. Geochem. 15 (2000) 97–116.

[13] S.W. Krasner, J. Croue, J. Buffle, E.M. Perdue, Three approaches for characterizing NOM, J. Am. Water Works Assoc. 88 (1996) 66–79.

[14] J.A. Leenheer, Systematic approaches to comprehensive analyses of natural organic matter, Ann. Environ. Sci. 3 (2009) 31–130.

[15] H.Z. Ma, H.E. Allen, Y.J. Yin, Characterization of isolated fractions of dissolved organic matter from natural waters and a wastewater effluent, Water Res. 35 (2001) 985–996.

[16] N.A. Marley, J.S. Gaffney, K.A. Orlandini, M.M. Cunningham, Evidence of radionuclide transport and mobilization in a shallow, sandy aquifer, Environ. Sci. Technol. 27 (1993) 2456–2461

[17] F. Caron, G. Mankarios, Pre-assessment of the speciation of 60Co, 125Sb, 137Cs and 241Am in a contaminated aquifer, J. Environ. Radioactivity 77 (2004) 29–46.

[18] J. Gaillardet, J. Viers, B. Dupré, Trace elements in river waters, in: J.I. Drever(Ed.), Treatise on Geochemistry, Elsevier, Amsterdam, (2003) 225–272.

[19] M. Plaschke, J. Romer, J.I. Kim, Characterization of Gorleben groundwater colloids by atomic force microscopy, Environ. Sci. Technol. 36 (2002) 4483–4488.

[20] E.M Thurman, R.L Malcom, Preparative isolation of aquatic humic substances, Environ. Sci. Technol. 15 (1981) 463–466.

[21] C.J. Miles, J.R. Tuschall Jr, P.L. Brezonik, Isolation of aquatic humus with diethylaminoethylcellulose. Anal. Chem., 55 (1983) 410–411.

[22] S.M. Serkiz, E.M. Perdue, Isolation of dissolved organic matter from the Suwannee River using reverse osmosis, Water Res. 24 (1990) 911–916.

[23] L. Sun, E.M. Perdue, J.F. McCarthy. Using reverse osmosis to obtain organic matter from surface and ground waters, Water Res. 29 (1995) 1471–1477.

[24] N. Chapman, J. Smellie, Introduction and summary of the workshop, Chem. Geol. 55 (1986) 167–173.

[25] S. Hong, M. Elimelech, Chemical and physical aspects of natural organic matter (NOM) fouling of nanofiltration membranes, J. Membr. Sci. 132 (1997) 159–181.

[26] H. Iwai, M. Fukushima, M. Yamamoto, T. Komai, Y. Kawabe, Characterization of seawater extractable organic matter from bark compost by TMAH-py-GC/MS, J. Anal. Appl. Pyrolysis 99 (2013) 9–15.

[27] M.J. Avena, L.K. Koopal, W.H. van Riemsdijk, Proton binding to humic acids: Electrostatic and intrinsic interactions. J. Colloid Interface Sci. 217 (1999) 37–48.

[28] W. Yuan, A.L. Zydney, Humic acid fouling during ultrafiltration. Environ. Sci. Technol. 34 (2000) 5043–5050.

[29] S.K. Hong, M. Elimelech, Chemical and physical aspects of natural organic matter (NOM) fouling of nanofiltration membranes. J. Membr. Sci. 132 (1997) 159–181.

[30] A. Seidel, M. Elimelech, Coupling between chemical and physical interactions in natural organic matter (NOM) fouling of nanofiltration membranes: implications for fouling control. J. Membr. Sci. 203 (2002) 245–255.

[31] C.Y. Tang, Y.N. Kwon, J.O. Leckie, Fouling of reverse osmosis and nanofiltration membranes by humic acid—effects of solution composition and hydrodynamic conditions, J. Membr. Sci. 290 (2007) 86–94.

[32] T. Iwatsuki, R. Furue, H. Mie, S. Ioka, T. Mizuno, Hydrochemical baseline condition of groundwater at the Mizunami underground research laboratory (MIU), Appl. Geochem. 20 (2005) 2283–2302.

[33] D. Saeki, T. Tanimoto, H. Matsuyama, Prevention of bacterial adhesion on polyamide reverse osmosis membranes via electrostatic interactions using a cationic phosphorylcholine polymer coating, Colloids and Surf. A: Physicochem. Eng. Asp. 443 (2014) 171‑176.

[34] F.A. Andersen, L. Brecevic, Infrared spectra of amorphous and crystalline calcium carbonate, Acta Chem. Scand. 45 (1991) 1018–1024.

[35] C.L. Tiller, C.R. Omelia, Natural organic matter and colloidal stability: Models and measurements, Colloids and Surf. A: Physicochem. Eng. Asp. 73 (1993) 89–102.

[36] K. Ghosh, M. Schnitzer, Macromolecular structures of humic substances, Soil Sci. 129 (1980) 266.

[37] F.J. Stevenson, Humus chemistry, John Wiley & Sons: New York, 1982.

[38] C. Sáiz-Jiménez, J.W. De Leeuw, Chemical characterization of soil organic matter

fractions by analytical pyrolysis-gas chromatography-mass spectrometry, J. Anal. Appl. Pyrolysis 9 (1986) 99–119.

[39] J.A. González-Pérez, G. Almendros, J.M. de la Rosa, F.J. González-Vila, Appraisal of polycyclic aromatic hydrocarbons (PAHs) in environmental matrices by analytical pyrolysis (Py–GC/MS), J. Anal. Appl. Pyrolysis 109 (2014) 1–8.

[40] M.A. Wilson, R.P. Philp, A.H. Gillam, T.D. Gilbert, K.R. Tate, Comparison of the structures of humic substances from aquatic and terrestrial sources by pyrolysis gas chromatography-mass spectrometry, Geochim. Cosmochim. Acta 47 (1983) 497–502.

[41] R. Sihombing, P.F. Greenwood, M.A. Wilson, J.V. Hanna, Composition of size exclusion fractions of swamp water humic and fulvic acids as measured by solid state NMR and pyrolysis-gas chromatography-mass spectrometry, Org. Geochem. 24 (1996) 859–873.

[42] X.Q. Lu, J.V. Hanna, W.D. Johnson, Source indicators of humic substances: an elemental composition, solid state 13 C CP/MAS NMR and Py-GC/MS study, Appl. Geochem. 15 (2000) 1019–1033.

[43] F. Martin, C. Sáiz-Jiménez, F.J. GonzaÁlez-Vila, Pyrolysis-gas chromatography-mass spectrometry of lignins, Holzforschung 33 (1979) 210–212.

[44] C. Sáiz-Jiménez, J.W. de Leeuw, Chemical structure of a soil humic acid as revealed by analytical pyrolysis. J. Anal. Appl. Pyrolysis 11 (1987) 367–376.

# Chapter IV

## Efficient condensation of organic colloids in deep groundwater using surface-modified nanofiltration membranes under optimized hydrodynamic conditions

### IV.1 Introduction

High-level radioactive waste (HLW) originating from the nuclear industry is legislated to be disposed of underground at a depth of more than 300 m [1]. The safety of the geological disposal of HLW is dependent on the migration of the radionuclides released from HLW into the underground environment. Organic colloids are present in deep groundwater [2,3], and the interaction between organic colloids and radionuclides affects the migration of radionuclides [4,5]. Therefore, for the safety assessment of HLW, it is imperative to understand the detailed composition of organic colloids and their interaction with radionuclides. Precise analysis of organic colloids from groundwater is difficult, caused by their low concentration [6,7]; hence, extraction techniques using adsorption resins [8,9] are widely applied. However, extracted samples using adsorption resins are exposed to severe chemical disturbances, and there is concern over their chemical changes. On the other hand, condensation using porous membranes has also been applied to afford high concentrations of organic colloids. Although porous membranes can rapidly condense organic colloids without chemical exposure [10–12], some amount of organic colloids from the condensed samples is lost because of their deposition on the membrane surface and subsequent blocking of pores (membrane fouling). For obtaining more accurate information on organic colloids, it is

imperative to prevent membrane fouling.

Effects of hydrodynamic conditions on membrane fouling by organic colloids have been investigated [13–15]. These studies have reported that membrane fouling is affected by chemical and hydrodynamic interactions. That is, the fouling of membranes by organic colloids is promoted by high concentrations of divalent cations ($Ca^{2+}$ and $Mg^{2+}$), high initial permeate flux, and low cross-flow velocity. Divalent cations neutralize the net negative charge of humic acids, which supposedly constitute the majority of organic colloids in groundwater, caused by strong affinity, resulting in the reduction of repulsion among humic acid molecules [16–18]. In addition, divalent cations can bridge humic acid molecules [19]. Thus, divalent cations accelerate the fouling of membranes, caused by the coagulation of humic acid molecules. The high permeate flux or low cross-flow velocity increases the concentration of divalent cations on the membrane surface, caused by concentration polarization, which in turn enhances membrane fouling [14]. Thus, increase in the cross-flow velocity and decrease in the permeate flux mitigate the fouling of membranes by organic colloids.

The surface modification of membranes using various hydrophilic polymers has also been effective for preventing membrane fouling [20]. Hydrophilic polymers, such as polyethylene glycol, and zwitterionic polymers have been frequently used for modifying the surfaces of porous membranes with the aim of preventing the adsorption of organic colloids and fouling of membranes [21–24]. We have developed a simple, facile method for modifying polyamide reverse osmosis (RO) membranes using zwitterionic polymers with the aim of preventing the adsorption of bacteria, an example of an organic colloid [25]. Negatively charged RO membranes were coated with poly(2-methacryloyloxyethyl phosphorylcholine-co-2-aminoethyl methacrylate)

(p(MPC-co-AEMA)), which is composed of cationic AEMA units and zwitterionic MPC units, by electrostatic interaction. The coated RO membranes exhibited high hydrophilicity and high resistance to bacterial adsorption. Therefore, membrane surface modification with p(MPC-co-AEMA) is also promising for preventing the fouling of membranes by organic colloids.

Previously, we have developed a method for the condensation of organic colloids in groundwater using nanofiltration (NF) membranes [12]. The use of NF membranes facilitated the condensation of organic colloids without severe reduction in flux, while condensation using RO membranes facilitated severe reduction in flux, caused by the precipitation of condensed inorganic substances. Organic colloids in actual condensed groundwater at a depth of 300 m in granitic rocks were successfully analyzed by pyrolysis gas chromatography coupled with mass spectrometry (Py-GC/MS), and their composition was similar to that of humic substances with high humification. However, the recovery yields of organic colloids were up to 57% at 20-fold condensation, caused by the fouling of organic colloids. Thus, the recovery yields need to be improved for the purpose of confirming the validity of the result obtained by Py-GC/MS.

This study aimed at preventing the fouling of membranes by organic colloids in the condensation of deep groundwater using NF membranes by optimizing hydrodynamic conditions and modifying the membrane surface. Commercial humic acids and bovine serum albumin (BSA) were used as models of organic colloids. The aqueous solutions of organic colloids were condensed using a cross-flow filtration apparatus equipped with sulfonated polyethersulfone NF membranes. The time courses of permeate flux and the recovery yield of humic acid and BSA were monitored. The effects of hydrodynamic conditions and modification of membrane surfaces with

p(MPC-co-AEMA) on condensation behavior were examined. Finally, actual deep groundwater was condensed using modified NF membranes under optimized hydrodynamic conditions. The composition of the organic colloids in the condensed deep groundwater was analyzed by Py-GC/MS.

## IV.2 Experimental

### IV.2.1 Materials

All solutions used in this study were prepared using ultrapure water and analytical-grade chemicals. Unless specified, all chemicals were obtained from Wako Pure Chemical Industries (Osaka, Japan) and were used without further purification. Commercial sulfonated polyethersulfone NF membranes were obtained from Nitto Denko (NTR7450; Osaka, Japan). Coal-derived humic acid (WHA; 088-04622; Wako Pure Chemical Industries) and peat-derived humic acid (AHA; H16752; Sigma-Aldrich, St. Louis, MO, USA) were used after purification according to a previous study [12]. A p(MPC-co-AEMA) (MPC:AEMA = 9:1, random copolymer) was generously supplied by NOF Corporation (Tokyo, Japan), and its weight-average molecular weight was $9.7 \times 10^5$ [25]. Coomassie brilliant blue (CBB) G-250 was purchased from Polysciences Inc. (Warrington, PA, USA).

Groundwater in the granitic rock was collected from the 09MI20 borehole in the −300 m Access/Research Gallery of Mizunami Underground Research Laboratory on December 25, 2014. The borehole was divided into six sections by impermeable packers, and the sections were numbered from 1 to 6 according to the distance from the base of the borehole. Groundwater samples were collected from section 1 and placed in the freezer until experiments were conducted. Detailed information of the borehole and

hydrochemistry of the examined groundwater has been summarized in our previous paper [12]. The groundwater contained 9.0 mg/L $Ca^{2+}$, and the pH was 8.5.

### IV.2.2 Condensation apparatus

Fig. IV.1 shows the laboratory-scale cross-flow membrane filtration apparatus used for condensation experiments [12]. For condensation experiments, a feed solution was fed into a cylindrical stainless steel membrane cell using a plunger pump (NPL-120; Nihon Seimitsu Kagaku, Tokyo, Japan) at a constant flow rate of 9.0 mL/min. The applied transmembrane pressure (TMP) was adjusted using a back pressure valve. The effective membrane area was 8.0 $cm^2$. The permeate solution was collected in a permeate reservoir. The retentate solution was circulated through the feed reservoir and was condensed. The feed solution in the cell was stirred using a cylindrical magnetic bar with a length of 3.0 cm. Permeate flux was calculated from the time course of permeate weight.

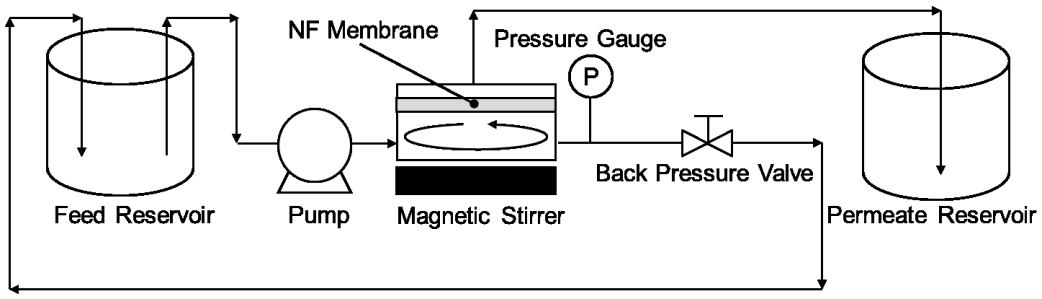


**Fig. IV.1 Schematic of the cross-flow condensation apparatus.**

### IV.2.3 Modification of membrane surface using a cationic phosphorylcholine polymer

A negatively charged NF membrane was modified using cationic

p(MPC-co-AEMA) by electrostatic interaction [25]. As shown in Fig. IV.1, the NF membrane was set into the membrane cell. An aqueous solution of 0.1 wt% p(MPC-co-AEMA) was fed into the membrane cell at a constant flow rate of 9.0 mL/min and a constant TMP of 0.75 MPa for 2 h. The feed solution of the membrane cell was magnetically stirred at 150 rpm. Then, the membrane was detached and washed by gentle shaking in an aqueous solution of 3.5 wt% NaCl for removing non-specifically adsorbed polymers. For evaluating the surface hydrophilicity of the membranes, the water contact angle was measured using a contact angle meter (DM-300; Kyowa Interface Science, Saitama, Japan). The ζ-potential was measured by streaming potential measurement using an electrophoretic light-scattering apparatus (ELSZ-1000, Otsuka Electronics, Osaka, Japan) in aqueous 10 mmol/L NaCl.

### IV.2.4 Condensation of humic acid and BSA

A feed solution of 5 mg/L of humic acid containing 1 mg/L $Ca^{2+}$ or 5 mg/L of BSA was condensed from 125 mL to 25 mL (5-fold condensation) using the raw NF membrane and p(MPC-co-AEMA)-coated NF membrane under different TMPs (0.75 or 1.5 MPa) and stirring rates (150 or 1500 rpm). The concentration of $Ca^{2+}$ in the feed solution of humic acid was adjusted using a $CaCO_3$ standard solution of 1000 mg/L in 0.1 mol/L $HNO_3$ (Wako Pure Chemicals).

The humic acid concentration was determined by optical density measurements at 254 nm using a UV–vis spectrometer (V-650; Jasco Corp., Tokyo, Japan). The BSA concentration was determined by a CBB method [26]. CBB was dissolved in methanol, and then phosphoric acid and ultrapure water were added. The final concentration of the components in this CBB solution was 0.025% (w/v) CBB, 12.5% (w/v) methanol,

and 70.83% (w/v) phosphoric acid. The CBB solution (0.2 mL) and 0.8 mL of the sample were mixed, and the optical density at 595 nm was measured using a UV–vis spectrometer.

### IV.2.5 Characterization of organic colloids

Condensation experiments were carried out using groundwater. The concentration of organic colloids in the groundwater was determined by the same method as that used for the determination of humic acid under the assumption that all organic colloids are humic acids. The condensed organic colloids were characterized by Py-GC/MS. Py-GC/MS analysis was carried out using a double-shot pyrolyzer (PY-2020id; Frontier Laboratories Ltd., Fukushima, Japan) attached to a GC/MS instrument (Agilent 6890N/Agilent 5973; Agilent Technologies Inc., Palo Alto, CA, USA) Py-GC/MS is a powerful tool for obtaining detailed compositional information of a polymer. Two humic acids derived from coal and peat were directly analyzed by Py-GC/MS. In the case of the organic colloids in condensed groundwater, the condensed water was further evaporated, dried under $N_2$, and then analyzed by Py-GC/MS. Py-GC/MS analysis was performed by the same method as in our previous paper [12].

## IV.3 Results and discussion

### IV.3.1 Analysis of commercial humic acids

First, two commercial humic acids WHA and AHA, which have been extensively used as model humic acids by several researchers [13–15,27,28], were analyzed by Py-GC/MS. Fig. IV.2 shows the Py-GC/MS pyrogram of WHA and AHA, and Table

IV.1 lists the detected compounds. The major products obtained from the pyrolysis of coal-derived WHA were aromatic compounds (n = 1, 3, 4, 5, 7, 8, 10, 13, 14, 17, 20, and 23) attributed to a high degree of humification; these compounds were consistent with brown coal humic substances [29]. On the other hand, the major products obtained from the pyrolysis of peat-derived AHA were a series of aliphatic compounds (n = 2, 6, 8, 9, 11, 12, 15, 16, 18, 19, 21, 22, and 24–32), attributed to lipids and paraffinic material in humic substances. The result obtained for AHA is similar to that obtained for peat-derived humic substances [29,30]. The composition of organic colloids in deep groundwater is similar to that of humic substances with high humification [12]. Thus, we used WHA as a model organic colloid in the following experiments.

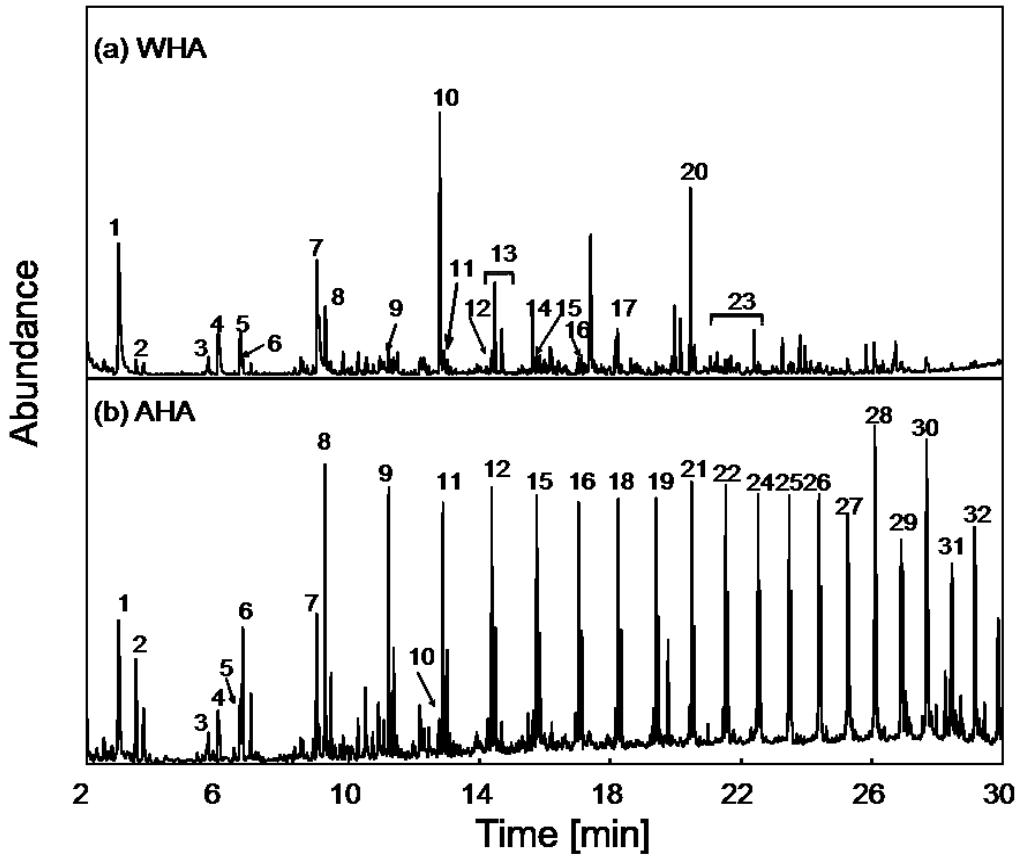


**Fig. IV.2 Py-GC/MS pyrogram of (a) WHA and (b) AHA. Table IV.1 shows the peak numbers.**

**Table IV.1 Typical compounds obtained from the pyrolysis of Wako humic acid (WHA), Aldrich humic acid (AHA), and organic colloids in groundwater condensed using the p(MPC-co-AEMA)-coated NF membrane under optimized hydrodynamic conditions (at 1500 rpm and 0.75 MPa).**

| Peak No. | Compound | Group |
|---|---|---|
| 1 | Toluene | aromatic |
| 2 | Octene | aliphatic carbon |
| 3 | Ethylbenzene | aromatic |
| 4 | Xylene | aromatic |
| 5 | Styrene | aromatic |
| 6 | Nonene | aliphatic carbon |
| 7 | Phenol and Benzonitrile | hydroxy benzene and N-containing |
| 8 | Decene and $C_3$-Alkylbenzene | aliphatic carbon and aromatic |
| 9 | Undecene | aliphatic carbon |
| 10 | Naphthalene | aromatic |
| 11 | Dodecene | aliphatic carbon |
| 12 | Tridecene | aliphatic carbon |
| 13 | Methylnaphthalene | aromatic |
| 14 | Biphenyl | aromatic |
| 15 | Tetradecene | aliphatic carbon |
| 16 | Pentadecene | aliphatic carbon |
| 17 | Fluorene | aromatic |
| 18 | Hexadecene | aliphatic carbon |
| 19 | Heptadecene | aliphatic carbon |
| 20 | Phenanthrene | aromatic |
| 21 | Octadecene | aliphatic carbon |
| 22 | Nonadecene | aliphatic carbon |
| 23 | Methylphenanthrene and Methylanthracene | aromatic |
| 24 | Eicosene | aliphatic carbon |
| 25 | Heneicosene | aliphatic carbon |
| 26 | Docosene | aliphatic carbon |
| 27 | Tricosene | aliphatic carbon |
| 28 | Tetracosene | aliphatic carbon |
| 29 | Pentacosene | aliphatic carbon |
| 30 | Hexacosene | aliphatic carbon |
| 31 | Heptacosene | aliphatic carbon |
| 32 | Octacosene | aliphatic carbon |

### IV.3.2 Condensation of humic acid

#### IV.3.2.1 Optimum hydrodynamic conditions

Firstly, the effects of the TMP and stirring rate on the recovery yield were investigated. Fig. IV.3 shows the recovery yield and experimental time required to condense the feed solution to 5 times on the WHA condensation tests. The recovery yield was defined as the amount of organic colloids in the condensed solution divided by that in the initial solution. The decreasing TMP increased both the recovery yield and experimental time (Fig. IV.3a). The experimental time at 0.75 MPa (recovery yield: 70%) was twice longer than that at 1.5 MPa, although the recovery yield at 0.75 MPa was 70%, higher than that at 1.5 MPa, 44%. Thus, the condensation test was conducted at 0.75 MPa as optimized TMP. About the stirring rate, the recovery rate maximally reached 70% over 750 rpm, and the experimental times were roughly same (Fig. IV.3b). Therefore, the condensation test was conducted at 1500 rpm, which was a maximum value. The optimum hydrodynamic condition of the stirring rate and TMP was decided as 150 rpm and 1.5 MPa, respectively.

Fig. IV.4 shows the effect of the optimization of the hydrodynamic conditions on the permeate flux and WHA concentration in the condensed solutions. In this figure, the theoretical concentrations in the condensed solutions with 100% recovery yield are represented as red dotted lines. Fig. IV.5 shows the surface view of the membranes after 5-fold condensation tests of WHA. The condensation test under all hydrodynamic conditions exhibited no reduction in flux (Fig. IV.4). However, all WHA concentrations in the condensed solutions were below the dotted line, indicating low recovery yields. As shown in Fig. IV.4a, the recovery yield after condensation at 150 rpm and 1.5 MPa was quite low, only 44% (Fig. IV.4a). This low recovery yield was caused by the

adsorption and deposition of humic acid on the membrane surface. As shown in Fig. IV.5a, large amounts of humic acids were deposited on the membrane surface. The stirring rate on the membrane surface is considered greater outside the membrane cell compared with that in the center. Thus, a large amount of deposits on the center of the membrane surface is probably caused by the distribution of the stirring rate. However, at this time scale, these deposits hardly affected the reduction in flux. As the stirring rate increased or TMP decreased, the recovery yields increased (Figs. IV.4b and c), and the amounts of humic acids deposited on the membrane surface decreased (Figs. IV.5b and c). The decreasing TMP and increasing stirring rate decrease the permeation drag and concentration polarization of solutes on the membrane surface, resulting in the prevention of membrane fouling. At a high stirring rate and low TMP, a high recovery yield of 80% was obtained (Fig. IV.4d), with small amounts of WHA deposited on the NF membrane (Fig. IV.5d). These results indicate that a high stirring rate and low TMP is optimum condition for high recovery yield.

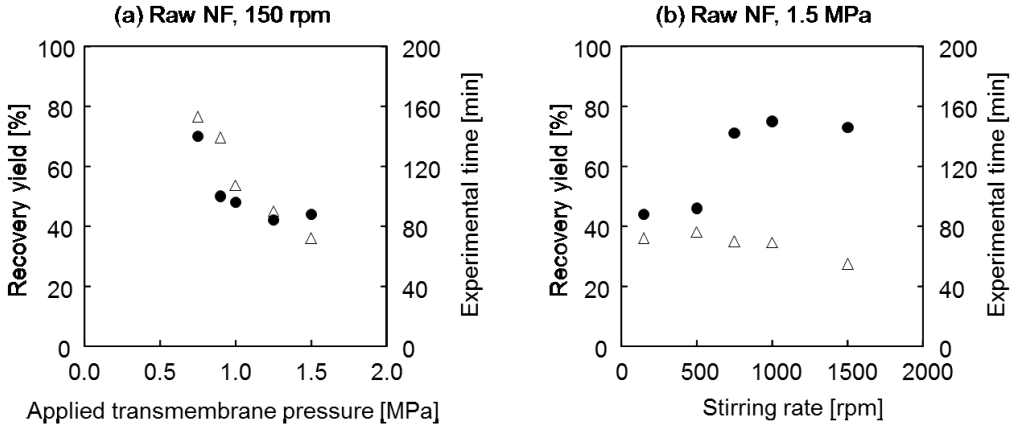


**Fig. IV.3 Effect of the TMP (a) and stirring rate (b) on the recovery yield and experimental time to condense the feed solution to 5 times on the WHA condensation test. Closed circles and open triangles indicate recovery yield and experiment time, respectively.**

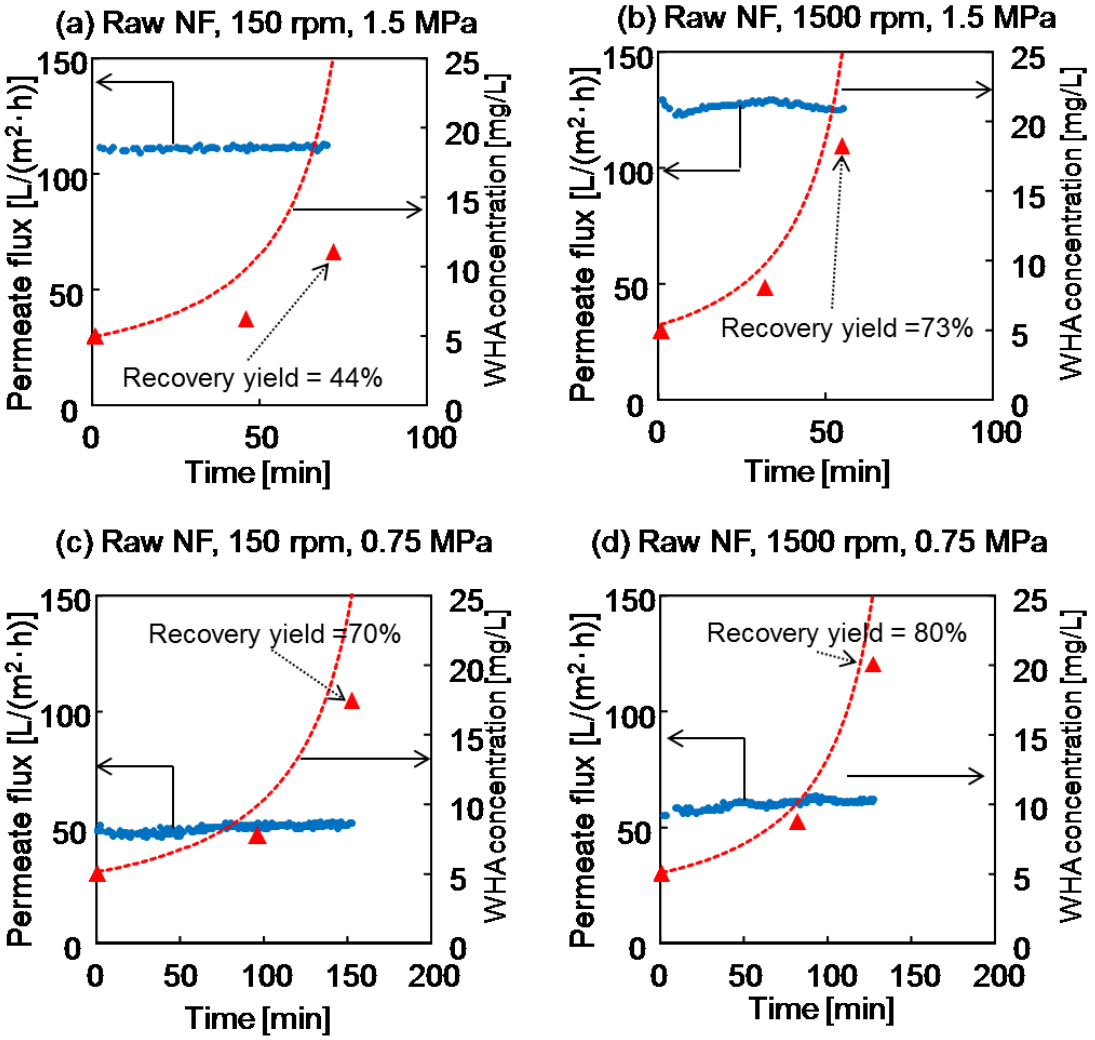


**Fig. IV.4 Time courses of the permeate flux and WHA concentrations in the condensed solutions from the condensation tests of WHA using (a) raw NF membrane under the original hydrodynamic conditions (at 150 rpm and 1.5 MPa), (b) raw NF membrane at 1500 rpm and 1.5 MPa, (c) raw NF membrane at 150 rpm and 0.75 MPa, (d) raw NF membrane under the optimized hydrodynamic conditions (at 1500 rpm and 0.75 MPa). Blue circles and red triangles indicate permeate flux and WHA concentration, respectively. Red dotted line indicates the theoretical concentrations of WHA assuming 100% recovery yield.**

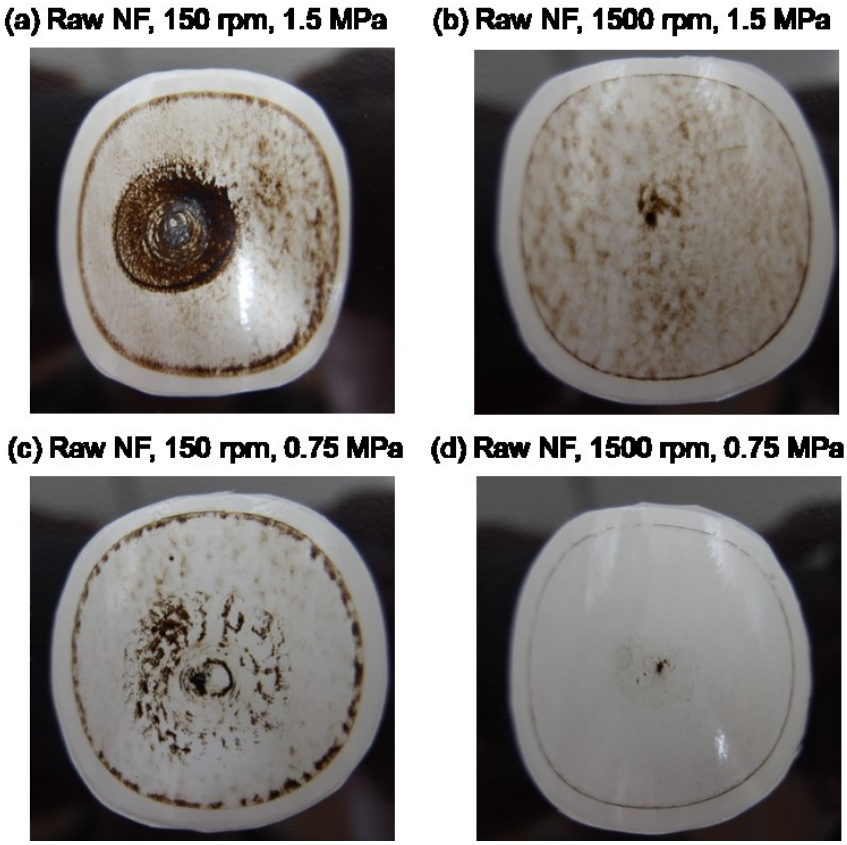


**Fig. IV.5 Surface view of the membranes after the 5-fold condensation tests of WHA using (a) raw NF membrane under the original hydrodynamic condition (at 150 rpm and 1.5 MPa), (b) raw NF membrane at 1500 rpm and 1.5 MPa, (c) raw NF membrane at 150 rpm and 0.75 MPa, (d) raw NF membrane under the optimized hydrodynamic conditions (at 1500 rpm and 0.75 MPa).**

### IV.3.2.2 Modification of membrane surface

To prevent the adsorption of organic colloids, the surface of the NF membrane was modified with zwitterionic polymer. Fig. IV.6 shows the ζ-potentials and water contact angles of the raw NF membrane and NF membranes coated with p(MPC-co-AEMA) of different concentrations. The ζ-potential of the NF membranes was neutralized by the coating with the aqueous solution of 0.0001 wt% p(MPC-co-AEMA). The water contact angle of the NF membrane decreased with increasing the p(MPC-co-AEMA) concentration and reached the minimum value at

0.01 wt% of p(MPC-co-AEMA). Fig. IV.7 shows the effect of the p(MPC-co-AEMA) concentration on the recovery yield and experimental time required to condensate the feed solution to 5 times on the WHA condensation test. The highest recovery yield was obtained at 0.1 wt% p(MPC-co-AEMA). Thus, the NF membranes were coated with 0.1 wt% of p(MPC-co-AEMA) on the following experiments.

We examined the effect of the modified membrane surface on the recovery yield of WHA. Fig. IV.8 shows the time courses of the permeate flux and WHA concentrations in the condensation tests using the p(MPC-co-AEMA)-coated NF membrane. Fig. IV.9 shows the surface view of the p(MPC-co-AEMA)-coated NF membrane after 5-fold condensation tests of WHA. As shown in Fig. IV.8, in the condensation test using the p(MPC-co-AEMA)-coated NF membrane (Fig. IV.8), reduction in flux was not observed. Although the amounts of humic acids deposited on the surface of the p(MPC-co-AEMA)-coated NF membrane (Figs. IV.9a and b) and raw NF membrane (Figs. IV.5a and d) seemed similar, recovery yields of 56% and 86% for the p(MPC-co-AEMA)-coated NF membrane shown in Figs. IV.8a and b were higher than those of the raw NF membrane under the same hydrodynamic condition (44% and 80% shown in Figs. IV.4a and d, respectively). Thus, modification of the membrane surface by p(MPC-co-AEMA) is effective against fouling by WHA, caused by improved hydrophilicity.

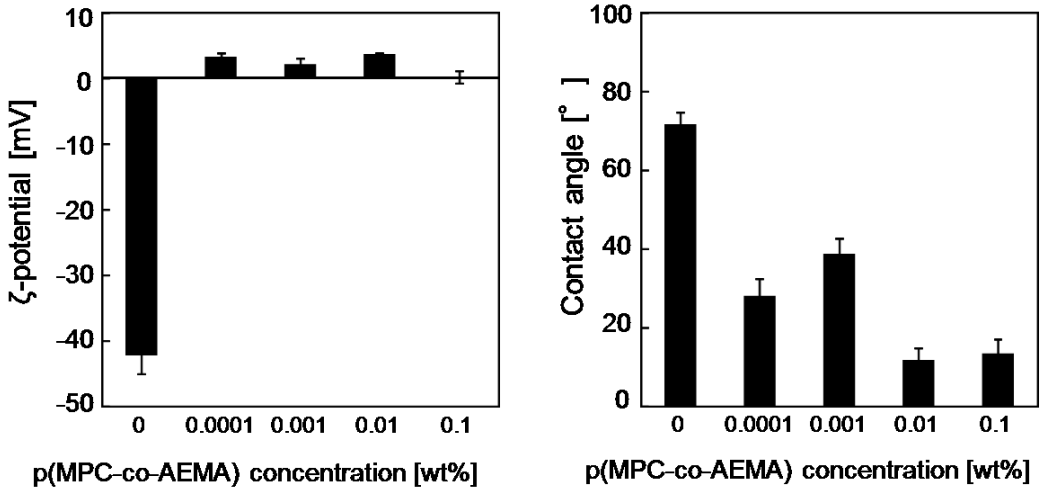


**Fig. IV.6 ζ-potentials and water contact angles of the raw NF membrane and NF membranes coated with p(MPC-co-AEMA) of different concentrations.**

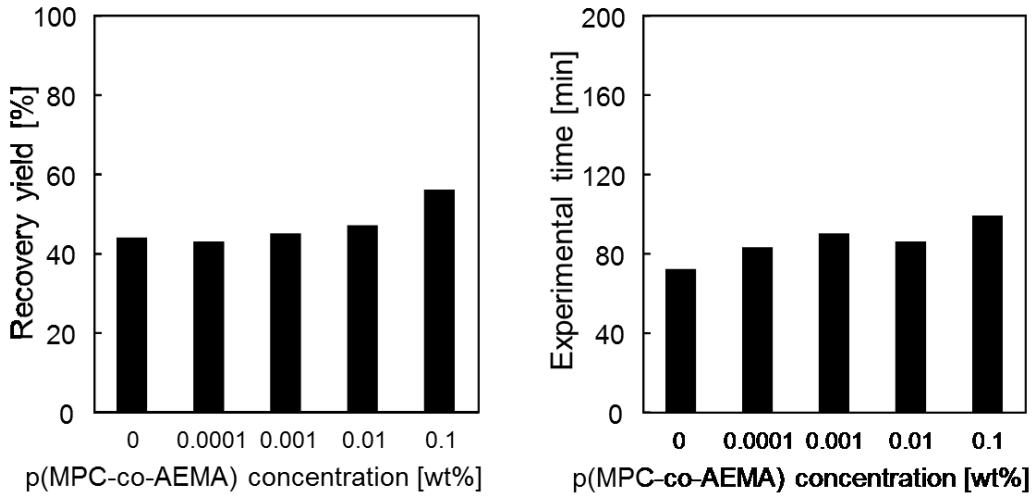


**Fig. IV.7 Recovery yield and experimental time of the 5-fold concentration test of the humic acid using raw NF membrane and NF membranes coated with p(MPC-co-AEMA) of different concentrations.**

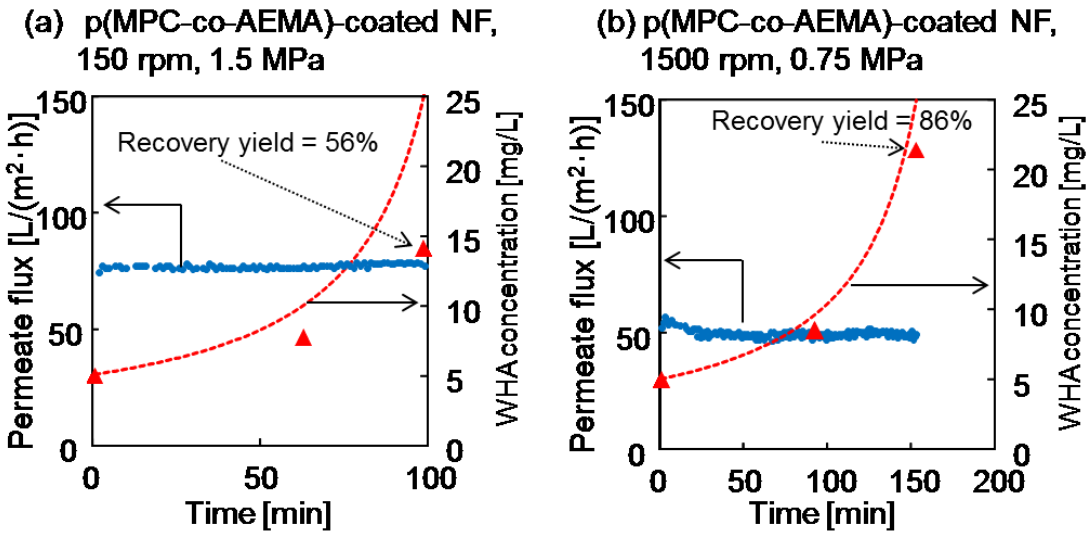


**Fig. IV.8 Time courses of the permeate flux and WHA concentrations in the condensed solutions from the condensation tests of WHA using (a) p(MPC-co-AEMA)-coated NF membrane under the original hydrodynamic conditions (at 150 rpm and 1.5 MPa), (b) p(MPC-co-AEMA)-coated NF membrane under the optimized hydrodynamic conditions (at 1500 rpm and 0.75 MPa). Blue circles and red triangles indicate permeate flux and WHA concentration, respectively. Red dotted line indicates the theoretical concentrations of WHA assuming 100% recovery yield.**

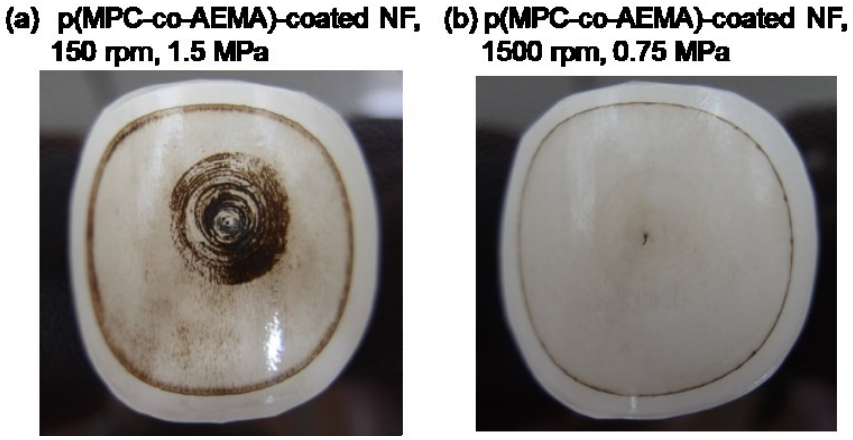


**Fig. IV.9 Surfaces view of the membranes after the 5-fold condensation tests of WHA using (a) p(MPC-co-AEMA)-coated NF membrane under the original hydrodynamic condition (at 150 rpm and 1.5 MPa), (b) p(MPC-co-AEMA)-coated NF membrane under optimized hydrodynamic conditions (at 1500 rpm and 0.75 MPa).**

### IV.3.3 Condensation of BSA

We examined the effects of hydrodynamic conditions and modified membrane surface on the recovery yields of BSA. Fig. IV.10 shows the time courses of the permeate flux and BSA concentration in the condensed solutions. The initial permeate flux value of the raw NF membranes (Figs. IV.10a and b) was significantly lower than those obtained from the condensation test of WHA under the same hydrodynamic condition (Fig. IV.3a and b), indicating that the permeate flux of raw NF membranes drastically declines immediately after the start of the condensation test of BSA. On the other hand, the permeate flux in the condensation tests using the p(MPC-co-AEMA)-coated membranes (Fig. IV.10c and d) exhibited almost the same values as those obtained from the condensation test of WHA under the same hydrodynamic conditions (Fig. IV.8a and b). Thus, the modification of the membrane surface by p(MPC-co-AEMA) is significantly effective for the prevention of the decrease in permeate flux by fouling with BSA. The recovery yields were significantly improved by the optimized hydrodynamic conditions (Fig. IV.10b) as compared to the membrane surface modified by p(MPC-co-AEMA) (Fig. IV.10c), indicating that the optimized hydrodynamic conditions are more effective than the membrane surface modified with by p(MPC-co-AEMA) for increasing the recovery yield of BSA.

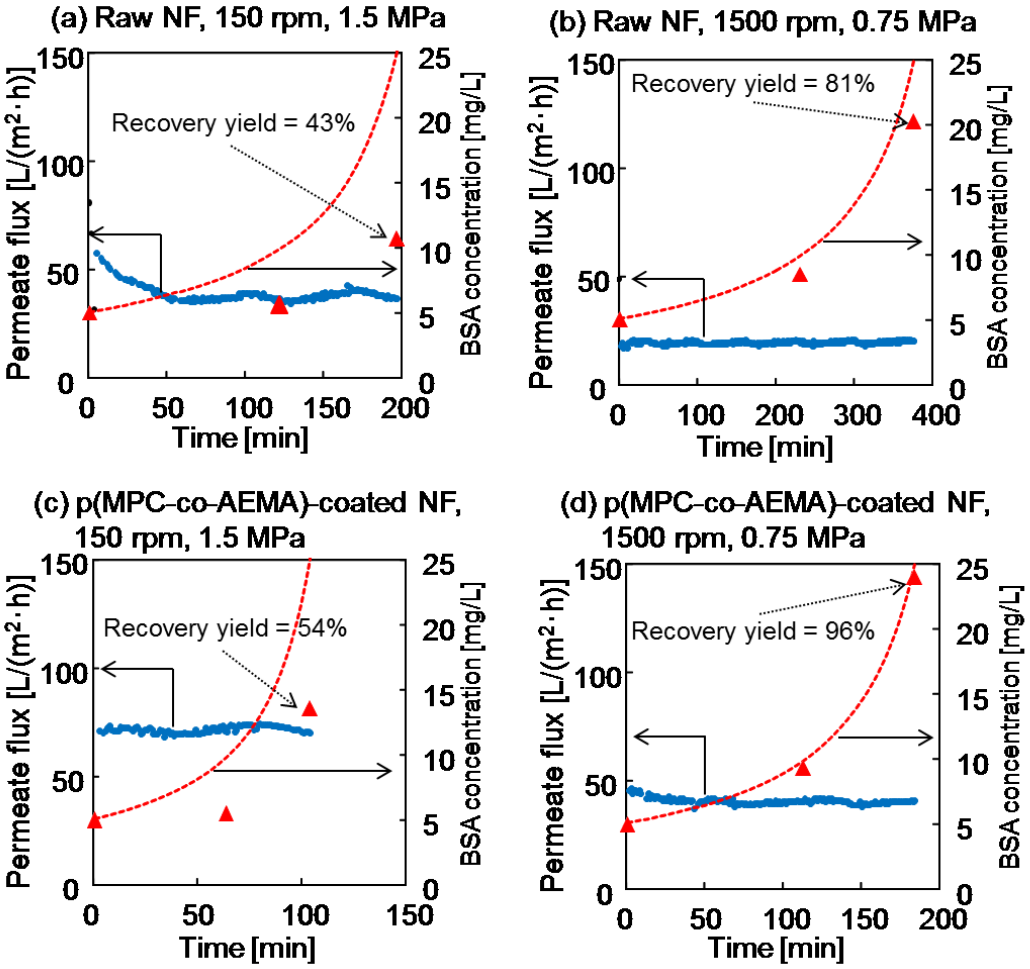


**Fig. IV.10 Time courses of the permeate flux and BSA concentrations in the condensed solutions from the condensation tests of the BSA using (a) raw NF membrane under the original hydrodynamic condition (at 150 rpm and 1.5 MPa), (b) raw NF membrane under the optimized hydrodynamic conditions (at 1500 rpm and 0.75 MPa), (c) p(MPC-co-AEMA)-coated NF membrane under the original hydrodynamic condition (at 150 rpm and 1.5 MPa), (d) p(MPC-co-AEMA)-coated NF membrane under the optimized hydrodynamic conditions (at 1500 rpm and 0.75 MPa). Blue circles and red triangles indicate permeate flux and BSA concentration, respectively. Red dotted line indicates the theoretical concentrations of BSA assuming 100% recovery yield.**

### IV.3.4 Condensation of groundwater

We examined the effects of hydrodynamic conditions and membrane surface modification on the recovery yield of organic colloids in groundwater. Fig. IV.11

shows the time course of the permeate flux and organic colloid concentration in the condensed solution. The condensation test using the raw NF membrane under the original hydrodynamic condition exhibited no reduction in flux, but the recovery yield at 5-fold condensation was only 62% (Fig. IV.11a). This low recovery yield is attributed to the adsorption of organic colloids on the membrane surface caused by membrane fouling. On the other hand, the condensation test using the p(MPC-co-AEMA)-coated NF membrane under the optimized hydrodynamic condition afforded a higher recovery yield of 92% at 5-fold condensation (Fig. IV.11b). For obtaining a sufficiently high concentration of organic colloids for Py-GC/MS measurement, the groundwater was condensed from 500 mL to 25 mL (20-fold condensation) using the p(MPC-co-AEMA)-coated NF membrane under the optimized hydrodynamic condition. Fig. IV.12 shows the results. The recovery yield obtained was 74% at 20-fold condensation, which was higher than that of 57% at 20-fold condensation in our previous study using the raw NF membrane under the original hydrodynamic condition (at 150 rpm and 1.5 MPa) [12]. Thus, we achieved improvement in the recovery yield of organic colloids by the combination of optimized hydrodynamic conditions and p(MPC-co-AEMA) coating.

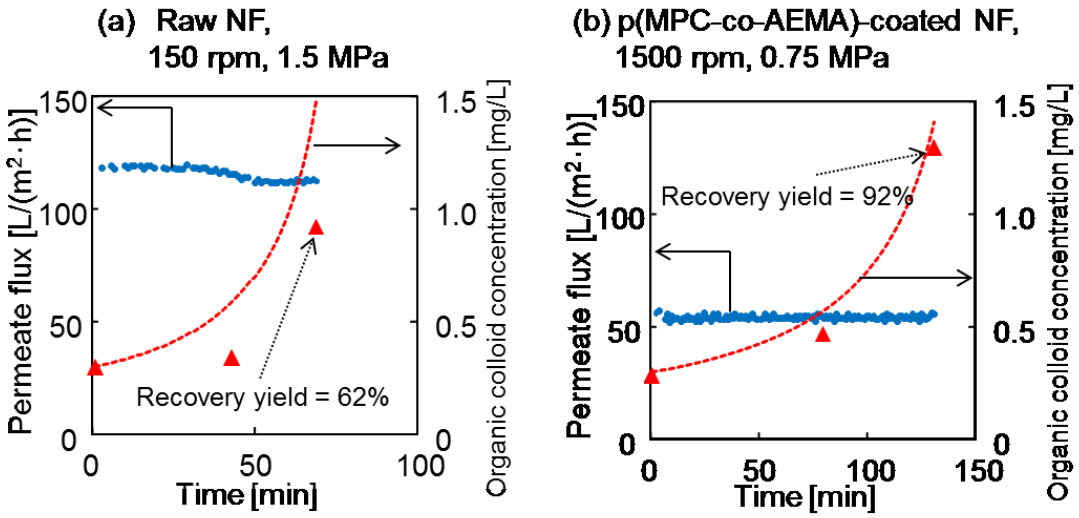


**Fig. IV.11 Time courses of the permeate flux and organic colloid concentration of the condensed solutions from the condensation test of the groundwater using (a) raw NF membrane under the original hydrodynamic condition (at 150 rpm and 1.5 MPa), (b) p(MPC-co-AEMA)-coated NF membrane under the optimized hydrodynamic conditions (at 1500 rpm and 0.75 MPa). The concentration of organic colloids was calculated under the assumption that all organic colloids were WHA. Blue circles and red triangles indicate permeate flux and organic colloid concentration, respectively. Red dotted line indicates theoretical concentrations of organic colloids assuming 100% recovery yield.**

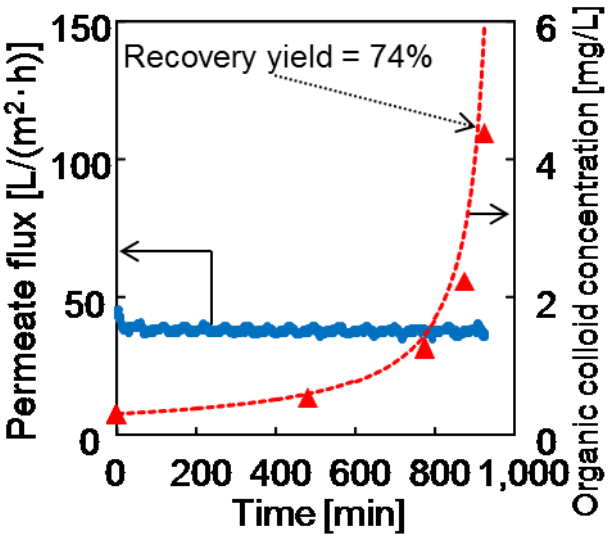


**Fig. IV.12 Time courses of the permeate flux and organic colloid concentration in the condensed solutions from the condensation tests of the groundwater using the p(MPC-co-AEMA)-coated NF membrane under optimized hydrodynamic conditions (at 1500 rpm and 0.75 MPa). The groundwater was condensed from 500 mL to 25 mL. The concentration of organic colloids was calculated under the assumption that all organic colloids were WHA. Blue circles and red triangles indicate permeate flux and organic colloid concentration, respectively. Red dotted line indicates theoretical concentrations of organic colloids assuming 100% recovery yield.**

### IV.3.5 Characterization of groundwater

Fig. IV.13 shows the Py-GC/MS pyrogram of the organic colloids in the condensed groundwater, and Table IV.1 lists the detected compounds. The major products obtained from the pyrolysis of organic colloids were aromatic products. This result indicates that the composition of a majority of the organic colloids in deep groundwater is similar to that of humic substances with high humification, as has been previously reported by our group [12]. Moreover, as shown in Fig. IV.13b, the major products obtained from the pyrolysis of p(MPC-co-AEMA), such as benzene, methyl methacrylate, and dimethylethanolamine, were not detected in the pyrogram of organic colloids, indicating that the p(MPC-co-AEMA) coating does not desorb from the NF

membrane surface and does not affect Py-GC/MS analysis. Although the result obtained from the Py-GC/MS pyrogram was not different from those obtained from our previous study [12], other components, which were not detected by Py-GC/MS, may be different. In particular, the result of rare earth elements (REEs) could be different, caused by their high affinity with organic colloids [31–33]. REEs are regarded as analogs of trivalent actinides [34] and are important for HLW. Therefore, REEs should be analyzed in future studies.

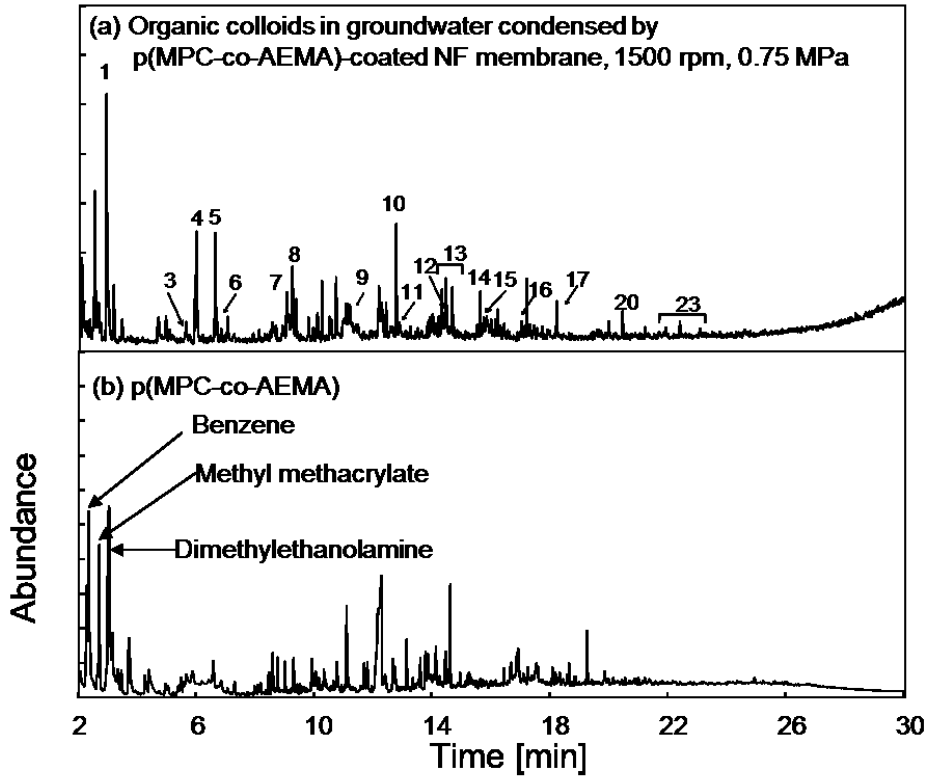


**Fig. IV.13 Py-GC/MS pyrogram of (a) organic colloids in groundwater condensed by the p(MPC-co-AEMA)-coated NF membrane under optimized hydrodynamic conditions (at 1500 rpm and 0.75 MPa), (b) p(MPC-co-AEMA). Table IV.1 shows the peak numbers.**

## IV.4 Conclusions

We examined the improvement in the recovery yields of organic colloids via the condensation of deep groundwater by utilizing optimized hydrodynamic conditions, such as transmembrane applied pressure and stirring rate, and modifying the surface of NF membranes with p(MPC-co-AEMA). The recovery yield of humic acid from the condensation test was increased by the optimized hydrodynamic conditions, attributed to the reduction of concentration polarization and permeate drag, and by the modification of membrane surfaces, attributed to the hydrophilization of the NF membrane surface. The recovery yield of BSA in the condensation test was also increased by the optimized hydrodynamic conditions and modified membrane surface. In addition, the modification of membrane surfaces was effective for preventing the decrease in permeate flux, caused by BSA fouling. The recovery yield of organic colloids in the condensation test of deep groundwater was significantly increased by the combination of optimized hydrodynamic conditions and the modified membrane surface. The Py-GC/MS analysis of organic colloids condensed by the improved method proposed in this study indicated that composition of organic colloids is similar to that of humic substance with high humification, same as in our previous study. The optimization of hydrodynamic conditions and modification of membrane surfaces, which were effective for the improvement in the recovery of organic colloids, will contribute to the prevention of organic fouling in various applications of NF membranes.

REFERENCES

[1] Minister of Economy, Trade and Industry, Designated Radioactive Waste Final Disposal Act (Act No. 117 of 2000), 2000.

[2] P. Vilks, D.B. Bachinski, Characterization of organics in Whiteshell Research area groundwater and the implications for radionuclide transport, Appl. Geochem. 11 (1996) 387–402.

[3] T. Saito, Y. Suzuki, T. Mizuno, Size and elemental analyses of nano colloids in deep granitic groundwater: implications for transport of trace elements, Colloids Surf. A: Physicochem. Eng. Asp. 435 (2013) 48–55.

[4] V. Moulin, G. Ouzounian, Role of colloids and humic substances in the transport of radio-elements through the geosphere, Appl. Geochem. 7 (1992) 179–186.

[5] V. Moulin, C. Moulin, Fate of actinides in the presence of humic substances under conditions relevant to nuclear waste disposal, Appl. Geochem. 10 (1995) 573–580.

[6] J. Gaillardet, J. Viers, B. Dupré, Trace elements in river waters, in: J.I. Drever(Ed.), Treatise on Geochemistry, Elsevier, Amsterdam, (2003) 225–272.

[7] M. Plaschke, J. Romer, J.I. Kim, Characterization of Gorleben groundwater colloids by atomic force microscopy, Environ. Sci. Technol. 36 (2002) 4483–4488.

[8] E.M. Thurman, R.L. Malcom, Preparative isolation of aquatic humicsubstances, Environ. Sci. Technol. 15 (1981) 463–466.

[9] C.J. Miles, J.R. Tuschall Jr., P.L. Brezonik, Isolation of aquatic humus with diethylaminoethylcellulose, Anal. Chem. 55 (1983) 410–411.

[10] S.M. Serkiz, E.M. Perdue, Isolation of dissolved organic matter from the

Suwannee River using reverse osmosis, Water Res. 24 (1990) 911–916.

[11] L. Sun, E.M. Perdue, J.F. McCarthy, Using reverse osmosis to obtain organic matter from surface and ground waters, Water Res. 29 (1995) 1471–1477.

[12] D. Aosai, D. Saeki, T. Iwatsuki, H. Matsuyama, Concentration and characterization of organic colloids in deep granitic groundwater using nanofiltration membranes for evaluating radionuclide transport, Colloids and Surf. A: Physicochem. Eng. Asp. 485 (2015) 55–62.

[13] S. Hong, M. Elimelech, Chemical and physical aspects of natural organic matter (NOM) fouling of nanofiltration membranes, J. Membr. Sci. 132 (1997) 159–181.

[14] A. Seidel, M. Elimelech, Coupling between chemical and physical interactions in natural organic matter (NOM) fouling of nanofiltration membranes: implications for fouling control, J. Membr. Sci. 203 (2002) 245–255.

[15] C.Y. Tang, Y.N. Kwon, J.O. Leckie, Fouling of reverse osmosis and nanofiltration membranes by humic acid—effects of solution composition and hydrodynamic conditions, J. Membr. Sci. 290 (2007) 86–94.

[16] M.J. Avena, L.K. Koopal, W.H. van Riemsdijk, Proton binding to humic acids: Electrostatic and intrinsic interactions. J. Colloid Interface Sci. 217 (1999) 37–48.

[17] C.L. Tiller, C.R. Omelia, Natural organic matter and colloidal stability: Models and measurements, Colloids and Surf. A: Physicochem. Eng. Asp. 73 (1993) 89–102.

[18] K. Ghosh, M. Schnitzer, Macromolecular structures of humic substances, Soil Sci. 129 (1980) 266–276.

[19] F.J. Stevenson, Humus chemistry, John Wiley & Sons: New York, 1982.

[20] D. Rana, T. Matsuura, Surface modifications for antifouling membranes, Chem.

Rev. 110 (2010) 2448–2471.

[21] G.D. Kang, M. Liu, B. Lin, Y.M. Cao, Q. Yuan, A novel method of surface modification on thin-film composite reverse osmosis membrane by grafting poly(ethylene glycol), Polymer 48 (2007) 1165–1170.

[22] G.D. Kang, H.J. Yu, Z.N. Liu, Y.M. Cao, Surface modification of a commercial thin film composite polyamide reverse osmosis membrane by carbodiimide-induced grafting with poly(ethylene glycol) derivatives, Desalination 275 (2011) 252–259.

[23] R. Bernstein, S. Belfer, V. Freger, Bacterial attachment to RO membrane ssurface-modified by concentration–polarization–enhanced graft polymerization, Environ. Sci. Technol. 45 (2011) 5973–5980.

[24] F. Razi, I. Sawada, Y. Ohmukai, T. Maruyama, H. Matsuyama, The improvement of antibiofouling efficiency of polyethersulfone membrane by functionalization with zwitterionic monomers, J. Membr. Sci. 401 (2012) 292–299.

[25] D. Saeki, T. Tanimoto, H. Matsuyama, Prevention of bacterial adhesion on polyamide reverse osmosis membranes via electrostatic interactions using a cationic phosphorylcholine polymer coating, Colloids and Surf. A: Physicochem. Eng. Asp. 443 (2014) 171‑176.

[26] T. Ikuma, K. Takeuchi, K. Sagisaka, T. Takasawa, Coomassie brilliant blue G250 dye-binding microassay for protein, Obihiro University Archives of Knowledge 23 (2002) 18–26

[27] Y. Muramatsu, S. Uchida, P. Sriyotha, K. Sriyotha, Some considerations on the sorption and desorption phenomena of iodide and iodate on soil, Water, Air, Soil Pollut. 49 (1990) 125–138.

[28] M. E. Alcántara-Garduño, T. Okuda, W. Nishijima, M. Okada, Ozonation of trichloroethylene in acetic acid solution with soluble and solid humic acid. J. Hazard Mater. 160 (2008) 662–667.

[29] X.Q. Lu, J.V. Hanna, W.D. Johnson, Source indicators of humic substances: an elemental composition, solid state 13 C CP/MAS NMR and Py-GC/MS study, Appl. Geochem. 15 (2000) 1019–1033.

[30] F.J. Gonzalez-Vila, J. del Rio, G. Almendros, F. Martin, Structural relationship between humic fractions from peat and lignites from the Miocene Granada basin, Fuel 73 (1994) 215–221.

[31] J.W. Tang, K.H. Johannesson, Speciation of rare earth elements in natural terres-trial waters: assessing the role of dissolved organic matter from the modeling approach, Geochim. Cosmochim. Acta 67 (2003) 2321–2339.

[32] Y. Yamamoto, Y. Takahashi, H. Shimizu, Systematic change in relative stabilities of REE–humic complexes at various metal loading levels, Geochem. J. 44 (2010) 39–63.

[33] F.J. Millero, Stability constants for the formation of rare earth–inorganic com-plexes as a function of ionic strength, Geochim. Cosmochim. Acta 56 (1992) 3123–3132.

[34] N. Chapman, J. Smellie, Introduction and summary of the workshop, Chem.Geol. 55 (3–4) (1986) 167–173.

# Chapter V

## Conclusions

In this chapter, the results obtained in previous chapters are summarized as conclusion, and perspectives for further research studies are discussed.

### V.1 Conclusions

The migration behavior of radionuclides in underground must to be understood for safety assessment of geological disposal of high-level radioactive waste (HLW). In this safety assessment, colloid study is widely conducted, because colloids affect the migration behavior of radionuclides. However, there are problems in colloid study that properties of colloids are influenced by changes in the chemistry of groundwater, and concentration of colloids is low. Therefore, development of analytical techniques to understand properties of colloids in groundwater accurately is required.

In this thesis, a separation technique using microfiltration/ultrafiltration (MF/UF) membranes was developed to analyze properties of colloids without alteration of colloids and a new condensation technique using nanofiltration (NF) membranes was developed to obtain highly condensed organic colloids with high concentration and to analyze properties of organic colloids in detail. Moreover, the condensation technique was improved for high recovery yields of organic colloids by surface modification of nanofiltration membranes and optimization of filtration conditions. The findings and conclusions of this thesis are summarized as follows:

## 1. Size and composition analyses of colloids in deep granitic groundwater using microfiltration/ultrafiltration while maintaining in situ hydrochemical conditions

To collect colloids and analyze properties of colloids in deep groundwater without significant changes of the groundwater chemistry, a MF/UF apparatus which can maintain in situ hydrochemical conditions (mainly hydraulic pressure and anaerobic condition) was developed. An air exposure experiment of groundwater indicated that Fe colloids were formed rapidly by oxidation due to exposure to the air, and the oxidation of groundwater influenced the partitioning of rare earth elements (REEs) depending on colloids size. Therefore, the microfiltration/ultrafiltration apparatus is indispensable for analyzing colloids and REEs in deep groundwater accurately. Actual groundwater was filtered using the developed apparatus at in-situ of a depth of 300 m at the Mizunami Underground Research Laboratory (MIU) to analyze size distribution and composition of colloids and partitioning of REEs depending on colloids size. Different types of colloids consisting of inorganic substances (e.g., Fe, Al, Mg, and Si) and organic substances (mainly humic substances) were observed with a wide size range. REEs characteristic partitioning, such as preferential association of light REEs with colloids of specific sizes range, were revealed. These results implicated that influence of organic colloids on radionuclides migration is stronger than that of inorganic colloids in the groundwater obtained from at the MIU and these findings are useful for understanding the migration of radionuclides in deep groundwater.

## 2. Concentration and characterization of organic colloids in deep granitic groundwater using nanofiltration membranes for evaluating radionuclide transport

In addition to my result, another study, which conducted speciation of REEs complexes based on thermodynamic calculation, implicated that chemical behavior of REEs in the groundwater obtained at MIU mainly depends on organic colloids. Therefore, I focused on organic colloids and developed a new condensation method using nanofiltration (NF) membranes to condense organic colloids rapidly without chemical disturbance for analyzing organic colloids accurately. Condensation performance of NF and RO membranes for aqueous solutions of humic acids, which considered as main organic colloids, were evaluated using a laboratory-scale cross-flow membrane filtration apparatus. The time course of permeate flux was monitored and recovery yields of humic acids were calculated. In condensation of groundwater using the RO, severe permeate flux decline was occurred owing to the precipitation of inorganic substances on the membrane surface and crosslinking of organic colloids with $Ca^{2+}$. Thus, it was difficult to concentrate the solution to more than 6-fold concentration using RO membrane. On the other hands, the NF membrane achieved 20-fold condensation of groundwater with 57% recovery yield of organic colloids. The low rejection of monovalent ions and high rejection of divalent ions of the NF membrane allowed the condensation of organic colloids in deep groundwater. Therefore, NF membranes were more suitable than RO membranes for the condensation of organic colloids in deep groundwater. The organic colloids concentrated by the NF membrane were successfully analyzed using Py-GC/MS. The result indicated that the composition of organic colloids in granite groundwater at a depth of 300 m is similar to those of

humic substances with high humification. Moreover, some REE concentrations in the groundwater condensed by NF membranes could be detected by inductively coupled plasma mass spectrometry (ICP-MS), while those in the raw groundwater were lower than the detection limit. This condensation method would be promising for condensing organic colloids and REEs in groundwater efficiently and for understanding the interaction between organic colloids and REEs.

### 3. Efficient condensation of organic colloids in deep groundwater using surface-modified nanofiltration membranes under optimized hydrodynamic conditions

A condensation method using NF membranes was improved by optimization of hydrodynamic conditions, such as the applied transmembrane pressure (TMP) and stirring rate, and membrane surface modification using a cationic phosphorylcholine polymer, poly(2-methacryloyloxyethyl phosphorylcholine-co-2-aminoethyl methacrylate) (p(MPC-co-AEMA)). The effect of the optimization of hydrodynamic conditions and membrane surface modification was evaluated using aqueous solutions of humic acid or bovine serum albumin (BSA), which were used as models of organic colloids. The time course of permeate flux was monitored and recovery yield of humic acids and BSA were calculated. The decreasing TMP and increasing stirring rate prevented membrane fouling and improved the recovery yield of humic acids and BSA. The membrane surface modified with p(MPC-co-AEMA) was significantly effective for preventing the decline in permeate flux, caused by fouling with BSA. Optimized hydrodynamic conditions were more effective than the membrane surface modification for improving the recovery yield of humic acids and BSA. Finally, the recovery yield of

organic colloids in deep groundwater was efficiently improved by the combination of optimized hydrodynamic conditions and membrane surface modification. The Py-GC/MS analysis of organic colloids condensed by the improved method indicated that the composition of organic colloids is similar to that of humic substance with high humification. This improved condensation method contributes to understanding of organic colloids property and interaction with radionuclides for safety assess of HLW.

## V.2 Perspectives

The separation technique using MF/UF membranes developed in this thesis can separate and analyze colloids in groundwater without changes of colloid properties by air exposure and pressure release during sampling. The change of colloid properties was not prevented sufficiently in previous studies. This technique will be able to widely apply in various sites especially the site where actual radionuclides present for reliable safety assessment of geological disposal of HLW.

The condensation technique using NF membranes developed in this thesis achieved highly condensation of organic colloids. However, at the present stage, the interaction between REEs and colloids is not unclear, because the condensation and recovery yield are not enough to detect REEs. Evaluation of condensation performance for REEs and detail analysis on the condensates are required to understand interaction between REEs and colloids more exactly.

The recovery yield of organic colloids on the condensation using NF membranes was efficiently improved by the prevention of membrane fouling with organic colloids by the combination of optimized hydrodynamic conditions and membrane surface modification. This improvement approach will be useful for further condensation of

colloids in groundwater and analysis of the interaction between REEs and colloids.

Finally, I hope that these techniques developed in this thesis and obtained findings for properties of colloids in groundwater contribute to safety of geological disposal of HLW.

# List of Publications

**Chapter II** ***Size and composition analyses of colloids in deep granitic groundwater using microfiltration/ultrafiltration while maintaining in situ hydrochemical conditions,*** **D. Aosai,** Y. Yamamoto, T. Mizuno, T. Ishigami, H. Matsuyama, Colloids Surf. A: Physicochem. Eng. Asp. 461 (2014) 279–286.

**Chapter III** ***Concentration and characterization of organic colloids in deep granitic groundwater using nanofiltration membranes for evaluating radionuclide transport***, **D. Aosai,** D. Saeki, T. Iwatsuki, H. Matsuyama, Colloids Surf. A: Physicochem. Eng. Asp. 485 (2015) 55–62.

**Chapter IV** ***Efficient condensation of organic colloids in deep groundwater using surface-modified nanofiltration membranes under optimized hydrodynamic conditions***, **D. Aosai,** D. Saeki, T. Iwatsuki, H. Matsuyama, Colloids Surf. A: Physicochem. Eng. Asp. 495 (2016) 68–78.

Doctoral Thesis, Kobe University
“Development of separation and condensation techniques using functional membrane for trace components in groundwater”, 112 pages
Submitted on January 19, 2016
The date of publication is printed in cover of repository version published in Kobe University Repository Kernel.